

MECHANICAL PROPERTIES OF MYOSIN CROSS-BRIDGES IN FROG STRIATED MUSCLE

David Graham Hirst

A Thesis Submitted for the Degree of PhD
at the
University of St Andrews



1975

Full metadata for this item is available in
St Andrews Research Repository
at:

<http://research-repository.st-andrews.ac.uk/>

Please use this identifier to cite or link to this item:

<http://hdl.handle.net/10023/14825>

This item is protected by original copyright

MECHANICAL PROPERTIES OF MYOSIN CROSS-BRIDGES
IN FROG STRIATED MUSCLE.

A Thesis

Submitted to the University of St. Andrews
for the degree of Doctor of Philosophy.

by

DAVID GRAHAM HIRST

Department of Physiology

University of St. Andrews

September, 1975.



ProQuest Number: 10166452

All rights reserved

INFORMATION TO ALL USERS

The quality of this reproduction is dependent upon the quality of the copy submitted.

In the unlikely event that the author did not send a complete manuscript and there are missing pages, these will be noted. Also, if material had to be removed, a note will indicate the deletion.



ProQuest 10166452

Published by ProQuest LLC (2017). Copyright of the Dissertation is held by the Author.

All rights reserved.

This work is protected against unauthorized copying under Title 17, United States Code
Microform Edition © ProQuest LLC.

ProQuest LLC.
789 East Eisenhower Parkway
P.O. Box 1346
Ann Arbor, MI 48106 – 1346

Th 8836

ACKNOWLEDGMENTS

I would like to express my gratitude and thanks to my supervisors, Dr. F.W. Flitney and Dr. W.G.S. Stephens, for their help and inspiration throughout this work.

I have also benefited considerably from valuable discussions with Dr. D.A. Jones and Dr. P.S. Agutter.

This work was supported by a James MCKenzie research fellowship.

DECLARATION.

I hereby declare that the research reported in this thesis was carried out by me and that the thesis is my own composition. No part of this work has been previously submitted for a higher degree.

The research was conducted in the Department of Physiology, United College of St. Salvator and St. Leonard, University of St. Andrews, under the direction of Dr. F.W. Flitney and Dr. W.G.S. Stephens.

ACADEMIC RECORD.

I first matriculated at the University of St. Andrews
in October 1968 and graduated with the degree of
~~B.Sc. Hons. (1st class)~~ in Physiology in June 1972.

I matriculated as a research student of the Department of Physiology, University of St. Andrews in
October 1972.

CERTIFICATE.

We hereby certify that David G. Hirst has spent nine terms engaged in research work under our direction, and that he has fulfilled the conditions of General Ordinance No. 12 (Resolution of the University Court No. 1 1967), and that he is qualified to submit the accompanying thesis for the degree of Doctor of Philosophy.

A cynic once remarked that the only thing that mankind can do is to move things. It would be pleasant to be able to add that at any rate he can understand how, if not why, he moves them.

A.V. HILL (1950)

CONTENTS.

	Page.
Summary	1
CHAPTER I : Introduction.	7
Sliding filament theory.	9
Cross-bridge models.	15
A structural basis for cross-bridge models.	30
Scope of the present study.	33
CHAPTER II : Materials and methods.	35
Apparatus.	36
CHAPTER III : Tension changes and sarcomere movements during ramp and hold stretches of large amplitude.	39
Part one. Tension responses.	39
Part two. Laser diffraction measurements of sarcomere movements.	42
Resting muscle.	45
Active muscle.	46
Discussion.	54
CHAPTER IV : Tension responses and sarcomere movements during cyclical length changes of large amplitude.	59
Discussion. Working hypothesis	66
CHAPTER V : The effect of temperature and velocity of length change on the form of the tension response.	71
Discussion.	78

CHAPTER VI : Tension responses to length changes of	
small and intermediate amplitude.	85
Intermediate amplitudes.	86
Small amplitudes.	89
Discussion.	91
CHAPTER VII : Work absorbed by contracting muscle	
during cycles of stretch and release.	96
Discussion.	103
CHAPTER VIII: Conclusions.	108
The concept of rapid 'give' as a transition	
between two steady states.	109
Structure of the actin active region and	
the possible nature of bonding to the myosin	
head.	110
Undamped elastic component of the cross-	
bridge.	113
Relation of the present results to other	
models in which the myosin cross-	
projections function as mechanical	
linkages.	116
Scope for further study.	118
References.	121

List of figures.

<u>Fig. no.</u>	<u>Facing page.</u>	<u>Fig. no.</u>	<u>Facing page.</u>	<u>Fig. no.</u>	<u>Facing page.</u>
1.1.	10.	3.7.	49.	5.7.	76.
1.2.	15.	3.8.	50.	5.8.	76.
1.3.	15.	3.9.	50.	5.9.	76.
1.4.	16.	3.10.	51.	5.10.	76.
1.5.	17.	3.11.	51.	5.11.	77.
1.6.	17.	3.12.	51.	5.12.	77.
1.7.	18.	3.13.	52.	5.13.	79.
1.8.	18.	3.14.	52.		
1.9.	21.	3.15.	52.	6.1.	86.
1.10.	22.	3.16.	54.	6.2.	86.
1.11.	23.			6.3.	87.
1.12.	24.	4.1.	59.	6.4.	88.
1.13.	24.	4.2.	60.	6.5.	88.
1.14.	25.	4.3.	60.	6.6.	89.
1.15.	28.	4.4.	62.	6.7.	89.
1.16.	31.	4.5.	64.	6.8.	90.
1.17.	31.	4.6.	65.	6.9.	91.
		4.7.	67.		
2.1.	36.	4.8.	69.	7.1.	96.
				7.2.	97.
3.1.	39.	5.1.	72.	7.3.	97.
3.2.	44.	5.2.	73.	7.4.	98.
3.3.	45.	5.3.	73.	7.5.	99.
3.4.	47.	5.4.	73.	7.6.	100.
3.5.	48.	5.5.	74.	7.7.	100.
3.6.	48.	5.6.	74.		

List of Tables.

<u>Table no.</u>	<u>Facing page.</u>
1.	45.
2.	45.
3.	46.
4.	46.
5.	75.
6.	82.

ABBREVIATIONS.

The following abbreviations are used in the text and for labelling figures :

P_0	Peak isometric tension.
S_1	The first inflection on the tension record, during an applied stretch.
S_2	The second inflection on the tension record, during an applied stretch.
P_{S_2}	Total muscle tension at S_2 .
l_0	Length of the muscle in the intact animal, with the legs at 180° .
ΔS	Change in sarcomere length.
ΔP	Change in muscle tension.
ΔL	Change in muscle length.
E_m	Stiffness of the muscle: $\Delta P / \Delta L$.
E_s	Stiffness of the sarcomeres: $\Delta P / \Delta S$.
C_v	Critical velocity.
FRT	Filamentary resting tension.
W	Work absorbed by the muscle.

SUMMARY.

A. A study has been made of the tension responses and relative sliding movements of the actin and myosin filaments which result when controlled length changes of variable amplitude and velocity are applied to contracting frog's muscle.

B. The tension increment produced by a 'ramp and hold' stretch of approximately 1mm (about 4 % of muscle length) consists of three phases whose limits are defined by two points, designated S_1 and S_2 , where the slope of the increase of tension changes abruptly. S_1 and S_2 correspond with muscle extensions of 40 - 45 μ m and 325 - 375 μ m, respectively.

C. Displacement of the actin and myosin filaments was recorded simultaneously by monitoring changes in the diffraction spectra produced by illuminating a small area of muscle with a laser. The spectra were projected onto a screen and photographed with a cine-camera. The spacing of the 1st order lines was measured and used to calculate sarcomere length.

D. Cine photography of diffraction spectra showed that a variable, and sometimes large, proportion of the length change applied to the muscle is taken up by extension of elastic elements arranged in series with the sarcomeres. During the early part of the stretch, filament displacement is less than would be anticipated if all of the external length change was distributed uniformly amongst the sarcomeres.

E. The way in which sarcomeres shorten during the onset and development of an isometric tetanus shows that the series elastic elements become progressively stiffer with increasing extension; at peak tetanic tension their compliance is found to be approximately $6.5 \times 10^{-4} \text{ m.N}^{-1}$.

F. When the actin and myosin filaments are forcibly displaced by about 11-12 nm from their 'steady state' position at the peak of an isometric tetanus, the sarcomere length increases abruptly by some 20-30 nm, a phenomenon referred to as rapid 'give'. The 11-12 nm displacement before rapid 'give' occurs, represents the range of movement of the filaments over which the myosin cross-bridges can be distorted yet remain attached to the actin active site. This range of movement is found to be independent of sarcomere length, and hence, of interfilamentary spacing. Cross-bridges are forcibly broken when the filaments are made to move by more than 11-12 nm. The sudden increase in compliance of the sarcomeres which results effects an abrupt shortening of the stretched elastic elements (elastic recoil) at the expense of the sarcomeres in series with them,

producing rapid 'give'.

G. The stiffness of the sarcomeres and the force they are able to bear immediately prior to rapid 'give' (the maximum 'holding' force, designated P_{S_2}) are both directly proportional to filament overlap. Hence, the stiffness of an individual cross-bridge and its affinity for the actin active region are quantities which must be independent of the surface-to-surface separation of the filaments. The minimum stiffness of a single cross-bridge is estimated to be around $2.7 \times 10^{-4} \text{ N.m}^{-1}$.

H. Tension changes and sarcomere movements during single and double cycles of stretch and release were recorded. The events occurring during a second cycle stretch differ markedly from those during a first. Cross-bridges can accommodate a wider range of filament movement without detaching, 18 nm as compared with 12 nm, if the second stretch is applied without delay after the preceeding release. The stiffness of the sarcomeres is approximately the same for a second cycle stretch ($5.3 \times 10^{12} \text{ N.m}^{-2}$ per metre extension of each half sarcomere) as for a first ($5.95 \times 10^{12} \text{ N.m}^{-2}$ per metre extension of each half sarcomere), indicating that the number of cross-bridges holding the filaments together is not altered appreciably. These results are compatible with Huxley & Simmons recent model. They suggest an actin active region of length 15 nm, made up of four regularly spaced ($\sim 5.0 \text{ nm}$ separation) attachment sites, corresponding with individual actin monomers. The myosin head can occupy one of

three possible stable positions (designated A, B and C) and the full range of movement of the head (the force generating process) is effected by two steps ($A \rightarrow B$ and $B \rightarrow C$). At peak isometric tension the majority of the heads spend most of their time in position B.

I. PS_2 increases with increasing speed of stretch until a critical velocity (C_V) is reached, beyond which it remains more or less constant. Muscle stiffness (E_m) varies in a similar fashion. The C_V 's for PS_2 and E_m increase with increasing temperature. At 0°C , the C_V is about 3.8mm.s^{-1} , corresponding with a relative sliding of the filaments of $0.163\mu\text{m.s}^{-1}$.

J. Arrhenius plots of the variation in the C_V for PS_2 and E_m with temperature show that neither of these two parameters is related in a straight forward way to the rate of cross-bridge cycling. The activation energy for the rate limiting step determining the C_V for PS_2 is found to be $9.78\text{kcal.mol}^{-1}.\text{K}^{-1}$ (over the range $0 - 30^\circ\text{C}$). The corresponding Arrhenius plot for the variation in the C_V for E_m is more complex, yielding two activation energies of $12.5\text{kcal.mol}^{-1}.\text{K}^{-1}$ (range: $0 - 12^\circ\text{C}$) and $4.0\text{kcal.mol}^{-1}.\text{K}^{-1}$ (range: $12 - 30^\circ\text{C}$). It is postulated that there may be two, parallel reactions requiring ATP, which are separately related to PS_2 and E_m .

K. Tension changes during length cycles of small amplitude (not sufficient to reach S_1) and intermediate amplitude (sufficient to reach

S_1 , but not S_2) were investigated. The results suggest that tension generated up to S_1 (for stretches of 40 - 45 μm) is due to extension of Huxley & Simmons' AB link without a change in the orientation of the attached myosin head, whereas beyond S_1 and up to S_2 , backward rotation of the head accounts for most (about 90 %) of the movement of the filaments.

L. Muscle length/tension 'loops' were recorded during cyclical length changes of different amplitudes, made at constant velocity (greater than C_v). The work absorbed by the muscle (given by the area of the 'loop') depends upon the amplitude of the length change; no detectable work is absorbed for cycles of amplitude less than that required to exceed S_1 ; beyond S_1 , the work absorbed per unit increment of length increases progressively up to S_2 ; beyond S_2 , the work absorbed by the muscle is more or less constant. Sarcomere length/tension loops indicate that most (80 - 90%) of the non-returnable work is absorbed by the sarcomeres themselves.

M. More non-returnable work is done on a muscle during the first cycle of a double stretch-release combination than during the second. Typical values obtained are: 4.6 $\text{mJ} \cdot \text{m}^{-2}$ per half sarcomere (1st cycle) and 3.75 $\text{mJ} \cdot \text{m}^{-2}$ per half sarcomere (2nd cycle), for stretch-release cycles of approximately 1mm. The greater amount of work absorbed during the first cycle as compared to the second is associated with a

correspondingly greater amount of filament sliding which takes place in the period immediately following rapid 'give' until the end of the stretch.

N. The work required to force a single cross-bridge head from position C \rightarrow B is found to be 0.2×10^{-19} J. if all the projections are active. This amount of energy may be provided by the hydrolysis of a single molecule of ATP (0.8×10^{-19} J).

O. The energy required to break a cross-bridge is estimated to be within the range $0.25 - 1.0 \times 10^{-19}$ J. This is close to the bond energy of a single hydrogen bond (0.35×10^{-19} J). Each point on the head may therefore be attached to the actin filament by a single hydrogen bond, although more numerous (electrostatic) weaker bonds are also possible.



CHAPTER I

INTRODUCTION.

It is understandable that the desire to unravel the mechanism of muscular contraction has provided a fascinating and irresistible challenge to countless generations of biologists, because the capacity for movement, in an apparently purposeful fashion, is one of the most striking attributes of living organisms. While it is true that not all organisms have 'muscles', it is becoming clear that many cell types contain actin and myosin, the two principal proteins found in muscle, and that their interaction at the molecular level is involved wherever movement of one kind or another takes place.

Latterly, there has been an almost explosive expansion in our knowledge of muscle. In a recent review, Fuchs (1974) mentions twenty-four similar review articles, covering the period 1970-73, dealing with the biochemistry of muscle proteins, the control of contraction by calcium and the regulatory protein system, and the mechanism of force generation, as well as several important books on muscular contraction, ranging from undergraduate texts to Needham's monumental 'Machina Carnis', an historical account of the biochemistry and physiology of muscle. It would not be practicable to present here a review of the entire field, or even attempt a survey of the relatively restricted area covered by the

present investigation; instead, this introduction is aimed at a statement of the sliding filament theory, with a brief account of the experimental evidence on which it is based, together with a more detailed consideration of some recently proposed models, which attempt to explain how the force for contraction is generated at the molecular level.

The work to be described is concerned with the tension responses produced by the application of controlled stretches and releases to contracting frog's muscle. The technique is by no means novel. An immense amount of experimental work of this nature has been done in the last 70 years, especially by A.V. Hill and his colleagues. The converse type of experiment, measuring length while subjecting muscles to sudden changes of load, has also been used extensively. Much of the earlier work on the mechanics of muscle was difficult to interpret, for two principal reasons. First, because the internal structure of muscle was imperfectly understood. It was not until the early 1950's that the characteristic banding pattern of striated muscle, undoubtedly its most striking structural feature, was recognised as being due to the existence of a double, partially interpenetrating array of filaments within the sarcomeres. This proved to be a milestone in the study of muscle and it came to light only when electron microscopy and X-ray diffraction methods were brought to bear on the problem. Secondly, many of the early experiments were confounded by the existence of inert (non-contractile) structures within the muscle whose presence seriously hampered attempts to interpret the results. It gradually became clear that a number of the 'physiological'

properties of muscle could be attributed to the existence of elastic elements in series with the contractile component, and indirect, often tedious, methods of analysis were needed to assess its contribution. A.V. Hill has referred, somewhat euphemistically, to the series elastic component as 'an unmitigated nuisance'. This it certainly was; but nowadays its effects can be almost entirely eliminated by the expedient of following changes in the length of the sarcomeres themselves. This task is greatly facilitated by the use of the laser, monitoring changes in the spacing of the diffraction spectra produced by the sarcomeres, while subjecting the muscle to controlled changes of length or load, a technique which has been used extensively in the present study.

The Sliding Filament Theory.

For many years it was thought that muscle shortening and the development of tension were brought about by a change of shape (coiling or folding) of the contractile material, which was supposed to be in the form of continuous filaments. Unfortunately, early electron microscopic investigations led to reports of the existence of continuous filaments in muscle (Hall, Jakus & Schmitt, 1946) and it was not until 1953 that evidence to the contrary began to accumulate. In 1954 two short papers appeared together in the May 22nd issue of Nature, one by A.F. Huxley & Neidergerke reporting observations made with the interference microscope on changes in the striation pattern of living fibres under different physiological conditions (passive stretch and during isometric and iso-

STANDARD FILAMENT LENGTHS

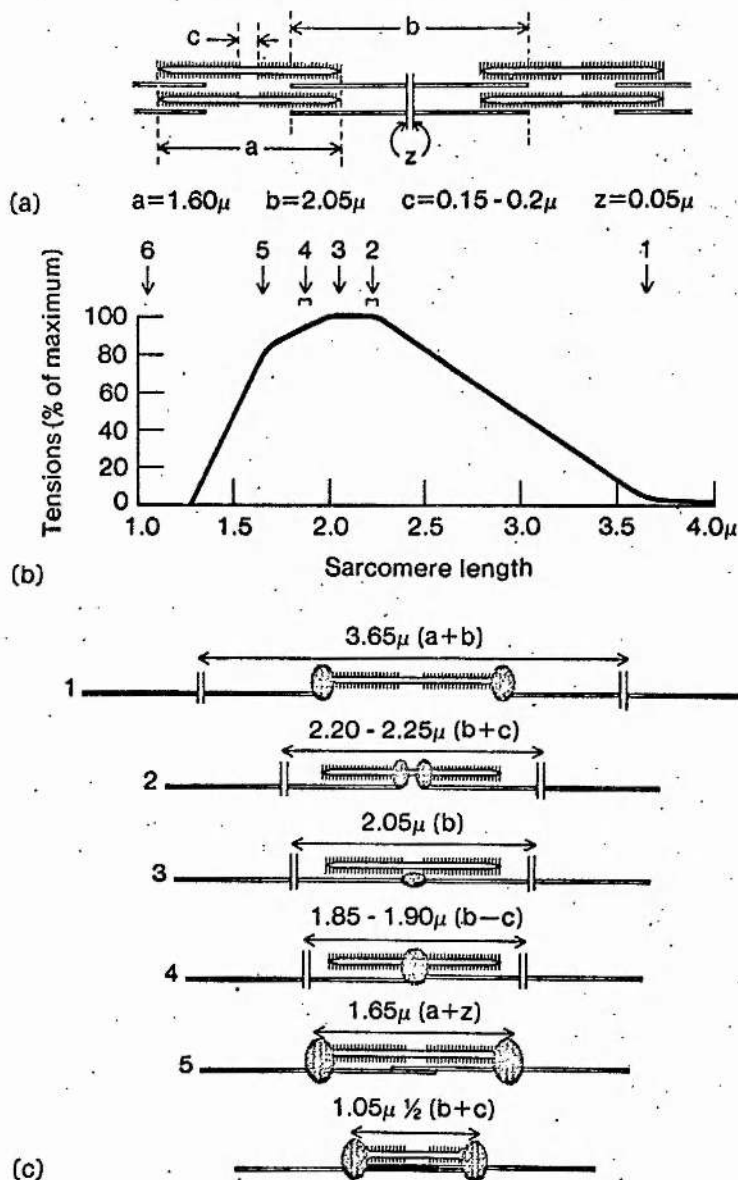


Fig. 1.1. (a) Standard filament lengths. (b) Length/tension curve from part of a single muscle fibre. The vertical arrows show the various critical stages of overlap portrayed in (c). (c) Critical stages in the increase in overlap of the thick and thin filaments as a sarcomere shortens. The numbers on the left refer to the discontinuities arrowed in (b). Shaded areas indicate regions of critical behaviour of the thick and thin filaments.

(From Carlson & Wilkie, 1974)

tonic contraction), and the other by H.E. Huxley & Hanson, summarising their observations made with the phase contrast microscope on the banding pattern of isolated myofibrils at rest and during contraction. The most significant result to emerge from both studies was that the width of the A-band region of the sarcomere remains constant under differing physiological conditions and that changes in muscle length can be accounted for by changes in the width of the I-bands. Electron microscopic observations (H.E. Huxley, 1953b) and X-ray diffraction studies (H.E. Huxley, 1953a) of muscle in rigor had earlier revealed the protein component to be in the form of elongated filaments, and it was shown by selective extraction experiments (H.E. Huxley & Hanson, 1954) that myosin is confined to the A-band. These observations led A.F. Huxley & Neidergerke and H.E. Huxley & Hanson to propose a new model for contraction which was widely accepted. This became known as the ~~sliding filament~~ theory. Briefly, it states that the contractile proteins are arranged within each sarcomere in the form of two sets of interdigitating filaments, organised in hexagonal arrays; the thin, actin-containing filaments, located principally in the I-band, and the thicker, myosin-containing filaments, located exclusively in the A-band. A change in the length of a muscle is brought about by a relative sliding movement of one set of filaments past the other and the force for contraction is generated by a number of independently-acting sites located where the two overlap. A diagram of the arrangement of filaments at different sarcomere lengths is shown in Fig. 1.1.

There are two important corollaries of this theory, which have been amply confirmed experimentally. First, if a change in the length of a muscle is brought about by a relative sliding motion of the two kinds of filaments, then their length ought to remain constant. This has been shown by electron microscopy (Page, 1964;1968), the length of the A filaments being $1.6\mu\text{m}$ and that of the I filaments, $2.1\mu\text{m}$ (frog muscle), and by wide angle diffraction studies of living muscle, which reveal that the spacing of the sub-units in the filaments remains constant, both at rest and during contraction, over a wide range of muscle lengths (Huxley & Brown, 1967). Secondly, the theory proposes that the force between the actin and myosin filaments is generated at a series of points of interaction located in the region of overlap in each sarcomere; accordingly, the tension developed per filament should be proportional to the number of these points, and therefore to the width of the overlap region. It has been known for some time that the peak isometric tension of a muscle is inversely related to its length, for sarcomere spacings greater than about $2.5\mu\text{m}$ (Ramsay & Street, 1940) and this has been strikingly confirmed by Gordon, Huxley & Julian (1966). It is an extremely important property of muscle, which fully accords with the idea that tension is produced by independent force generators, located in the region of overlap between the actin and myosin filaments.

With improvements in electron microscopic techniques, it became clear that, under certain conditions, physical linkages are formed

between the thick and thin filaments, and in 1957, A.F. Huxley proposed that in living muscle temporary cross-bridges are formed between the filaments and that these are responsible for the generation of force. Interaction between actin and myosin is supported by evidence from biochemical studies of proteins in solution. The ATPase activity of myosin alone under physiological conditions is low, but it is greatly enhanced by the presence of actin (Hasselbach, 1952), indicating that actin can, by itself, cause activation of myosin. This interaction is inhibited in the absence of calcium ions by troponin and tropomyosin, the regulatory proteins (Ebashi, 1963; Ebashi & Ebashi, 1966), which in vertebrate skeletal muscle are found to be associated with the thin filaments (Ebashi, Endo, Nonomura, Masaki & Otsuki, 1966; Pepe, 1966).

It is reasonable to assume that the enzymically-reactive part of the myosin molecule forms part of the mechanical linkage; furthermore, since relatively large sliding movements of the filaments occur, it must be assumed that each cross-bridge is capable of performing repetitive, cyclical movements. During part of each cycle it must form an attachment with the actin filament and at the same time undergo a change of shape so as to cause relative sliding movement of the filaments. The performance of each cycle is accompanied at some stage by the splitting of ATP, which provides the energy required by the system in doing work.

The way in which individual myosin molecules are assembled in the

myosin filament was clarified by H.E. Huxley (1961, 1963) using negatively stained preparations. As a result of this work it became clear that the myosin filament is polarised and that the direction of orientation of the molecules is reversed in either half of each filament. The consequence of this arrangement is that the tendency for the filaments to move relative to one another is equal and opposite in each half-sarcomere and individual cross-bridges act in parallel.

One of the earliest and most important results to emerge from the application of X-ray diffraction techniques to the study of muscle was H.E. Huxley's (1953) finding that the volume occupied by the filament lattice is constant at all muscle lengths; that is, the product of sarcomere length and the square of the interfilamentary spacing has a fixed value. It follows that the lateral spacing of the filaments varies inversely with sarcomere length, and for frog's muscle their centre-to-centre spacing is found to range from 19.0 - 26.0 nm (Elliot, 1964). The sum of the radii of the actin and myosin filaments is about 15 nm (Elliot, Lowy & Worthington, 1963) which means that their surface-to-surface separation may be as little as 4 nm or as great as 11.0 nm in the range of sarcomere lengths over which contraction is possible. These, then, are the limits of distance over which a cross-bridge must be capable of operating and it poses an interesting question, for the relationship between filament overlap and maximum isometric force shows clearly that a cross-bridge is equally effective at generating force, regardless of the distance over which it operates.

Using low angle X-ray diffraction techniques, Huxley, Brown & Homes (1965) were able to obtain diffraction patterns which revealed some of the changes which occur in the filaments when a muscle contracts; the diffraction lines produced by the actin filaments show little change in spacing or in their relative intensity, but the reflections produced by the regular helical arrangement of cross-bridges in the myosin filament become very much less intense. These observations indicate that cross-bridges undergo asynchronous movements which take place both radially and longitudinally with respect to the long axis of the myosin filament. Furthermore, the relative intensities of the equatorial reflections arising from the 1,0 and 1,1 lattice planes reverse during contraction. This results from the transfer of material from the thick filaments to the vicinity of the thin filaments.

A considerable amount of evidence has accumulated recently which shows that a large part of the so-called series elastic component is actually located within the sarcomeres. A.V. Hill (1970) has shown that the elastic component becomes stiffer as muscle force develops, a finding confirmed recently by Bressler & Clinch (1974), who also observed that the stiffness is dependent on the length of the muscle, and hence on the extent of filament overlap. A similar dependence of stiffness on filament overlap was demonstrated by Huxley & Simmons (1971a). It seems most likely that this elasticity is a colligative property of the cross-bridges themselves, since the filaments have been shown to be relatively inextensible (H.E. Huxley & Brown, 1967).

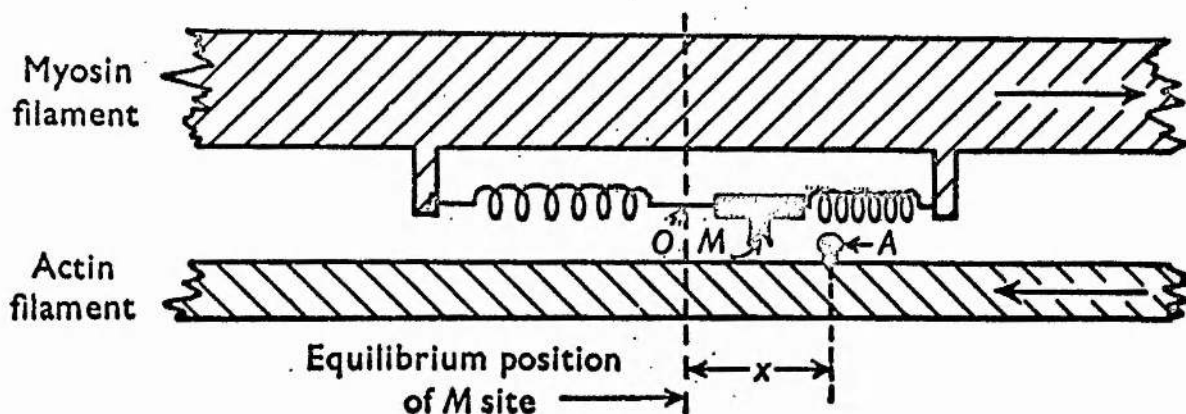


Fig. 1.2. Mechanism of contraction proposed by A.F. Huxley (1957). The part of the filaments shown is in the right hand half of an A band. The myosin 'side piece' (M) is capable of binding to the actin sites (A, only one shown). O is the equilibrium position of M, where there is no net force in the elastic linkages. x is the displacement of A from O.

(From A.F. Huxley, 1957.)

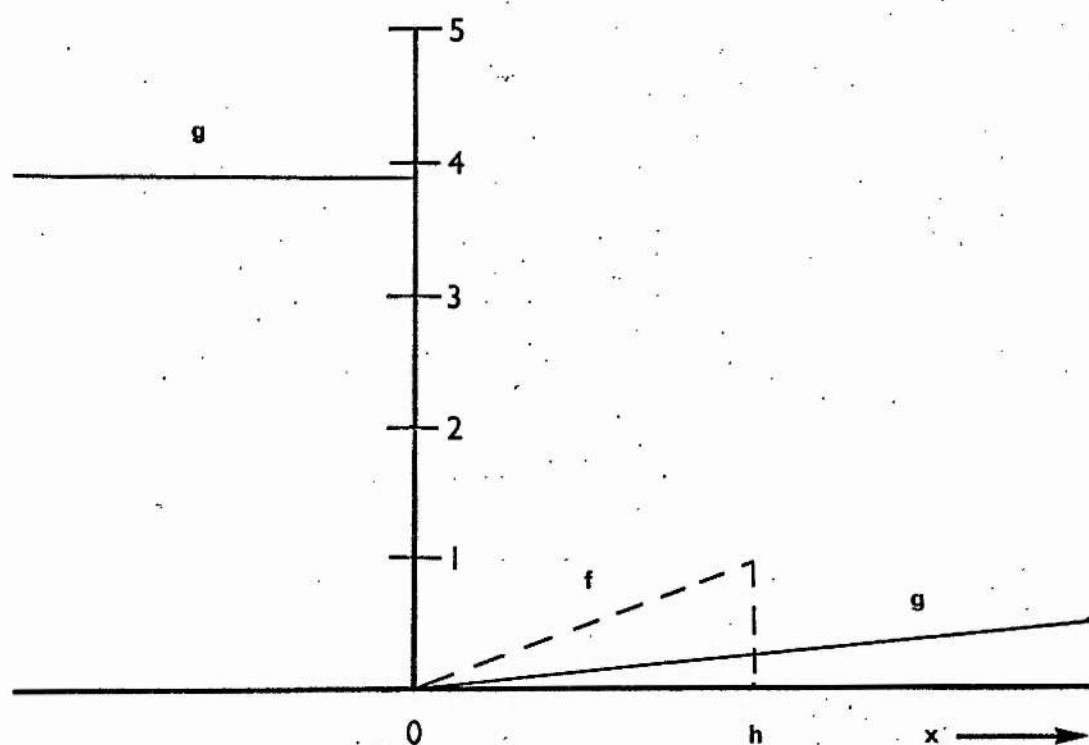


Fig. 1.3. Dependence of f and g on x , where f (broken line) is the rate constant for formation of actin-myosin cross-links and g (continuous line) is the rate constant for detachment, x is the distance of A from 0, the position where there is no net force in the elastic link. h represents the maximum value of x , at which attachment can occur. (From A.F. Huxley, 1957.)

Cross-bridge Models.

A number of models for the myosin cross-bridge have been proposed to account for the observed mechanical properties of contracting muscle, and it is of interest to compare the most important of these and to consider the experimental evidence on which they are based.

A.F. Huxley's 1957 theory. The first attempt to account for the observed physiological properties of muscle in terms of the kinetics of cross-bridge cycling was made by A.F. Huxley in 1957. He estimated the rate constants for making and breaking cross-bridges by fitting the steady state force-velocity and force-energy relations of the model to those found experimentally by A.V. Hill (1938). It was necessary to postulate a relatively small rate constant for the making of cross-bridges, so that the number formed at a given time is a function of the relative speed of sliding of the filaments. Consequently, as the load (tension) on the muscle decreases, its speed of shortening increases, in the manner observed experimentally. He made the additional assumption that one molecule of ATP is required for one cross-bridge to complete a single cycle.

The essential elements of the model are illustrated in Fig. 1.2 and the system works in the following way. Beginning from the condition in which the myosin and actin active regions (M and A), are detached: M is in a state of constant oscillation about its equilibrium position (O) under the influence of thermal agitation. If, as a result of this movement,

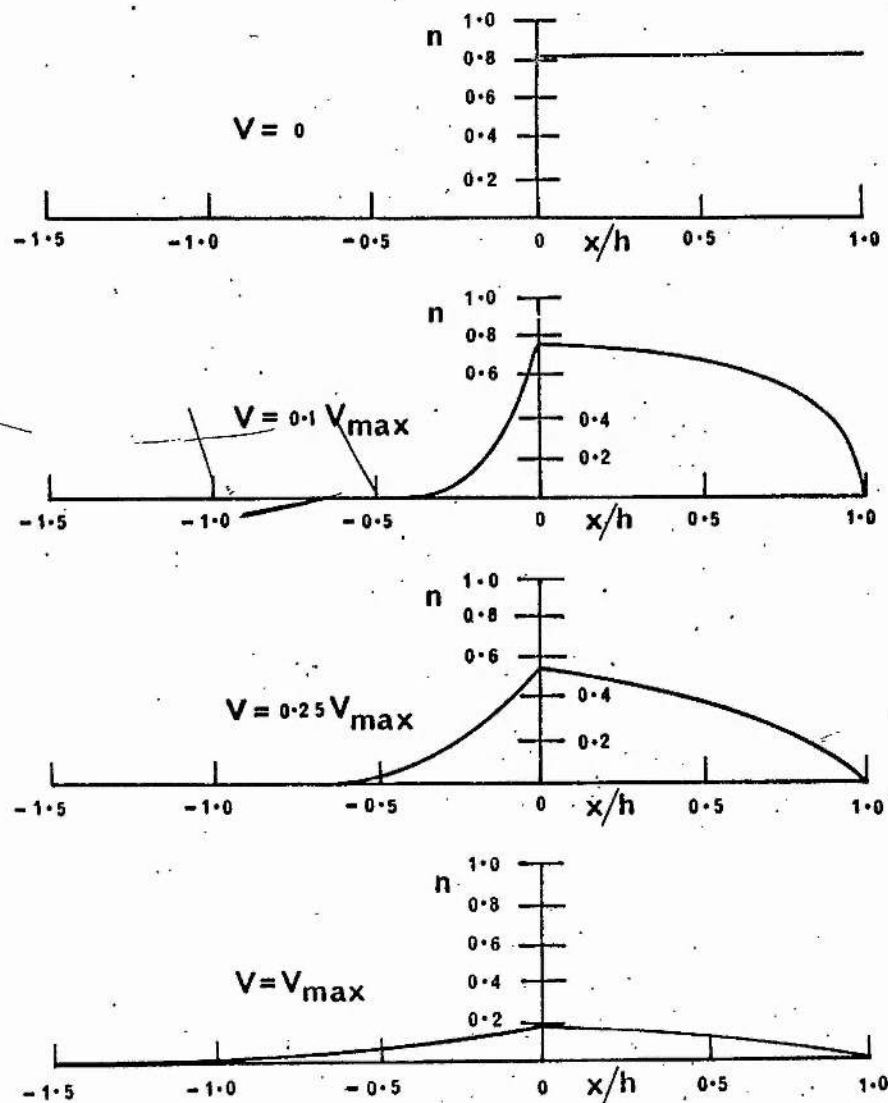


Fig. 1.4. Changes in n (proportion of sites where an actin-myosin linkage is formed), with x (position of A relative to the equilibrium position of M), for the steady state at velocities of shortening from 0 (isometric contraction) to V_{\max} (maximum speed of shortening in an unloaded, isotonic contraction). (From A.F. Huxley, 1957.)

M is brought close to A, there is a chance that the two active sites will interact and combine, and tension in the linkage connecting M to the myosin filament will be transmitted to the actin filament. This will either appear as muscle tension, or will result in a relative sliding movement of the filaments, if external conditions permit. The probability of a cross-bridge existing between the filaments at different distances, X , from O is depicted in Fig. 1.3, where f and g are the rate constants for bridge formation and breakage respectively. The AM combination occurs to the right of the point O and the tension generated in the elastic link promotes muscle shortening, so that the AM combination moves towards O. During this time there is a small chance that the cross-bridge will detach (to permit muscle relaxation when activation ceases) but when the point O is passed, g rises abruptly and the link is rapidly broken. However, at high rates of shortening, many of the links remain attached long enough for a force to be in the direction which opposes shortening. The maximum speed of shortening is reached when this force equals that generated on the other side of the point O, and overall tension is zero.

Fig. 1.4 illustrates more clearly how the model can account for the characteristic force/velocity relationship of muscle. The graphs show the proportion of A and M sites which are combined at different positions relative to the equilibrium position of the M site, over the range of shortening velocities from $V=0$ (isometric tension) to $V=V_{\max}$.

Although Huxley's 1957 theory can account satisfactorily for the

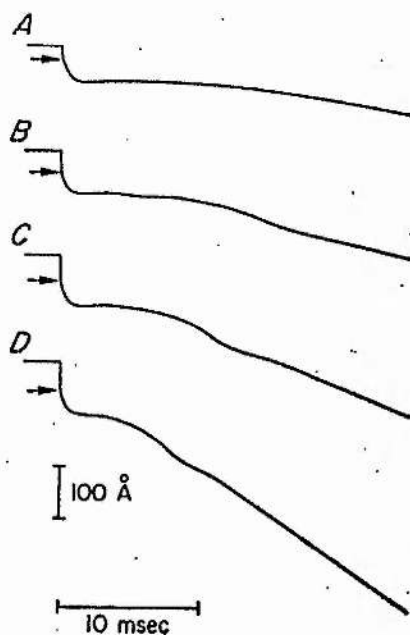


Fig. 1.5.

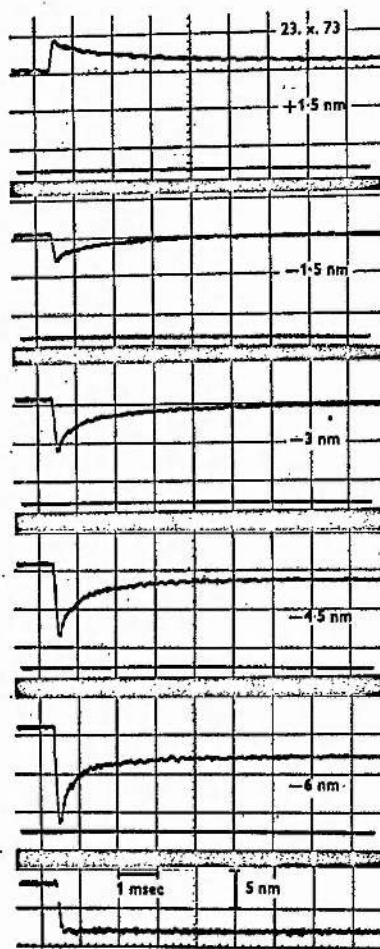


Fig. 1.6.

Fig. 1.5. Length responses to imposed 'step' reductions in load of different amplitude. The size of the initial instantaneous length change is shown by the arrow. Tension values immediately after the applied load 'step' are :-

- A - $0.5 \times P_0$.
- B - $0.3 \times P_0$.
- C - $0.15 \times P_0$.
- D - $0.01 \times P_0$. (From Julian et al., 1973)

Fig. 1.6. Group of tension 'transients' produced by 'step' changes in length. The figures on the right of each frame refer to the size of the length step. (From A.F. Huxley, 1974.)

force/velocity relationship and, with some modification, the liberation of energy under different conditions of load and speed, recent experiments have revealed muscle phenomena which cannot be accommodated so easily. These are the dynamic, or non-steady state, responses which result from rapid perturbations of length or load.

The transient mechanical behaviour of muscle. The assumption made in Huxley's 1957 theory, that tension generated in the link by thermal agitation is instantaneously transmitted to the actin filament whenever an AB combination occurs, cannot readily account for the behaviour of muscle fibres to 'step' changes of length or load.

The responses of contracting frog muscle fibres to step changes of load were investigated by Civan & Podolsky (1966) and Armstrong, Huxley & Julian (1966) and the kind of length changes they observed are shown in Fig. 1.5. The converse type of experiment was made by Huxley & Simmons (1970a, 1971a,b) in which abrupt changes of length were applied to muscle fibres and the resulting tension changes recorded. Some of their records are reproduced in Fig. 1.6. The dynamic responses of muscle fibres to a step reduction of length or load can be summarised as follows :-

- 1) During the length/tension step, a rapid, simultaneous drop of tension/shortening occurs.
- 2) This is followed in the next few milliseconds by a period of rapid early tension recovery/rapid early shortening.

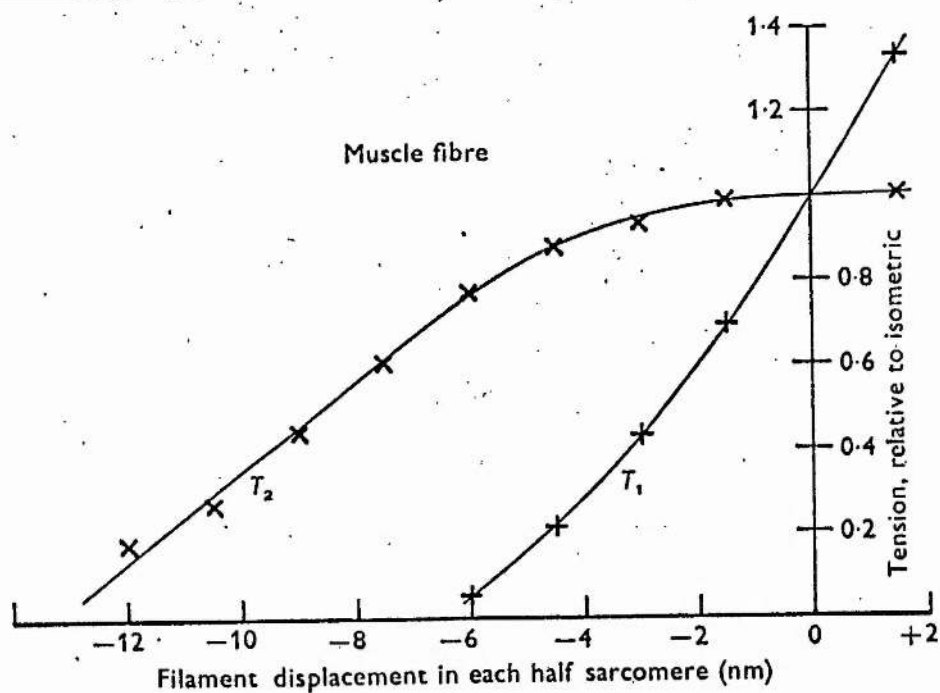


Fig. 1.7. T_1 and T_2 curves, constructed from a group of records such as those shown in Fig. 1.6. (From A.F. Huxley, 1974.)

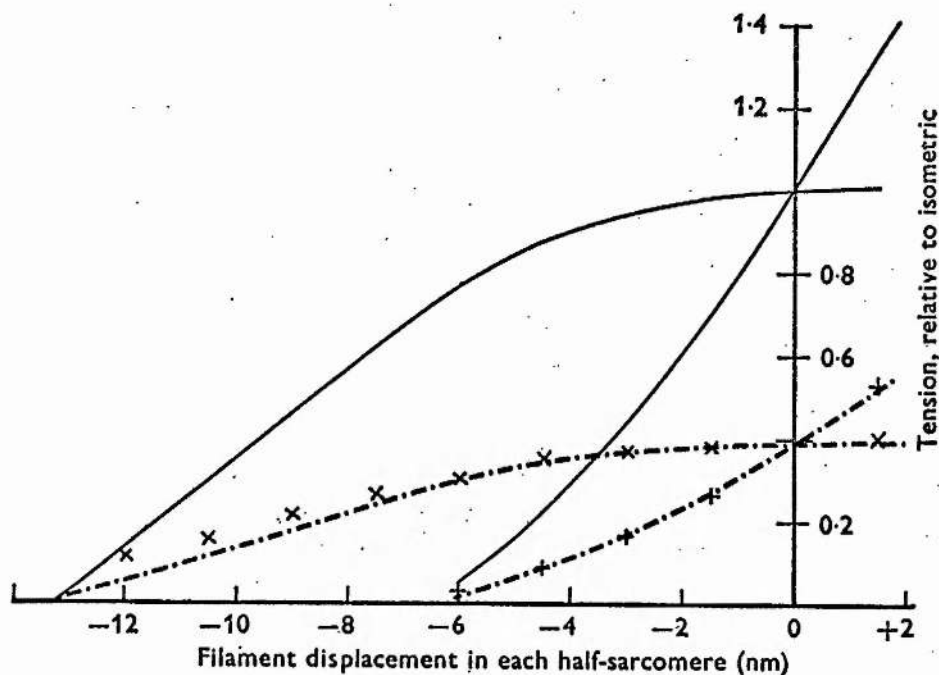


Fig. 1.8. T_1 and T_2 curves obtained from tension transients recorded from the same muscle fibre at two different lengths. The continuous line is the same as that shown in Fig. 1.7, where the sarcomere length was $2.2\mu\text{m}$. The lower symbols were derived from the fibre, stretched to a length where the sarcomere length was $3.1\mu\text{m}$. (From A.F. Huxley, 1974.)

3) During the next 5 - 20 ms., there follows a period of extreme reduction or even reversal of the rate of tension recovery / shortening speed.

4) Gradual tension recovery to P_0 / steady shortening, occurs during the remainder of the response.

Huxley & Simmons' (1971 a) tension records reveal two features of particular interest. First, tension drops abruptly during a step release to a value (T_1) which is dependent on the size of the step; and second, rapid tension recovery raises the tension level to a value (T_2) which also varies with the size of the shortening step. The way in which the values of T_1 and T_2 are influenced by the size of the length change is shown in Fig. 1.7. The application of a step increase of length produces a tension response such as the one shown at the top of Fig. 1.6, and the values for T_1 (in this case, the peak tension value) and T_2 (the tension after rapid early tension decline) may be plotted in the same way as those for releases. This yields two continuous curves, intersecting at zero length change.

Huxley & Simmons' (1970 a) initial interpretation of these observations was that the simultaneous tension drop represents an abrupt shortening of the filaments themselves, without relative sliding taking place, and that the early rapid recovery is brought about by the action of cross-bridges re-extending the filaments. An alternative explanation is that both features are properties of the cross-bridges and that filament lengths do not change appreciably, either during, or immediately

following a release. This question was quickly resolved by Huxley & Simmons (1971 a). A similar series of length steps were applied to a muscle fibre held at a longer length, where the overlap region in each sarcomere is reduced, and hence where there are fewer possible interaction sites. Fig. 1.8 shows the results they obtained. It is clear that although the shape of the T_1 and T_2 curves is not changed by the procedure, the values for T_1 and T_2 for a given length step are reduced in proportion to the reduction in the amount of filament overlap. As a result, it would be safe to assume that the observed transient effects are properties of the cross-bridges and in what follows, the compliance of the filaments and Z lines are considered small enough to be disregarded.

Interpretation of the tension responses to step changes of length. It is convenient to consider the behaviour of the muscle during each of the four stages already described, and then to compare the various explanations which have been offered to account for them :

Stage 1: Huxley & Simmons attribute the simultaneous fall of tension to a rapid change of length in an elastic component which forms part of each cross-bridge. In view of the rapidity of the event, it is suggested that no appreciable change in the number of cross-bridges (i.e. no attachment or detachment) occurs. Theoretically, no alteration in the length of any other cross-bridge component should occur during this stage, but very abrupt steps must be applied if the

changes responsible are to be separated from those thought to be responsible for the events observed during the next stage, (2).

Stage 2: The rapid, early tension recovery is to some extent predicted by Huxley's 1957 theory, because rapid shortening must result in the detachment of cross-bridges which have been displaced to a position where they develop negative tension (i.e. to the left of 0, Fig. 1.3.). However, the theory does not account for the rather abrupt transition from rapid early recovery to the more gradual recovery or reversal which is seen.

As shown in Fig. 1.7 the tension levels reached following a step change of length (T_1) and after rapid early recovery (T_2) vary with the size of the applied step. Curve T_1 shows an almost linear dependence on the amplitude of the length change, only deviating appreciably from a straight line for large releases, where the value of T_1 approaches zero. It has been shown that the more rapid the length step, the more closely the curve approaches a straight line, so that in proposing a model to fit their observations, Huxley & Simmons assumed the T_1 curve to be linear and to have a finite intercept on the displacement axis under 'ideal' experimental conditions. The curve T_2 , which shows the tension level approached during quick recovery, is concave downwards for releases and upwards for stretches, and is almost flat when the length steps are small.

Finally, the speed of rapid recovery becomes greater as the size of release increases, but less with increasing size of stretch. This is

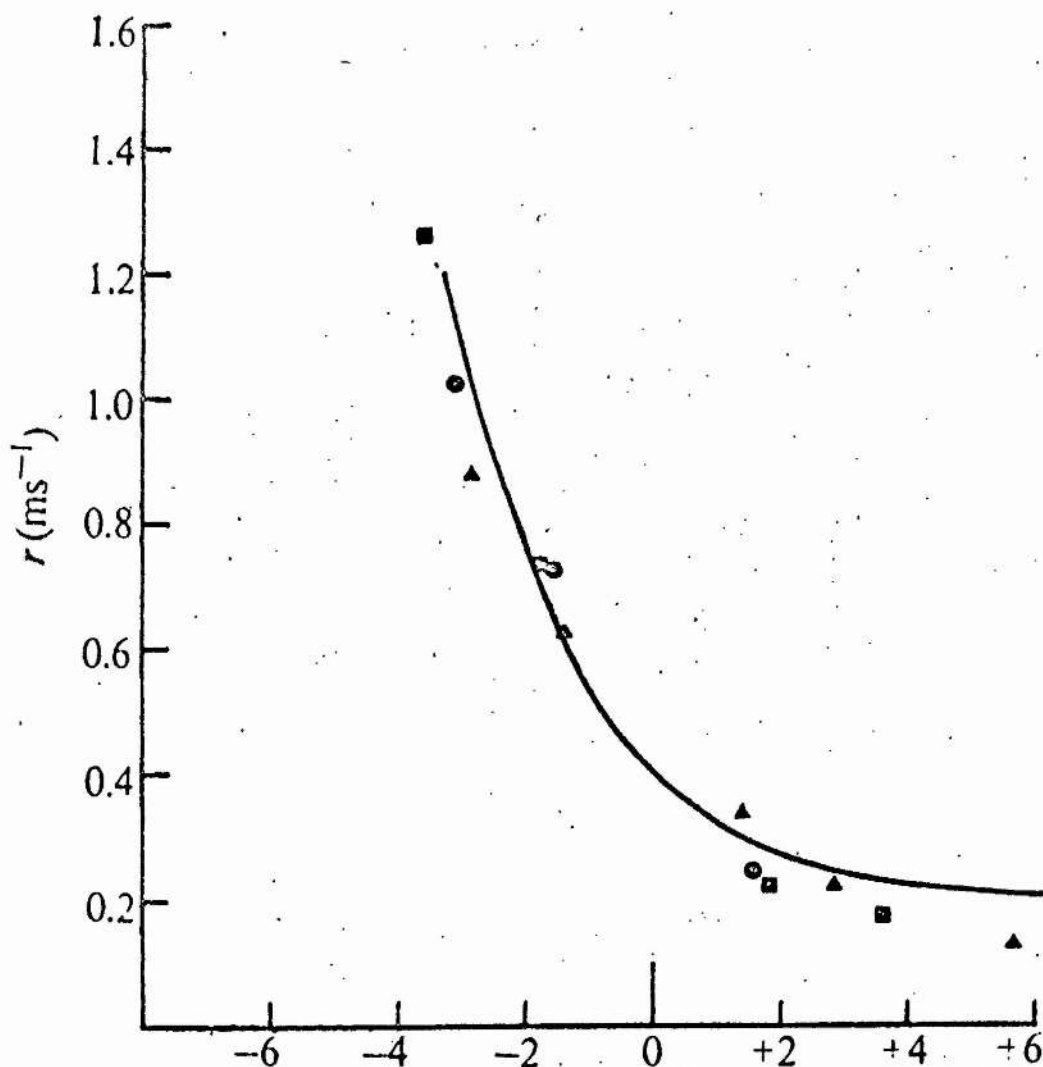


Fig. 1.9. Changes in the rate constant for the quick recovery phase, following 'step' changes in length of different size. The amplitude of the applied length changes (both stretches and releases) is given in nm per half sarcomere on the abscissa. (From Huxley & Simmons, 1973.)

clearly illustrated in Fig. 1.9 in which the rate constants for rapid recovery are plotted against the size of the length step.

Stage 3: The extreme reduction or reversal of the rate of recovery of tension during this stage is difficult to account for. However, if some modifications are made to the values of the rate constants for cross-bridge attachment and detachment (f and g in Huxley's 1957 theory) it is possible to achieve a condition in which a delayed fall of tension would occur following release. If the value of g increases after a shortening step, while f does not have time to change, a net decline in tension will result, and any influence which tends to delay cross-bridge reattachment will make the effect more pronounced, and tension will fall further before stage 4 returns it to the isometric level.

Stage 4: During this stage, cross-bridges undergo a number of cycles of detachment and reattachment at positions further along the filament, and so muscle tension returns to the same level as before the applied length change.

Huxley & Simmons' cross-bridge model. To account for the transient behaviour of muscle, Huxley & Simmons made two basic assumptions about the cross-bridges.

(A) The movement of a cross-bridge while it is attached to the actin filament takes place in a number of discrete steps, from one to the next of a series of stable positions with progressively lower potential energy.

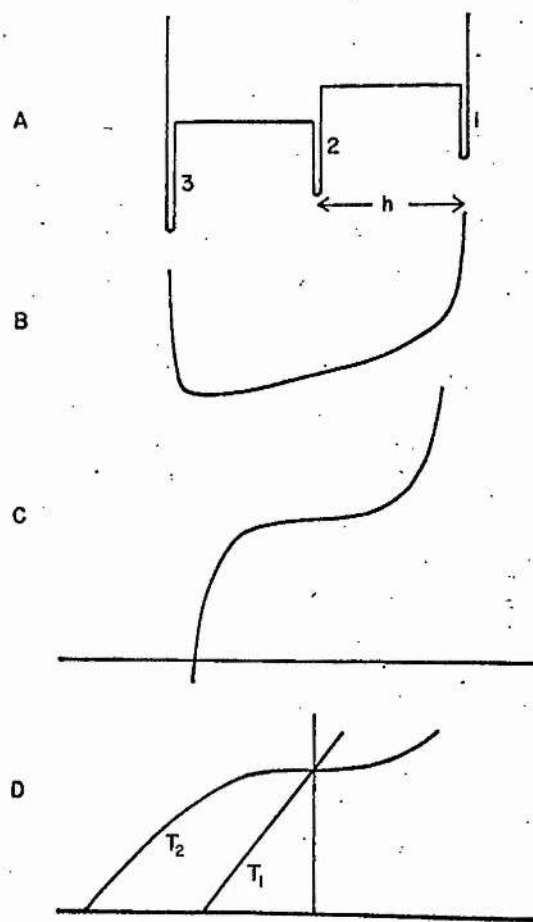


Fig. 1.10. A. Diagram of the potential energy in the force generating element (1), assuming 3 stable positions. Abscissa is the length of element 1, L_1 .

B. Time average of the potential energy curves shown in Fig.1.10.A, plotted against the time average of L_1 .

C. The slope of B, which represents the tension generated by the tendency of the element to spend more time in positions of lower potential energy.

D. T_1 , is the assumed linear, length / tension relation of elastic element ii. T_2 , is the length / tension relation obtained by combining, in series, the T_1 line and the curve C.

(From Huxley & Simmons, 1973.)

(B) There exists within each cross-bridge an instantaneous elasticity which permits it to move from one stable position to the next without simultaneous displacement of the actin and myosin filaments relative to one another.

The structures responsible for the above changes must be thought of as being in series and thus relative movement of the filaments must result in a change in the length of each. The cross-bridge can therefore be depicted by i) an element which generates force as a result of its tendency to move to positions of lower potential energy, the movement taking place at a finite rate, and ii) a passive element with instantaneous elastic properties, lying in series with the force generating element.

When considered in conjunction with assumptions A and B, such a model shows the kind of nonlinear responses to step length changes observed in experiments with real fibres (Huxley & Simmons, 1971 b). The stable positions which the force generating element (i) is capable of adopting can be represented in the form of a potential energy diagram. Fig.1.10.A shows the potential energy in the element in each of the stable positions it is capable of adopting. Under the influence of thermal agitation the cross bridge jumps between one position and another, the amount of time spent in each being dependent on the tension in ii), the instantaneous elastic connection. When the time average of the potential energy in element i) is plotted against its length a curve of the form shown in Fig.1.10.B is obtained. The change in

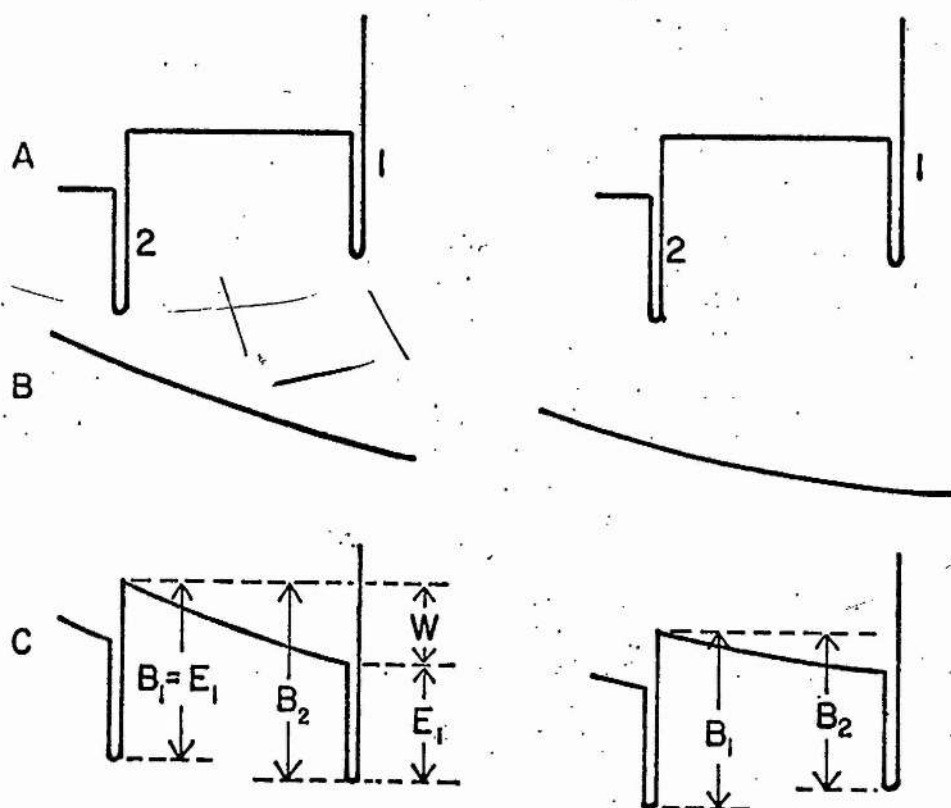


Fig. 1.11. The dependence of the rate constant for early recovery on the size of the step.

A. Potential energy diagram for positions 1 and 2 of Fig. 1.10.A

B. Potential energy / length diagram for the instantaneous elastic element.

C. Sum of A and B, giving the total potential energy in the cross-bridge as a function of L_i , (in the case where the total length of the cross-bridge is constant i.e. no relative movement of the filaments). B_1 and B_2 refer to the activation energies for the transition from position 2 to 1 and 1 to 2 respectively. W is the energy stored in the elastic element and E is the depth of the potential energy well, which constitutes a stable position.

(From Huxley & Simmons, 1973.)

slope of this curve represents the length/tension characteristics of the force generating element, Fig. 1.10.C. Since it is in series with an instantaneous elastic element (assumed to be Hookean), the length/tension diagram for both the cross-bridge elements (i and ii) is given by the curves T_1 and T_2 in Fig. 1.10.D, which resemble closely the experimental curves obtained with muscle fibres.

Finally, the dependence of the rate constant for rapid recovery on the size of the length step can be explained by the model. Consider the stable states 1 and 2, where the rate constant for rapid recovery is proportional to the size of the potential energy step required in going from state 1 to state 2. Fig. 1.11 shows that the size of this step is influenced both by the depth of the energy well which constitutes the stable position and by the energy developed in the elastic link in making the transition from 1 to 2. Clearly the depth of the well does not alter during stretch or release, but the energy in the link is dependent on its length. Consequently, the activation energy for the transition from 2 to 1 is unaffected by the length change, but that from 1 to 2 is decreased by a release and increased by a stretch. Thus a step decrease in length increases the rate of rapid recovery and a step increase in length decreases it, as is seen in actual muscle fibres.

The Podolsky - Nolan cross bridge model. In Huxley's 1957 theory it is implied that the rate constant for the attachment of cross-bridges (f) is relatively small, and thus, as the speed of muscle shortening

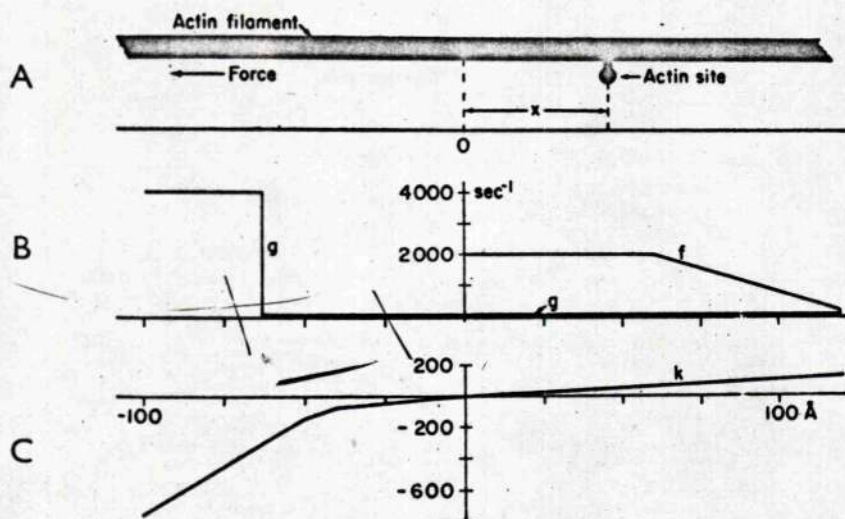


Fig. 1.12. A. Diagram of Podolsky & Nolans' system, in which x and 0 are the same as in Fig. 1.2.

B. Probability of making a bridge, f and breaking a bridge, g , for different values of x . Compare with Huxley's Fig. 1.3.

C. Dependence of the mean force (k) on x .

The ordinate scales in B and C may be treated as arbitrary.

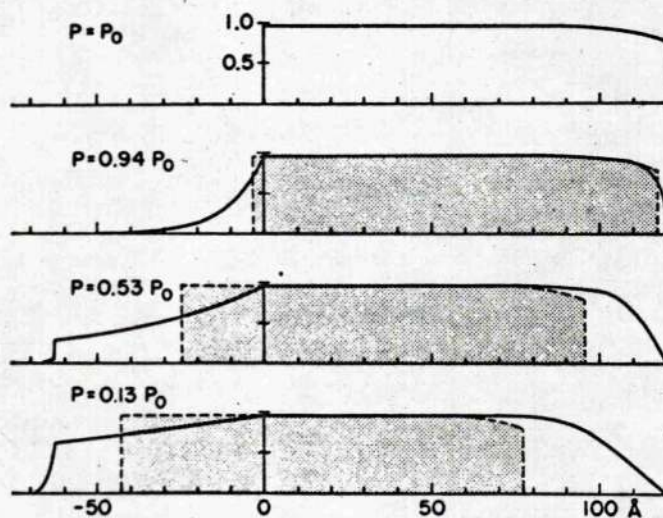


Fig. 1.13. Variation in the distribution of cross-bridge lengths during contraction, for various force steps. Tension immediately after each step is given on the left. Areas enclosed by continuous lines are the steady state distribution of cross-bridge lengths. Shaded areas should be disregarded for the purpose of this discussion. (From Podolsky & Nolan, 1973.)

increases, a greater proportion of the cross-bridges are unable to attach and do not contribute to the overall muscle tension (Fig. 1.4). Experiments made by Podolsky (1960) and Civan & Podolsky (1966), in which step reductions of force produced velocity transients similar to those reported by Armstrong, Huxley & Julian (1966), led Podolsky & Nolan (1971) to modify Huxley's original (1957) theory in a way which accounts for the transient behaviour. It was necessary to adjust the values of f and g , the rate constants for formation and detachment of cross-bridges respectively. Fig. 1.12 shows how the rate constants f and g change as the actin active site moves to the right and left of the position (O) at which the net force in the linkage is zero. It can be seen that g remains small for all positions of the site to the right of a point 6.3 nm to the left of O, beyond which it increases abruptly. (In contrast, the value of g in Huxley's 1957 theory rises to a high level at O.) This ability of cross-bridges to retain contact under a large negative force is an important feature of Podolsky & Nolans' explanation of the force/velocity relationship of muscle. Fig. 1.13 illustrates the distribution of cross-bridge lengths which they predict following various step changes of load, permitting shortening at different speeds. Under isometric conditions, Fig. 1.13 ($P = P_0$), all cross-bridges are in positions to the right of O and are thus under positive tension, but with increasing speed of shortening, the cross-bridge population shifts to the left so that some are under negative tension and the net tension level is reduced. Ultimately, when the force step reduces tension to zero, the

force contribution from cross-bridges to the left of O is equal to that from those on the right.

This whole argument rests on the assumption that cross-bridge cycling is very rapid and that, regardless of the speed with which the filaments move relative to one another, the probability of attachment is so high that when an actin site passes a myosin projection, a cross-bridge is almost invariably formed. This can then account for the high probability of cross-bridges existing over the 6.3 nm range to the left of O, even at high velocities of filament movement.

Podolsky & Nolan propose an explanation for the transient mechanical properties of muscle which differs considerably from that of Huxley & Simmons. Their account of the events which occur during and immediately after a step reduction in muscle length can best be summarised by a cross-bridge distribution diagram of the kind shown in Fig. 1.14. Before the step is applied, the distribution is that which corresponds to the steady isometric tension (Fig. 1.14. i). The application of a length step displaces the whole population to the left which results in a drop of tension as already described (Fig. 1.14. ii). Finally, cross-bridge turnover, and the attachment of some of those cross-bridges which previously had no site for attachment in the isometric state, brings about a redistribution of the cross-bridge population and an increase in tension (Fig. 1.14. iii).

The principal differences, then, between this model and that of Huxley & Simmons may be summarised as follows :-

1) A small shortening step causes the cross-bridges to change, almost instantaneously, from a condition in which they exert considerable force (isometric tension) to one in which they exert little force (T_1), by a) shortening of the instantaneous elastic element in each cross-bridge (Huxley & Simmons); or b) redistribution of the whole cross-bridge population to a position where the net force is greatly reduced (Podolsky & Nolan).

2) Immediately following the shortening step, tension is partially regenerated by a) stepwise movement of the force generating element in each cross-bridge, re-extending the instantaneous elastic element, without appreciable detachment or attachment of cross-bridges (Huxley & Simmons); or, b) redistribution of the whole cross-bridge population by a process of rapid cycling to a position where the net force is increased, and by the attachment of those cross-bridges which, due to unavailability of actin sites, were previously unattached (Podolsky & Nolan).

Clearly, this last statement (2b) implies that the total number of attached cross-bridges ought to be greater following rapid release than at peak isometric tension, and therefore the muscle should show a higher stiffness. Ford, Huxley & Simmons (1974) have demonstrated that this is not the case. They applied a quick release to a tetanised fibre, allowed rapid recovery to occur, and then applied a step increase in length. The tension generated by the stretch was marginally less than that produced by the same length change applied at the peak of

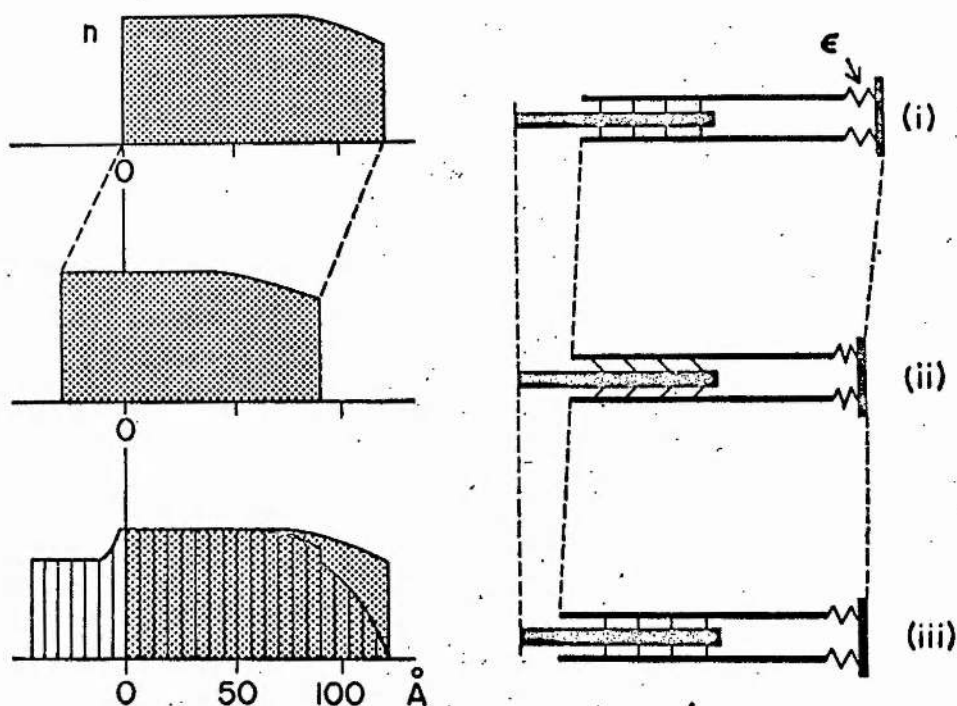


Fig. 1.14. A means of calculating tension redevelopment, following 'step' changes in length. Distribution functions (left, shaded areas) and filament configurations (right) at :

- i) the initial length, immediately before the tension step ;
- ii) just after the tension step ;
- iii) after tension has redeveloped; the lined area shows the distribution at a stage, intermediate between ii and iii, while tension redevelopment is occurring.

E is a passive elastic element, lying in series with the filaments.
(From Podolsky & Nolan, 1973.)

an isometric tetanus, and so it must be concluded that no increase (and possibly a small decrease) in the number of attached cross-bridges takes place during the early recovery phase.

It is difficult, in the light of this result, to see how Podolsky & Nolans' model, as it stands, can provide an acceptable explanation of rapid early recovery; this does not necessarily imply that Huxley & Simmons' model is the only explanation of the phenomenon, or that a model which permits some degree of cross-bridge detachment and reattachment, is ruled out.

A model for muscle contraction by Julian, Sollins & Sollins. A recent model based on the observations and interpretations of Huxley & Simmons (1971 b) has been presented by Julian, Sollins & Sollins (1973). Its fundamental proposals are that the attachment and force generating steps are completely separate, in that there is no force in the link when the cross-bridge first attaches to the actin filament. They suggest that force is generated following attachment by an abrupt conformational change or 'flip' of the force generating part of the cross-bridge. This is capable of attaching to the thin filament at only one (a) of two stable positions and only when there is no tension in the elastic link of the cross-bridge. Once attached, a cross-bridge may 'flip' reversibly to the second stable state (b) causing extension of an elastic link and the development of tension. In addition, it is only possible for detachment to take place from the b state.

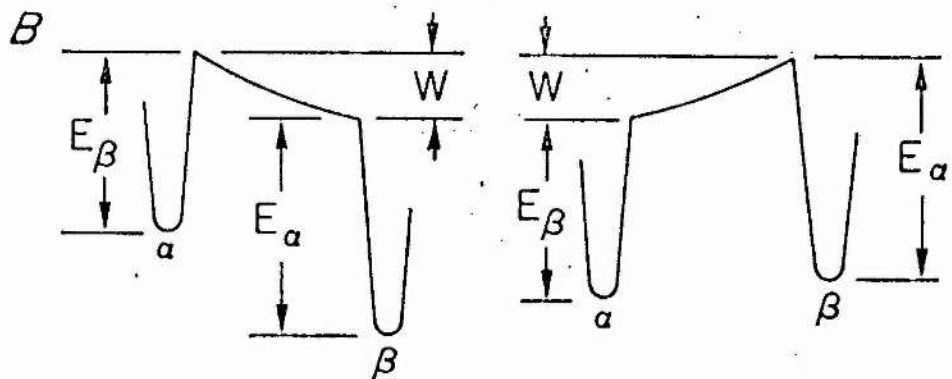


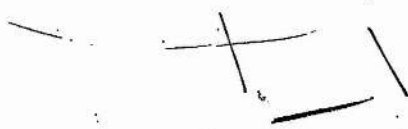
Fig. 1.15. Potential energy diagram for the force generating elements, analogous to Fig. 1.11.C, in Huxley & Simmons scheme. The energy wells are labelled α and β , corresponding to the two stable states a and b, proposed in this model. As in Fig. 1.11.C, the work term for extension of the elastic link is only effective, when it is positive, in opposing the 'flip' from a to b, and when it is negative, in opposing the 'flip' from b to a. (From Julian et al., 1973.)

How well does the model predict the behaviour of real muscle fibres subjected to abrupt length changes? The dependence of the rate constant for rapid recovery on the size of the length step can be explained by an argument similar to that put forward by Huxley & Simmons. The probability of a 'flip' from the unloaded state (a) to the loaded state (b) is dependent on the activation energy for the step, which is given by the depth of the energy well which constitutes the stable position and a term for the work (W) required to extend the elastic link. It can be shown (Fig. 1.15) that only when it is positive does the work term influence the activation energy for the step from a to b. Conversely, only when it is negative does it influence the step from b to a. Consequently, when W is made more positive, following an applied stretch, the activation energy for the force generating step a to b is increased and when it is made less positive, during a release, it is reduced. Since the rate constant for the step a to b is inversely related to the exponential function of the activation energy, the rate constant for rapid recovery would be predicted to show the same (roughly exponential) dependence on the size of the step, as is found experimentally.

The model does not permit the existence of attached cross-bridges in any state other than a and b for any appreciable length of time, and so the steady isometric distribution of cross-bridges is depicted by two spikes, one representing the component of the cross-bridge population in the a state, where link extension is zero, and another

representing the component in state b, where the link is extended.

Movements of the filaments will result in both population spikes being spread out either towards smaller link extensions, in the case of shortening, or towards greater link extensions, in the case of the muscle being stretched; the degree of spreading is dependent both on the speed of movement and on the rate constants for cross-bridge formation and detachment.



A structural basis for cross-bridge models.

Biochemical studies of the myosin molecule have shown it to be a rod shaped, two chain α -helix, about 150 nm in length, with a globular region at one end (Lowey, Goldstein, Cohen & Luck, 1968; Lowey, Slayter, Weeds & Baker, 1969). The actin binding sites of the molecule and its ATPase activity have been shown to be associated with this globular region. At two points along its length the myosin molecule is highly susceptible to the action of proteolytic enzymes. Trypsin has the effect of cleaving the molecule at a position about 60 nm from its globular end, known as the heavy meromyosin end (HMM), leaving about 90 nm of helical chain, the so called light meromyosin (LMM), remaining. LMM is capable of aggregating under physiological conditions into long filaments, which has lead to the conclusion that it forms the 'back-bone' of the intact myosin filament. HMM can be further split by papain, which detaches the globular fragment of HMM, known as the S_1 subunit. The remainder of the molecule, the S_2 subunit, resembles LMM structurally but it does not form aggregates, either on its own or with light meromyosin. This property suggests that in the intact myosin filament this part of the molecule is not bound tightly, enabling the HMM component to hinge outwards towards the actin filament (Lowey, Slayter, Weeds & Baker, 1969).

Evidence for this is found in the equatorial X-ray diffraction pattern. The relative intensity of the two principal reflections produced by the

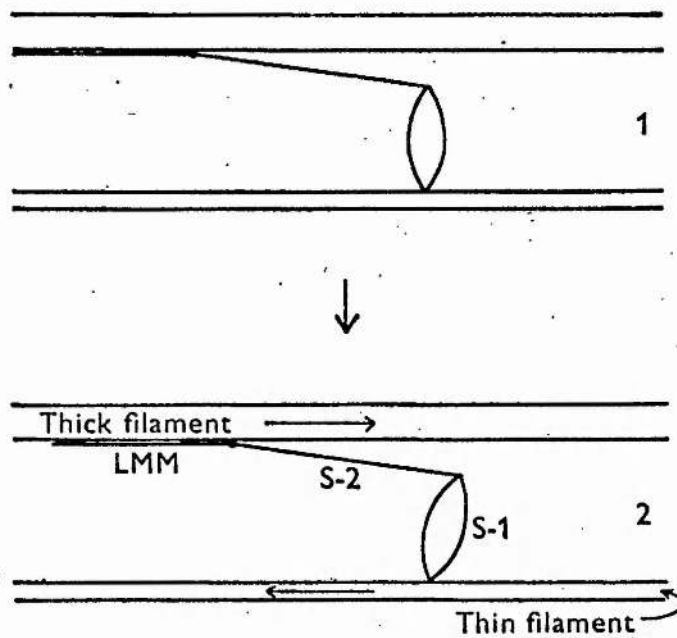


Fig. 1.16. A model of the cross-bridge by H.E. Huxley (1969). Relative movement of the filaments results from a tendency for the the S_1 subunit of HMM to undergo a change of orientation, while attached to the thin filament.

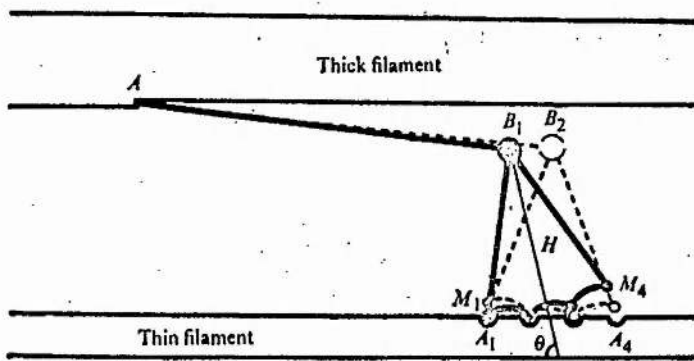


Fig. 1.17. Diagram of the cross-bridge, incorporating the features used by A.F. Huxley & Simmons (1971) as a structural basis for their theory. The myosin head (H) is connected to the thick filament by an undamped elastic link, AB. Solid lines show the head position with sites M_1A_1 and M_2A_2 attached; broken lines show position with M_2A_2 and M_3A_3 attached.

filament lattice reverses, which suggests that a large mass of material, normally associated with the thick filaments in resting muscle, is transferred to the actin filament when a muscle goes into rigor. The most probable explanation for this change is that when a muscle is activated, the S_2 -HMM component of the myosin molecule swings outward from the filament, carrying with it the S_1 subunit, thereby allowing it to engage with an active site on the actin filament. By this means, the cross-bridge is capable of forming a linkage over a wide range of filament spacings (4.0-11.0 nm) and the S_1 subunit is always 'offered-up' to the actin filament at the appropriate angle.

H.E. Huxley's (1969) model of a cross bridge incorporates such a flexible linkage. He proposed that the force generating potential of the cross-bridge resides in a tendency for the S_1 subunit to alter its angle of attachment while still in contact with the actin filament, and that the resulting force is transmitted to the myosin filament through the inextensible S_2 subunit (Fig. 1.16). This was used by Huxley & Simmons (1971a) as the basis for their model of the cross-bridge. A number of modifications to H.E. Huxley's model to render it compatible with their experimental findings, were necessary :


- 1) The limited number of stable positions required for Huxley & Simmons' model corresponds to the different angular orientations of the myosin head relative to the actin filament.
- 2) Any two consecutive sites on the myosin head (M_1, M_2, M_3, M_4)

when combined to the two corresponding sites on the actin filament (A_1, A_2, A_3, A_4), constitutes a stable linkage.

3) The elastic element of the cross-bridge is probably located in the S_2 subunit which connects the myosin head to the thick filament.

Fig. 1.17 is a diagrammatic representation of H.E. Huxley's (1969) model incorporating A.F. Huxley & Simmons' modifications. Although the AB link is thought to be the most likely site of the instantaneous elasticity of the cross-bridge, it should be pointed out that the head itself may be extensible, or that it is a property of the region where the head interacts with the actin filament. The site of the stepwise movement of the cross-bridge is also uncertain and may be a property of the head or of the actin active site.

The model shown in Fig. 1.17 affords a structural basis for Huxley & Simmons' proposals and with a modification to the number of stable positions, the model of Julian et al also. Since Podolsky & Nolan do not propose any stepwise movement of the cross-bridge, a more simple structural model, like H.E. Huxley's original one of 1969, could account for their interpretation of muscle transients.



Scope of the present study.

The work to be described is concerned with the effects of servo controlled length changes (stretches and releases) on the tension produced by contracting frog's muscle. It differs from recent work of this kind in two important respects. First, relatively slow stretches and releases were employed; and secondly, movements of the actin and myosin filaments were monitored simultaneously with muscle tension by cine photography of laser diffraction spectra produced by the sarcomeres. It will be seen that meaningful results can be obtained only when consideration is given to the question of how much of the external length change applied to the ends of the muscle is absorbed by the sarcomeres. The alternative approach to the problem, that of length-clamping the sarcomeres (eg. by means of a spot-follower device like that used by Gordon, Huxley & Julian, 1966b) and of studying the tension responses from controlled perturbations of sarcomere length was not used, because it is technically much more difficult with a whole muscle. Some consideration is given later (Chapter VIII; Discussion) to a device which might be gainfully employed in future work with whole muscles, using a photoelectric positional detector to monitor continuously movements of the diffraction spectra, incorporated in a negative feed-back circuit to control the displacement transducer.

The results have provided information which permits some specific conclusions to be reached concerning the physical properties of the cross-bridges and some speculative suggestions concerning the structure of

the actin active regions. In addition, they offer important clues about the nature of the temporary bonds which must be formed when actin and myosin interact during contraction.

Preliminary accounts of some aspects of the work have been presented to the Physiological Society; Flitney & Hirst (1974), Flitney & Hirst (1975a, b), Flitney, Hirst & Stephens (1975).

CHAPTER II

MATERIALS AND METHODS.

Sartorius muscles of the frog Rana temporaria were used in most of the experiments. Frogs were obtained from Gerrard and Haig Ltd. and kept at 4°C for several days before dissection. Diseased animals were removed from the tank and were not used in the experiments.

Bathing solution. A solution with the following composition was used (mM) : Na Cl, 115; K Cl, 2.5; Ca Cl₂, 1.8; Na HCO₃, 5.0 ; pH 7.3. The solution was oxygenated continuously throughout the experiments.

Stimulation. Muscles were stimulated by passing current through two parallel plate platinum electrodes of dimensions 4 cm x 0.5 cm, positioned on either side of the muscle. Square pulses, at an intensity of 12 V.cm⁻¹ were used. The duration of each pulse was 0.5 ms (single shocks) and 0.1 ms (tetanic stimulation). The stimulation parameters were chosen to comply with the recommendations of Rudel & Taylor (1969). The frequency of stimulation varied from 15 - 100 Hz over the temperature range from 0°C - 23°C and the polarity of the electrodes was reversed with alternate shocks to minimise polarisation effects. At least ten minutes recovery time was allowed between successive tetani and under these conditions no deterioration in the performance of the muscle occurred during the experiments.

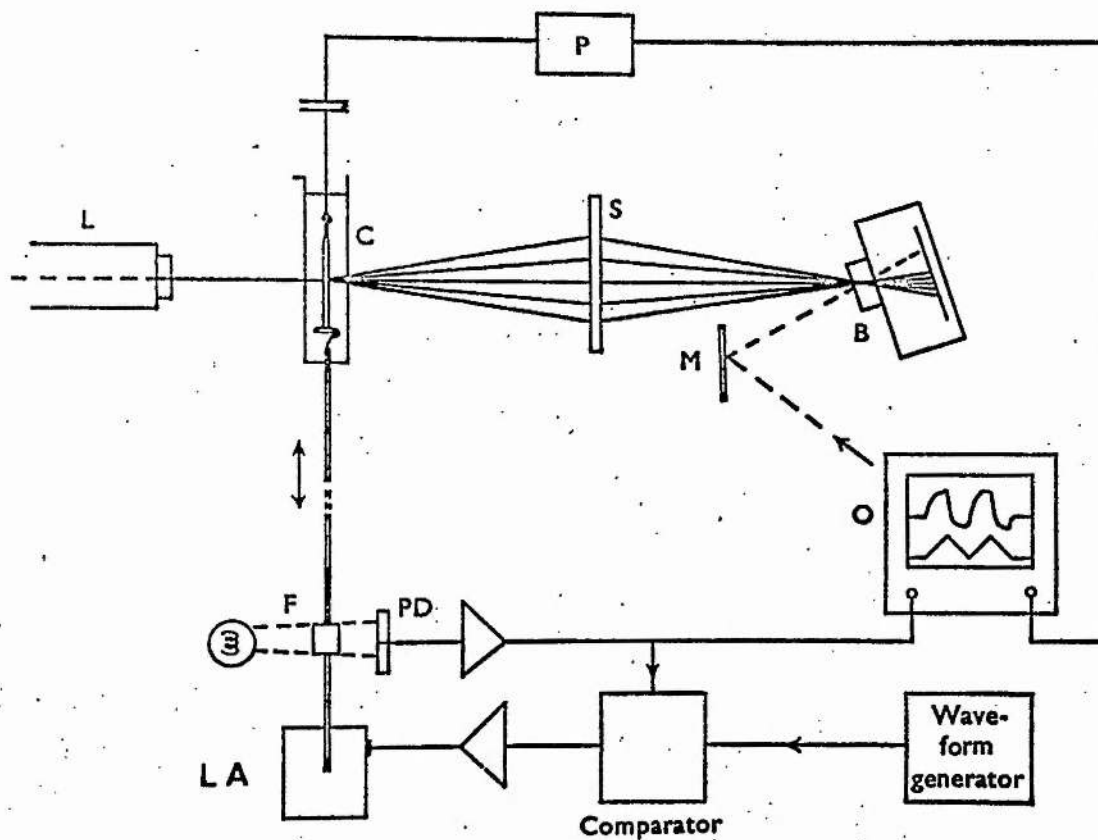


Fig. 2.1. Schematic representation of the apparatus. P, tension recorder; C, muscle chamber; S, screen; B, Bolex H 16M cine-camera; M, mirror; PD, photoelectric displacement sensor; F, vane to interrupt light beam; L, He-Ne laser; LA, vibrator unit; O, oscilloscope.

Apparatus

Muscles were suspended vertically in a narrow, glass-sided chamber containing Ringer's solution, (Fig. 2.1). The tibial tendon was attached by a fine gold plated chain to a tension recorder and the pelvic end of the muscle, retaining a small piece of pelvic bone, was held in a loop formed at one end of a platinum rod. The rod was connected at its lower end to an electromagnetic displacement transducer. Cooling of the chamber was effected by a thermoelectric module (type 12-15 G, De La Rue Frigistors Ltd.) clamped to the side of the chamber. The temperature of the bathing solution was measured continuously throughout the experiment by means of a thermocouple positioned close to the muscle; in all experiments, temperature was maintained at $0 \pm 0.1^\circ \text{C}$ unless otherwise stated. Thorough mixing of the solution was achieved by bubbling oxygen through the chamber.

Length changes. Changes of muscle length were produced by a moving coil electromagnetic unit (Ling-Altec vibrator, model 201), controlled by a servo-amplifier incorporating positional and velocity feed-back. Displacement was monitored by a photo-electric device, comprising a light source, a vane attached to the platinum rod and two silicon photodiodes, (Ferranti, type MS 1AE). The system was driven by a wave-form generator (Servomex LF 141), permitting voltage ramps of variable speed and amplitude to be applied to the length transducer. Linear length changes of up to 1.5 mm could be made in less than 10 ms.

Tension recorder. A variable capacitance gauge similar to that described by A.F. Huxley & Simmons (1968) was used to record muscle tension. The natural frequency of the recorder was approximately 2 k Hz and the compliance of the whole system was $0.1 \mu\text{m} \cdot \text{mN}^{-1}$. The output of the capacitance bridge amplifier was displayed on one channel of a dual-beam storage oscilloscope (Tektronix 5103 N); the applied length change, as recorded by the displacement monitoring device, was displayed on the other channel.

Laser diffraction system. Measurement of sarcomere lengths. The characteristic banding pattern of vertebrate skeletal muscle, produced by alternate regions of relatively high (A band) and low (I band) refractive index, causes a muscle to act as a diffraction grating (Sandow, 1936a). The diffraction pattern produced when a parallel beam of light passes through a muscle may be used to measure the mean repeat distance between the I bands, and hence the sarcomere spacing. Sarcomere length (S) may be calculated from the relationship $S = n \lambda / \sin \theta$, where n is the order of the diffraction line, λ , the wavelength of the light and θ is the angle between the zero and n^{th} order lines. The most distinct patterns are produced by coherent, monochromatic light and so a laser was used in all experiments. Muscles were illuminated with a continuous wave Helium - Neon laser (Metrologic) with a power output of 3 mW; the beam diameter was about 1 mm. Diffraction patterns were displayed on

a screen and photographed at 64 frames per second with a cine camera (Bolex H 16 mm). Kodak 4X film was used. A system of mirrors enabled the oscilloscope display of muscle tension and applied length changes to be photographed simultaneously. A diagram of the optical system is shown in Fig. 2.1. The technique permitted muscle tension, overall muscle length and mean sarcomere length (within the area illuminated by the beam) to be recorded with a time resolution of approximately 15 ms. The diffraction spectra from individual frames of the cine film were scanned with a Vickers Instruments (M 85) microdensitometer and the density profiles obtained were displayed on a chart recorder. Traces produced by this method show sharp peaks, corresponding with the zero and first order diffraction lines (Fig. 3.2). Changes in sarcomere spacing of $\pm 0.2\%$ could be detected, which is equivalent to a relative displacement of the thick and thin filaments of ± 2.5 nm.

Two synchronised Devices digitimers (type 3290) were used to co-ordinate events.

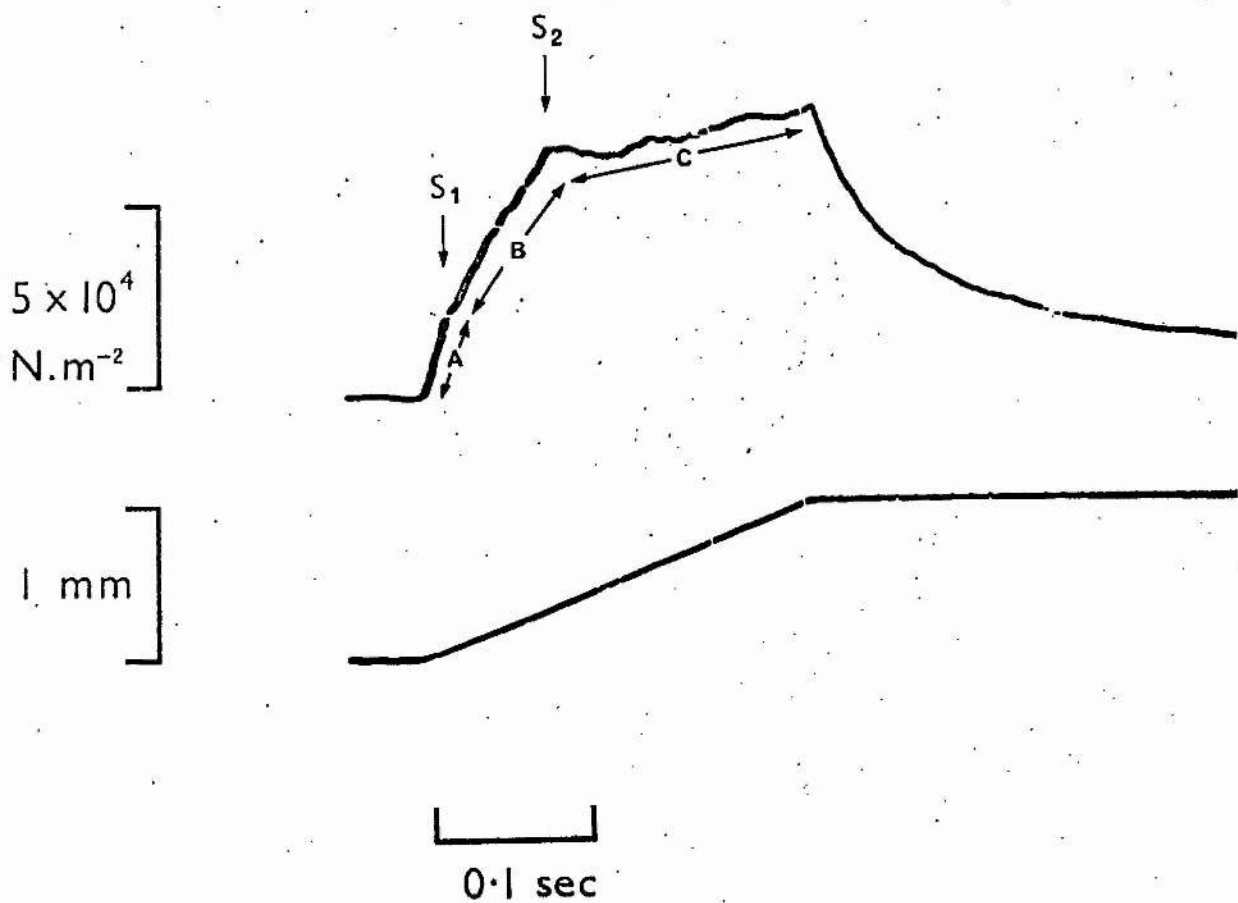


Fig. 3.1. Oscilloscope traces of a linear 'ramp and hold' stretch of $1060\mu\text{m}$ (lower trace), at a velocity of 4.24 mm.s^{-1} , during the plateau of an isometric tetanus. The characteristic form of the tension response (upper trace), showing inflections at the points S_1 and S_2 .

CHAPTER III

TENSION CHANGES AND SARCOMERE MOVEMENTS DURING RAMP AND HOLD STRETCHES OF LARGE AMPLITUDE.

Part one. Tension responses.

Characteristic form of the tension record. Fig. 3.1 is a typical record showing the non-linear form of the tension increment produced by a ramp and hold stretch of $1060\ \mu\text{m}$ (velocity, $4240\ \mu\text{m}\cdot\text{s}^{-1}$) applied to a tetanically stimulated muscle. The muscle was set up in the chamber at its rest length ($28\ \text{mm}$) and the temperature was maintained at 2.5°C .

Three distinct phases can be seen in records of this kind :

- 1) An early phase (A) where tension rises steeply and in a linear fashion, for muscle extensions of up to $40 - 45\ \mu\text{m}$.
- 2) An intermediate phase (B) for extensions greater than $40 - 45\ \mu\text{m}$ and less than $300 - 350\ \mu\text{m}$, during which tension rises less steeply than in phase A.
- and 3) A third, more variable phase (C) where tension may actually fall, or at best, show only a small increase.

The points designated S_1 and S_2 in Fig. 3.1 serve to delimit these three phases: S_1 marks the transition from phase A \rightarrow B and S_2 the transition from phase B \rightarrow C.

It will be seen later that the exact form of the response, in particular

the tension held by the muscle at the points S_1 and S_2 , varies with the speed of stretch. It is sufficient for the present to note that at the temperature used in the experiment of Fig. 3.1, a stretch velocity of 4.24 mm.s^{-1} is in the range (above 3.8 mm.s^{-1}) where the form of the response is largely independent of the speed of stretching.

The amount of muscle extension to S_1 and S_2 can be used to estimate the relative sliding movement of the filaments at the limits of phases A and B, assuming that these amounts of extension are wholly accounted for by uniform extension of the sarcomeres. The increase in length of each half sarcomere is equivalent to the longitudinal displacement of the filaments. Consider the record of Fig. 3.1. The initial muscle length was 28 mm or $2.8 \times 10^4 \mu\text{m}$. The amounts of extension required to reach S_1 and S_2 were $42 \mu\text{m}$ and $330 \mu\text{m}$ respectively, or 0.15% and 1.2% of the total muscle length. If all of this was transmitted to the sarcomeres their length would increase by $0.0036 \mu\text{m}$ up to S_1 and by $0.029 \mu\text{m}$ up to S_2 , which is equivalent to a sliding movement of the actin and myosin filaments of 1.8 nm and 14.5 nm respectively.

The results for several records analysed in this way give the following average values:

filament sliding up to S_1 :- 1.86 ± 0.05 (1 S.D.; $n = 6$) nm.

filament sliding up to S_2 :- 16.50 ± 1.5 (1 S.D.; $n = 13$) nm.

There are two important sources of error in estimates of this kind. First, evidence is presented later to show that a considerable fraction of the externally applied length change is taken up by elastic elements

arranged in series with the contractile component and consequently the above method over estimates the amount of filament displacement required to reach S_1 and S_2 . Secondly, shortening of the sarcomeres occurs during the development of a tetanus (6 - 9%), so that the sarcomere length in the muscle at rest is substantially longer than at the time of stretching.

Tension borne by the muscle at S_1 and S_2 . There is obviously a limit to the amount of extra force (above the peak isometric tension) that a muscle can support. There are conflicting reports in the literature concerning the magnitude of this limit; Katz, (1939) gives a figure of around $1.8 \times P_0$, but more recent work by Sugi, (1972) suggests that it may be as high as $3 \times P_0$. The dependence of the tension response on the speed of stretch was alluded to above, and there is no doubt that part of the discrepancy can be accounted for by differences in the speed of stretching. The complexity of the tension response also raises the question of which feature one should measure. Sugi (1972) simply recorded the maximum tension borne by the muscle, which sometimes, but not always, coincided with the end of the stretch, whereas Katz (1939) and more lately A.F. Huxley (1971), applied loads of varying size to isotonically contracting muscles and observed the resulting changes of length. There is strong evidence from cine films of diffraction spectra made during stretch which shows that the tension borne by the muscle at the point S_2 (PS_2) represents the maximum force that the contractile elements

can sustain. In the case of the tension response shown in Fig. 3.1 this reaches $1.366 \times P_O$, and the tension at S_1 (PS_1), $1.110 \times P_O$.

The following values were obtained for several muscles under comparable conditions:

$$PS_1 \quad - \quad 1.075 \pm 0.014 \text{ (1 S.D.; } n=6) \times P_O.$$

$$PS_2 \quad - \quad 1.362 \pm 0.030 \text{ (1 S.D.; } n=13) \times P_O.$$

Muscle stiffness. The stiffness of the muscle during the three phases A, B and C is measured from the slope of the tension records. The following values were obtained:

$$A \quad - \quad 5.30 \pm 0.70 \times 10^8 \text{ N.m}^{-2} \text{ per metre extension.} \\ \text{(1 S.D.; } n=6)$$

$$B \quad - \quad 1.97 \pm 0.31 \times 10^8 \text{ N.m}^{-2} \text{ per metre extension.} \\ \text{(1 S.D.; } n=13)$$

$$C \quad - \quad 1.58 \pm 3.5 \times 10^7 \text{ N.m}^{-2} \text{ per metre extension.} \\ \text{(1 S.D.; } n=13).$$

Part two. Laser diffraction measurements of sarcomere movements.

A laser diffraction technique was used to record sarcomere movements during the development and maintenance of a tetanus and as a result of superimposed length changes. The spacings between the various spectral orders of the diffraction pattern are a function of the mean sarcomere

length in the area of muscle illuminated. These distances (for example, between the two first order reflections) and the distance of the muscle from the recording film, can be accurately measured, and the use of optical diffraction combined with cine photography of the spectra affords a precise means of investigating the dynamics of sarcomere movements in a contracting muscle (Cleworth & Edman, 1972; Kawai & Kuntz, 1973; Nassar, Manring & Johnson, 1974). The variation in the lengths of the sarcomeres within a whole muscle is greater than in a single fibre, but because it is transparent and relatively thin, reasonably 'crisp' diffraction patterns can be obtained from the frog sartorius muscle. Indeed there are certain advantages of a whole muscle; as a result of multiple diffraction effects, relatively more of the light incident upon the muscle is deviated into the higher orders (D.K. Hill, 1953a), producing a pattern of more uniform intensity, which may be photographed without the need to mask the zero order line.

Intensity and width of diffraction lines. This study is concerned principally with changes in the spacing of the diffraction bands and consequently no detailed investigation of band intensity or line dispersion was made. These are important only in so far as they affect the accuracy of the measurements. Decreases in the intensity of the diffraction lines (up to 50%) have been reported in experiments with single muscle fibres (Kawai & Kuntz, 1973) and muscles whose thickness is only a few layers of fibres (D.K. Hill, 1953b), but in the experiments described here, large changes (visible to the naked eye) were observed only in those muscles which were unable to

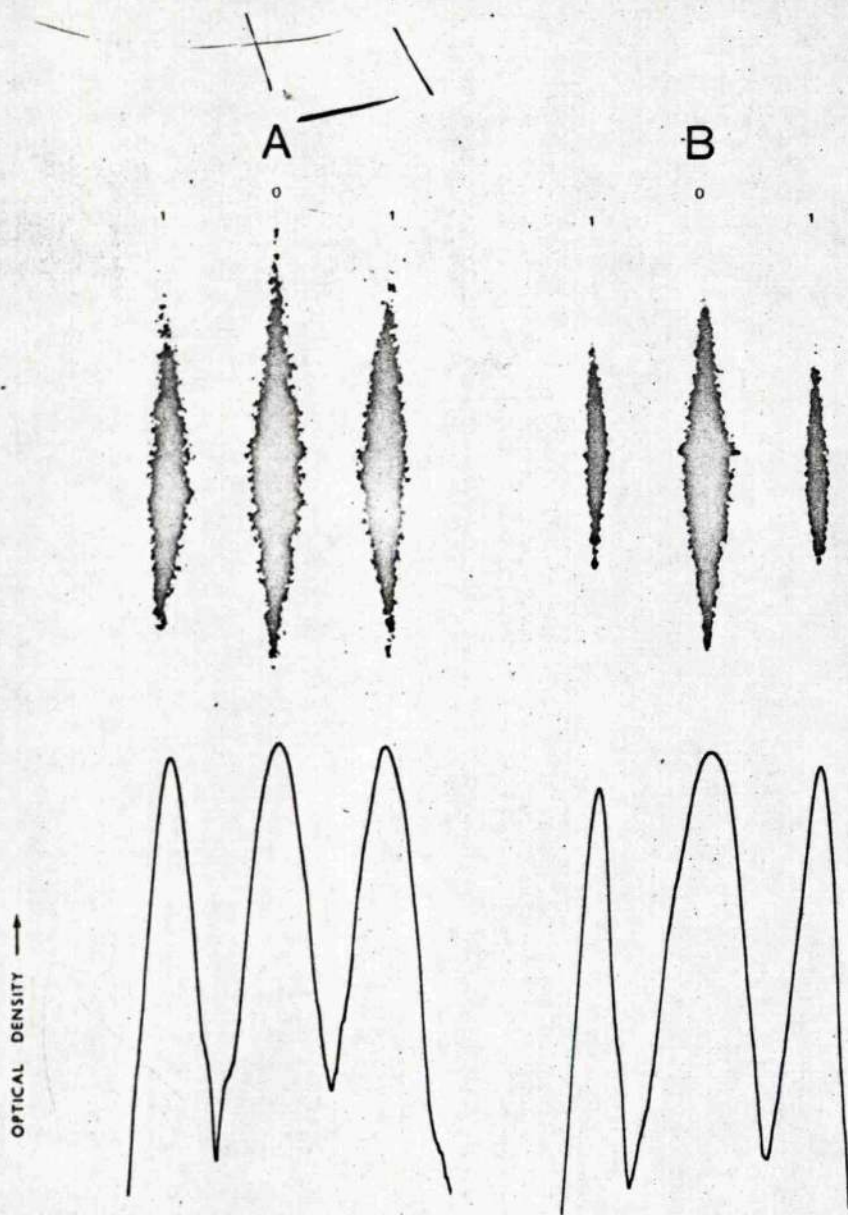


Fig. 3.2. Typical diffraction spectra from A, resting muscle and B, the same muscle 500msec after the beginning of tetanic stimulation. The density profiles of each spectrum, as obtained by scanning each frame with a densitometer, are also shown.

maintain a steady force and recordings of this kind were not included in the analyses. One cause of poorly maintained levels is undoubtedly inadequate stimulation. In all experiments from which records were used for analysis there was no appreciable decrease in diffraction band intensity.

Kawai & Kuntz (1973) showed that a small increase in the width of the first order diffraction lines occurs when a muscle fibre is stimulated. Fig. 3.2 shows the diffraction spectra and their optical density profiles from resting (A) and maximally tetanised (B) muscle. It can be seen that the peak intensity of the individual bands is little changed, but that the width of the first order diffraction lines is decreased during contraction. This is an interesting observation because it is the converse of the change seen in single fibres, and from the practical point of view it leads to greater accuracy in determining sarcomere spacing.

Finally, it has been shown that an increase of light scattering is associated with the transition from rest to activity (D.K. Hill, 1949). The location of the structures responsible is uncertain, but since the loss of intensity at peak tension is small (about 5%, in red light; Hill, 1949; Barry & Camay, 1969), this has a negligible effect on the quality of the diffraction pattern.

Reference is first made to some observations on the movement of sarcomeres during stretches of resting muscle because there are important qualitative differences between those and the movements produced by identical stretches applied to tetanised muscle.

At l_0	
Position mm from pelvic end	Sarcomere length μ
24	2.424
20	2.415
16	2.440
12	2.454
8	2.454
4	2.460

Table 1.

At $1.25 \times l_0$	
Position mm from pelvic end	Sarcomere length μ
24	2.992
20	2.981
16	3.000
12	2.987
8	3.000
4	2.987

Table 2.

Tables 1 and 2. Sarcomere lengths recorded at various positions along the length of a muscle, by a laser diffraction method.

Measurements were carried out at two muscle lengths, l_0 and $1.25 \times l_0$.

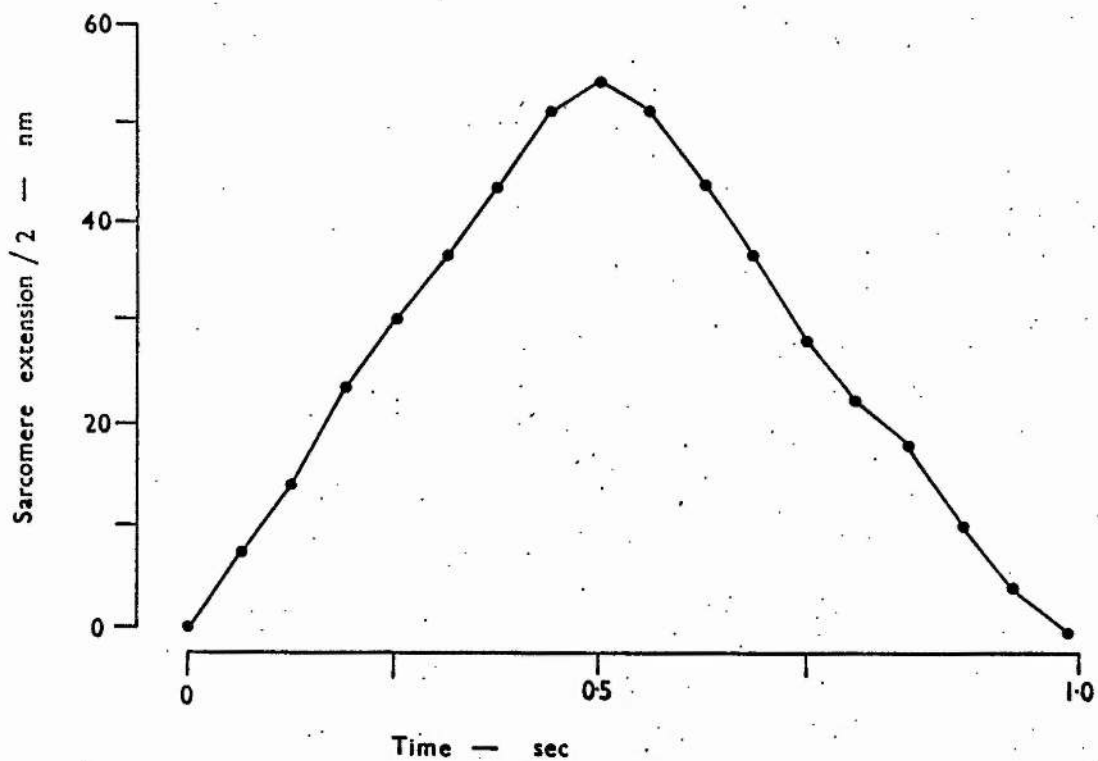


Fig. 3.3. Diffraction measurements of sarcomere length, made during the application of a linear stretch of $1060\mu\text{m}$, followed by an immediate release of the same amplitude. The recording position was 4mm from the pelvic end of the muscle.

Resting muscle.

Sarcomere length and its variation in the resting state. Muscles

were illuminated at six different positions and sarcomere lengths were measured from photographs of the resulting diffraction spectra. Values obtained initially at the in situ resting length (l_0) and then with the muscle extended to 7mm above the resting length ($1.25 \times l_0$) are shown in Tables 1 & 2 respectively. At l_0 the mean sarcomere length was found to be $2.44 \mu\text{m}$ and the coefficient of variation ($\text{S.D.}/\text{mean} \times 100$) was 0.7%. At $1.25 \times l_0$ the mean sarcomere length was $2.99 \mu\text{m}$ and the coefficient of variation was 0.3%.

There is evidence that the sarcomeres at the extreme ends of the muscle tend to be shorter (Huxley & Peachey, 1959) but the greater amount of connective tissue and the method of attaching the muscle to the apparatus made it impossible to obtain satisfactory spectra from those regions.

Sarcomere movements during stretches applied to resting muscle. It

has been known for many years (Sandow, 1936a) that the steady state sarcomere length increases in proportion to overall muscle length, and Tables 1 & 2 confirm this. However, there is no information in the literature on the movements of sarcomeres during stretch. To investigate this point diffraction spectra were photographed with a cine camera while the muscle was subjected to a stretch and release cycle of $1060 \mu\text{m}$

At l_0	
Position mm from pelvic end	Sarcomere extension nm
24	114
20	118
16	110
12	120
8	108
4	114

Table 3.

At $1.25 \times l_0$	
Position mm from pelvic end	Sarcomere extension nm
24	128
20	124
16	135
12	130
8	130
4	124

Table 4.

Tables 3 and 4. Sarcomere extensions produced by stretches of $1060\mu\text{m}$ as recorded at different positions along the length of the muscle. Starting sarcomere lengths were those given in Tables 1 and 2.

at a velocity of $4.24 \text{ mm} \cdot \text{s}^{-1}$.

Fig. 3.3 shows sarcomere spacing recorded 4 mm from the pelvic end of the muscle plotted against time (cine-frame number). The sarcomere length increases in an approximately linear fashion although the final length is roughly 8% greater than would be predicted theoretically. Table 3 shows sarcomere extensions recorded from different regions of the muscle and the values obtained from each position are broadly similar (mean 110 nm ; coefficient of variation, 4 %). A similar series of values are given in Table 4, but in this case the starting sarcomere length was $2.99 \mu\text{m}$. Once again, the extension is uniformly distributed throughout the sarcomeres sampled (mean 128 nm ; coefficient of variation, 6 %). In this case the maximum extension was 12 % greater than that predicted theoretically.

Active muscle.

Sarcomere movements during the development and maintenance of an isometric tetanus. Cine recordings of zero and first order diffraction bands were made during isometric tetani. An increase in the spacing of the spectral lines was observed, corresponding with the onset of tension development, signifying shortening of the sarcomeres at the expense of the elastic elements in series with them. The extent of internal shortening is a function of the force generated by the sarcomeres and the length tension characteristics of these elements.

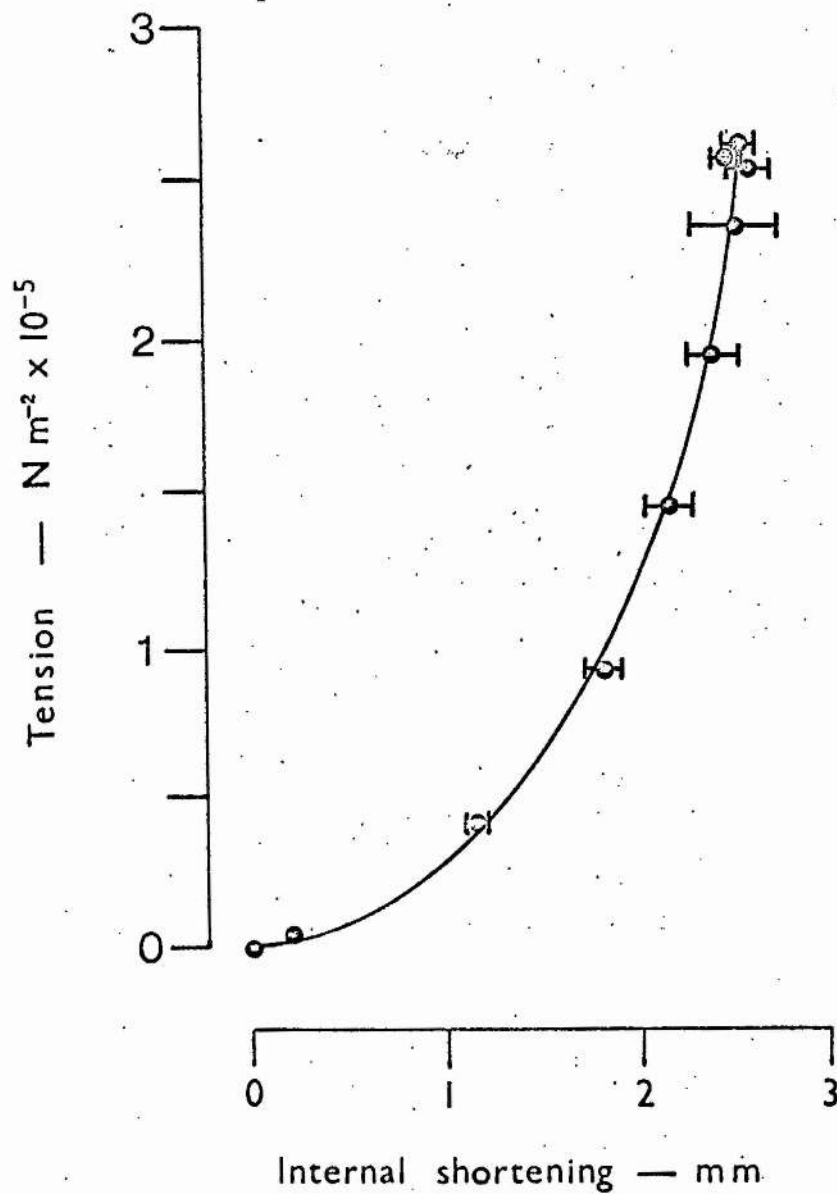


Fig. 3.4. A length / tension plot for all the elastic elements lying in series with the sarcomeres. The curve was constructed from recordings of sarcomere length, made during tension development, at the start of an isometric tetanus. Points are the mean values from four different recording positions, 4mm, 12mm, 16mm and 20mm from the pelvic end. Error bars show \pm one standard error, ($n=4$).

Measurements of sarcomere spacing during tension development were made at four levels in the muscle (4mm, 12mm, 16mm and 20mm from the pelvic end). Fig 3.4 shows isometric force plotted against mean internal shortening for the four positions sampled and thus it portrays the length/tension characteristics of all elastic elements (including 'stray' compliance in the apparatus) lying in series with the sarcomeres. The curve is very non-linear and as with many biological materials the stiffness increases with increasing amounts of extension. At peak isometric tension the compliance of the 'lumped' series elements is $6.34 \times 10^{-4} \text{ m.N}^{-1}$.

Fluctuations in the lengths of the sarcomeres during the tension plateau of a tetanus have been reported (Goldspink, Larson & Davies, 1970) in chick anterior and posterior latissimus dorsi muscle, in which maximum oscillations of 90 nm (3.75%) with a period of approximately 75 ms were observed. No fluctuations of this magnitude were detected with the system described here, although very much smaller changes in sarcomere length ($\pm 3 \text{ nm}$ per sarcomere) cannot be ruled out. This result is in agreement with the findings of Cleworth & Edman (1972) and Kawai & Kuntz (1973) from experiments with single fibres.

The dynamics of sarcomere movements during stretch of contracting muscle. The movements of sarcomeres during stretches applied to contracting muscle are strikingly different from those produced by stretching a resting muscle. Fig. 3.5 shows a single frame from a

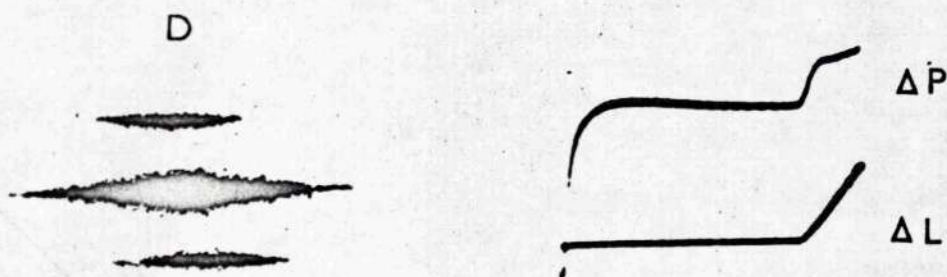


Fig. 3.5. A frame from the cine film, showing the diffraction pattern (D), applied length change (ΔL) and muscle tension (ΔP). This technique enabled sarcomere spacing to be related precisely to muscle tension and extension, at intervals of 15ms throughout a tetanus and/or an applied length change.

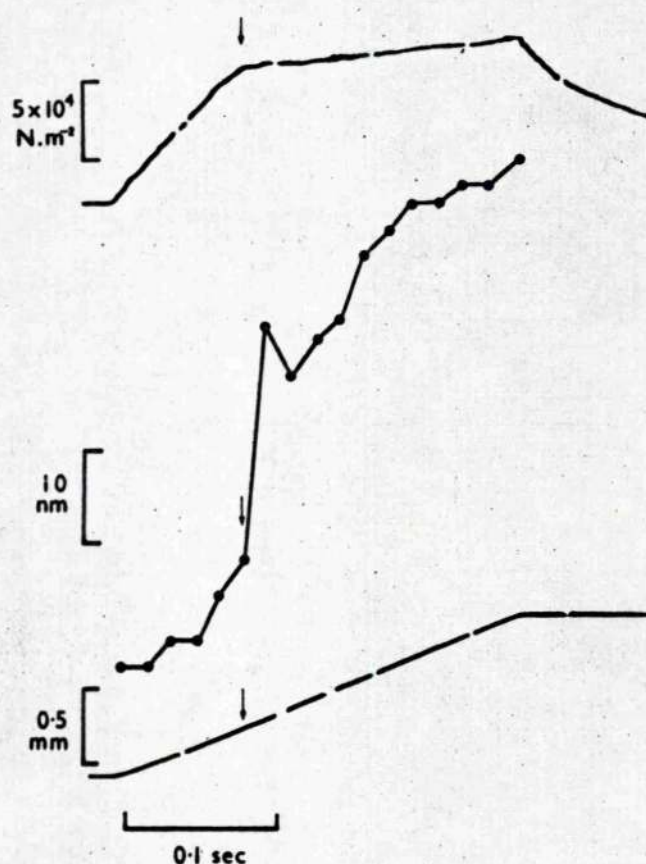


Fig. 3.6. Recorded changes in muscle tension (upper trace), sarcomere spacing (middle trace) and external muscle length (lower trace), made during the application of a 'ramp and hold' stretch of $1060\mu\text{m}$, to a tetanised muscle, at a velocity of 4.24mm.s^{-1} . Temperature was 0°C . The point S_2 is indicated by the arrows.

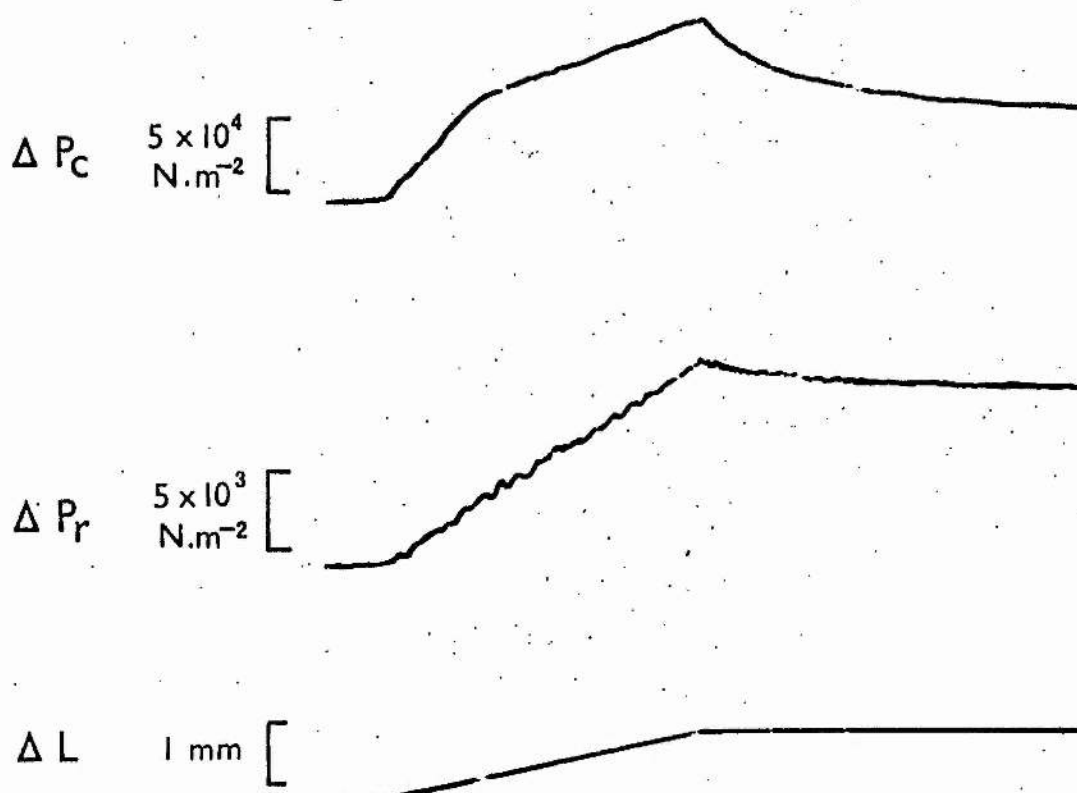


Fig. 3.7. Tension changes produced by a ramp and hold stretch (ΔL) of $1060\mu\text{m}$, at a velocity of 4.24mm.s^{-1} , applied to contracting muscle (ΔP_C) and resting muscle (ΔP_R).

Tension generated in a resting muscle is subtracted from that generated in a contracting muscle for a length change of the same amplitude, so that the contribution from parallel elastic elements, not involved in force development, may be allowed for.

The muscle length before the application of the stretch was in this case $1.7 \times l_0$.

cine film, with diffraction spectra, muscle tension and external length change displayed. The changes observed in sarcomere length, muscle force and muscle extension throughout the period of stretch are shown in Fig. 3.6. The tension record has a similar form to the one described earlier (Fig. 3.1) with a clearly defined 'slip' point at S_2 . There are three important points to notice about the way in which the sarcomeres elongate during stretch:

First, in the period up to S_2 they are extended at a rate which is considerably less than would be predicted theoretically. The following figures serve to illustrate the point. The initial muscle length was 28 mm and the sarcomere length at peak isometric tension was $2.37 \mu\text{m}$. The external length change was 1.06 mm, applied at a speed of $4.24 \text{ mm} \cdot \text{s}^{-1}$. This would be expected to cause the sarcomeres to extend at a velocity of $0.39 \mu\text{m} \cdot \text{s}^{-1}$, whereas the value estimated from the first six frames of the film is only $0.22 \mu\text{m} \cdot \text{s}^{-1}$. This result shows that a substantial fraction, in this case about 0.4, of the externally applied length change is not taken up by extension of the sarcomeres, but, presumably, by elastic elements in series with them.

Secondly, when the muscle is extended to the point S_2 , the sarcomere length increases abruptly. This sudden elongation is referred to hereafter as rapid 'give'. In the record of Fig. 3.6, it occurs when the actin and myosin filaments are displaced by about 11.5 nm from their equilibrium position at peak isometric tension. During the period of rapid 'give' they move by a further 21.4 nm, bringing the total extension

to 32.9 nm.

Third, extension of the sarcomeres in the period following rapid 'give' follows the external length change reasonably closely (velocity, $0.34 \mu\text{m} \cdot \text{s}^{-1}$, compared with $0.39 \mu\text{m} \cdot \text{s}^{-1}$), although, in nearly all of the records some 'overshoot' is seen. This transient shortening of the sarcomeres is shown clearly in Fig 3.6. By the time the stretch is terminated, the sarcomeres have been extended by an amount which is close to that which would be predicted theoretically; thus a 4% change in muscle length results ultimately in a 4% change in sarcomere length.

The most straightforward interpretation of these observations is that extension of the muscle ultimately results in forcible detachment of the cross-bridges holding the filaments together, with the resulting shortening of the extended series elastic elements (elastic recoil) causing sudden elongation of the sarcomeres.

Dependence of sarcomere stiffness on filament overlap. If this is the correct interpretation, then the resistance to stretch of the muscle up to S_2 ought to be inversely related to the length of the sarcomeres, since the number of cross-bridges potentially capable of contributing to the effect is proportional to the extent of overlap of the actin and myosin filaments.

Experiments were therefore made in which stretches were applied to tetanised muscles at lengths ranging from $0.93 - 1.38 \times l_0$. Sarcomere

lengths at rest and then during stretch were monitored by cine photography of diffraction spectra. Stretches of $960\text{ }\mu\text{m}$ were employed.

The method of analysing the records was as follows. First, at lengths greater than about $1.1 \times l_0$ there is an appreciable contribution to the tension record from elastic elements other than those associated with the contractile component, and to compensate for this the tension developed during stretch of a resting muscle was subtracted from that produced by the same stretch applied to the muscle during an isometric tetanus (Fig. 3.7). Secondly, measurements were made of the stiffness from a) the slope of the early part of the corrected tension response ($\Delta P / \Delta L$, where ΔL is the external movement) and b) the slope of the line relating internal sarcomere movement to muscle tension ($\Delta P / \Delta S$, where ΔS is the change in sarcomere length).

The results were all related to the sarcomere spacing at peak isometric tension immediately prior to the application of the stretch, rather than to sarcomere length at rest. In this way, due allowance was made for the shortening of sarcomeres (and the consequent change in filament overlap) which occurs during the development of the tetanus.

Fig 3. 8 . shows P_0 (filled circles) plotted against values for the sarcomere length at peak tetanic tension, just prior to the application of a stretch. The extrapolated region of the resulting length/tension diagram intercepts the abscissa at a value of $3.61\text{ }\mu\text{m}$, close to the expected theoretical value of $3.65\text{ }\mu\text{m}$, at which length the filaments no longer overlap (Page, 1964 a). The values obtained for muscle

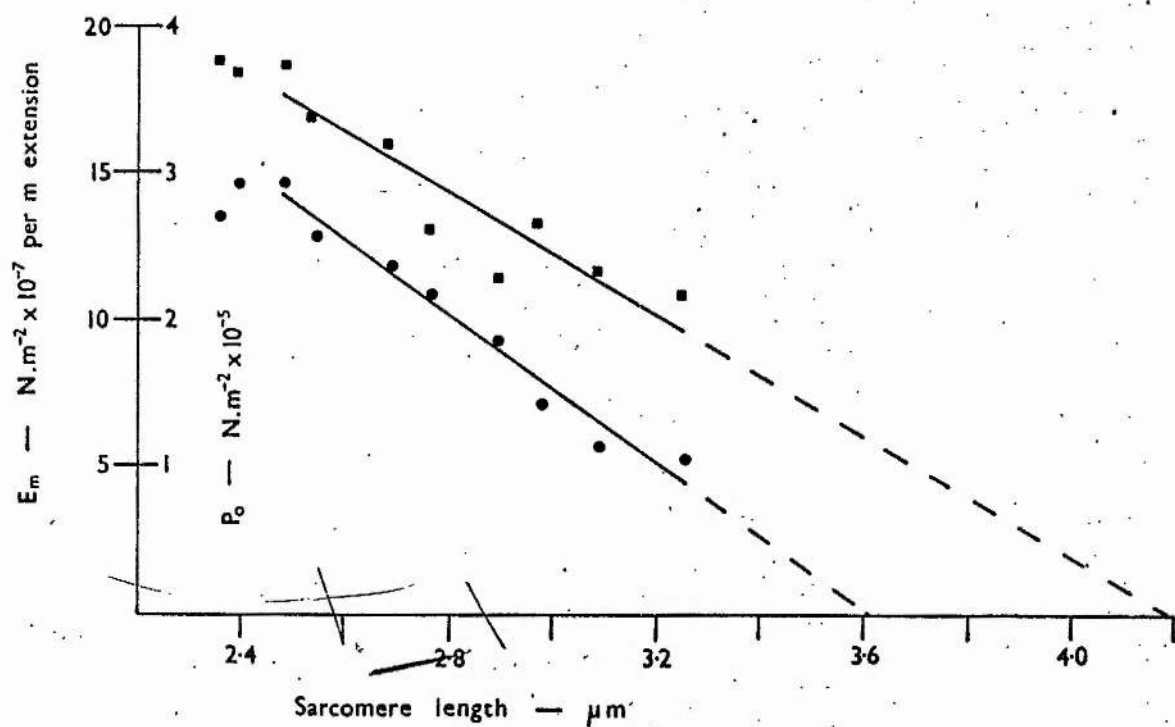


Fig. 3.8. Values for peak tetanic tension, P_0 , (circles) and mean muscle stiffness up to S_2 , E_m , (squares), obtained from the relationship $\Delta P / \Delta L$, plotted against sarcomere length.

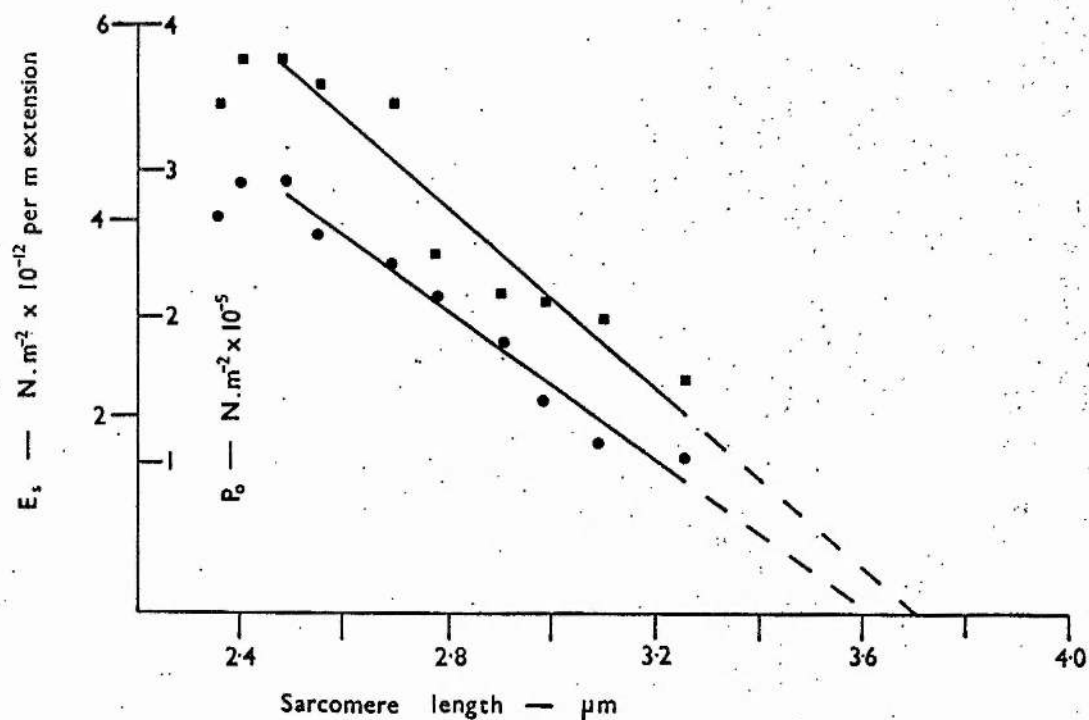


Fig. 3.9. Values for P_0 (circles) and the mean stiffness of the sarcomeres, E_s , (squares), obtained from the relationship $\Delta P / \Delta S$, plotted against sarcomere length.

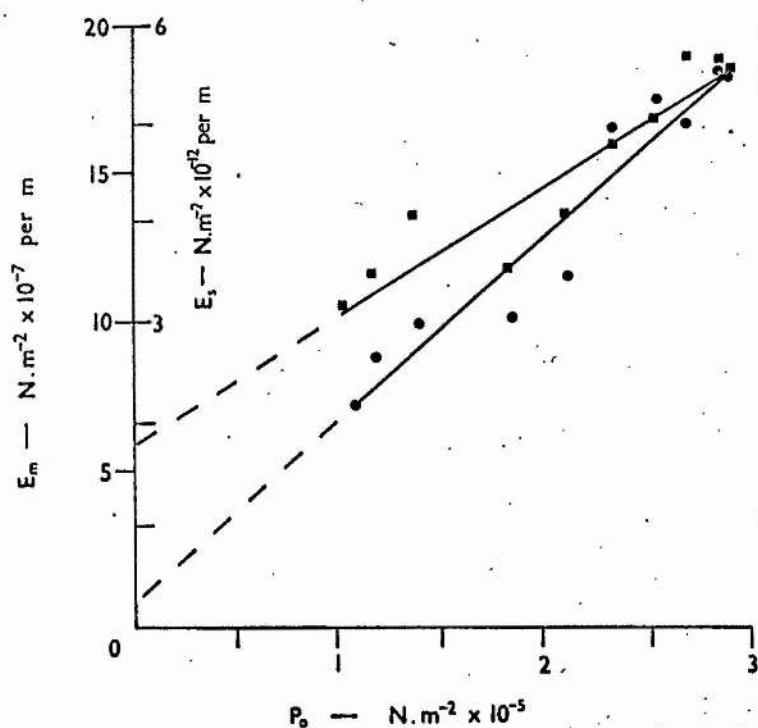


Fig. 3.10. Values for E_m (squares) and E_s (circles) plotted against P_o .

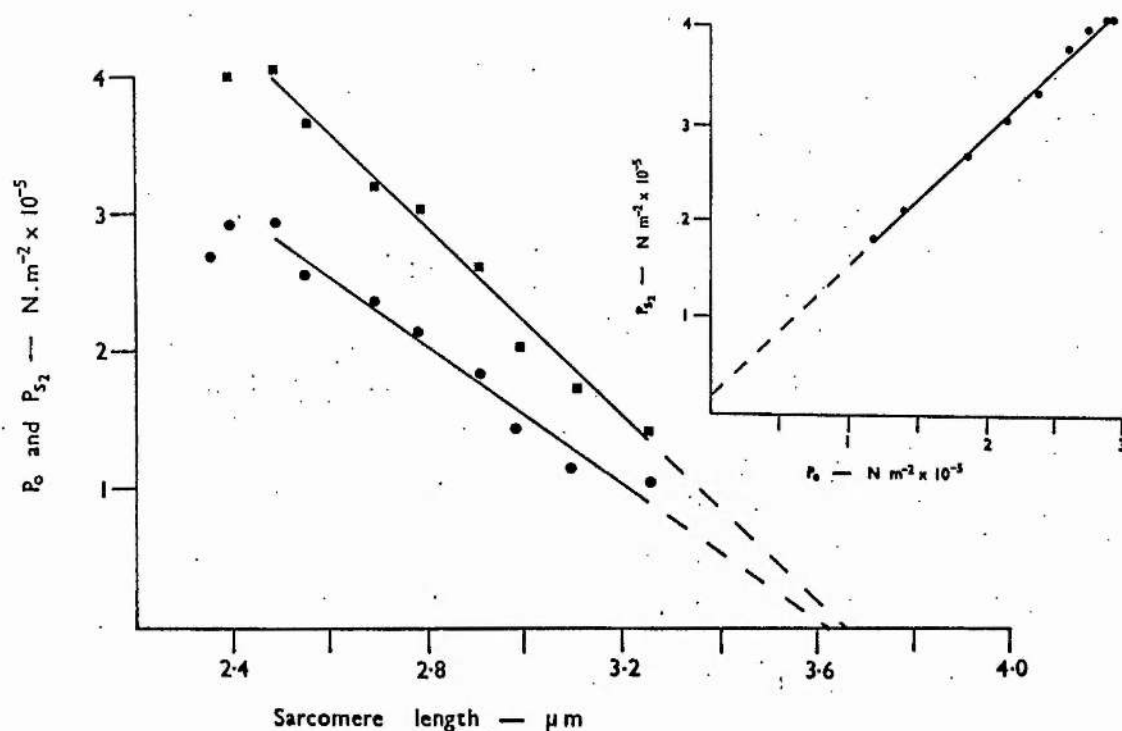


Fig. 3.11. The maximum force the sarcomeres are capable of holding (total active tension at P_o , P_{S_2}), (squares), and P_o , (circles), plotted against sarcomere length.

Fig. 3.12. (inset) P_{S_2} plotted against P_o .

stiffness, when referred to the external length change, denoted by E_m , are also shown (squares). The regression line fitted to the eight points, corresponding with those values of P_0 which clearly lie on the descending limb of the length/tension diagram, intercepts the abscissa at a value of $4.20 \mu\text{m}$, which is greatly in excess of the predicted value of $3.65 \mu\text{m}$. This is not an unexpected result. The experiments described previously showed that a considerable fraction of the externally applied length change is taken up by elastic elements arranged in series with the sarcomeres, and this fraction is likely to vary with muscle length. Fig. 3.9 shows the same values for P_0 plotted against sarcomere length and the corresponding values for muscle stiffness, calculated from the sarcomere movements, denoted by E_s (squares). In this case, the regression line fitted to the last eight points intercepts at a sarcomere length of $3.71 \mu\text{m}$. This is sufficiently close to the theoretical intercept of $3.65 \mu\text{m}$ to make it seem certain that the stiffness up to S_2 is directly related to filament overlap, and therefore represents the collective stiffness of the cross-bridges joining the filaments together.

Fig. 3.10 shows values for E_m and E_s plotted against P_0 . Both show linear relationships, but with different intercepts. The extrapolated region of the E_s line intercepts close to the origin, as would be expected, but that for E_m shows a finite intercept of 0.85 N.m^{-2} per metre extension of the whole muscle.

'Holding' force of muscle at S_2 . The maximum force the sarcomeres are

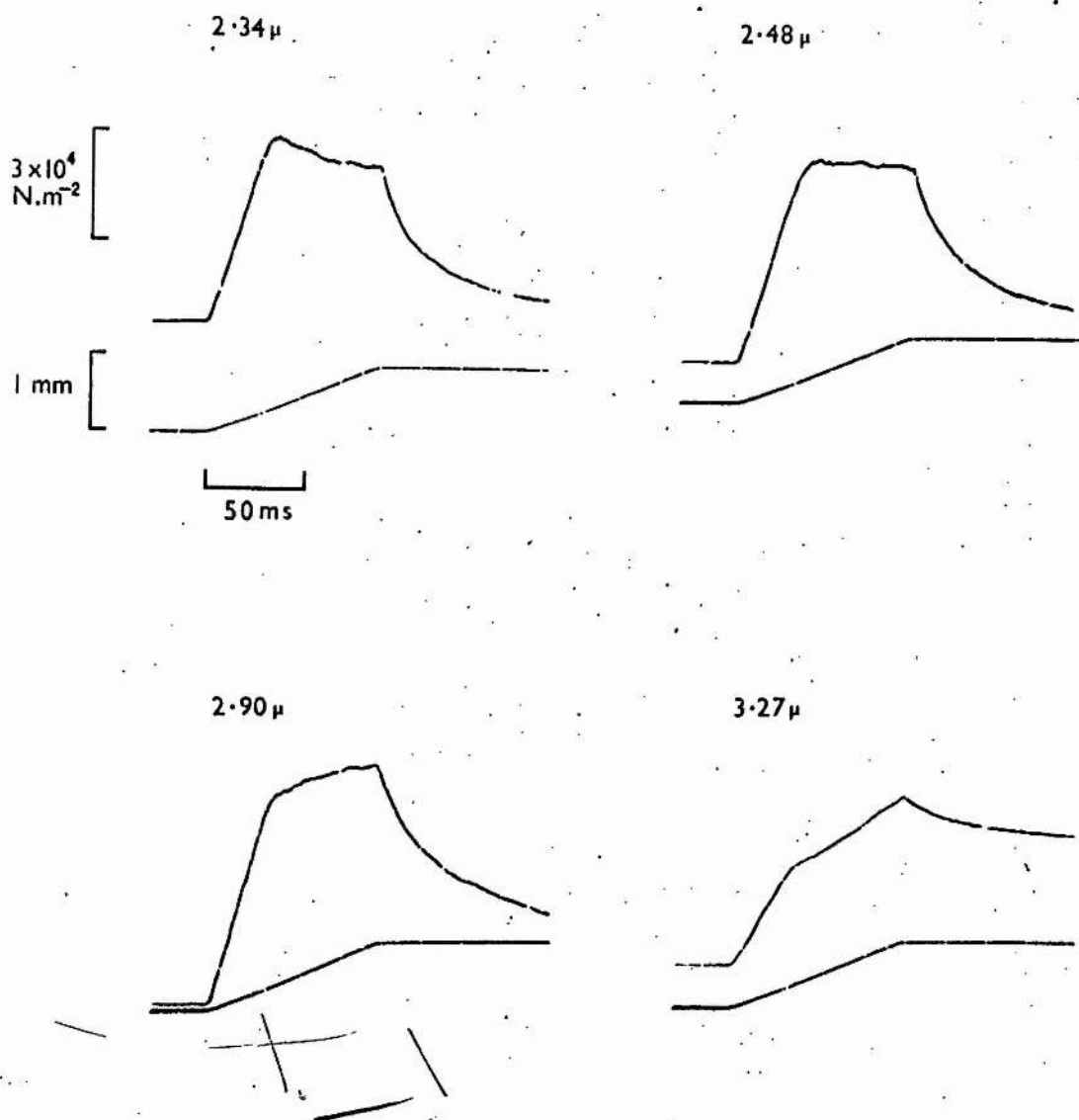


Fig. 3.13. Tension responses to stretches of $960\ \mu\text{m}$ (11.5mm.s^{-1}), applied to a tetanised muscle, at different sarcomere lengths (shown above each trace). Traces of this kind were used to obtain values for P_{S_2} , E_m and $\Delta L \rightarrow S_2$.

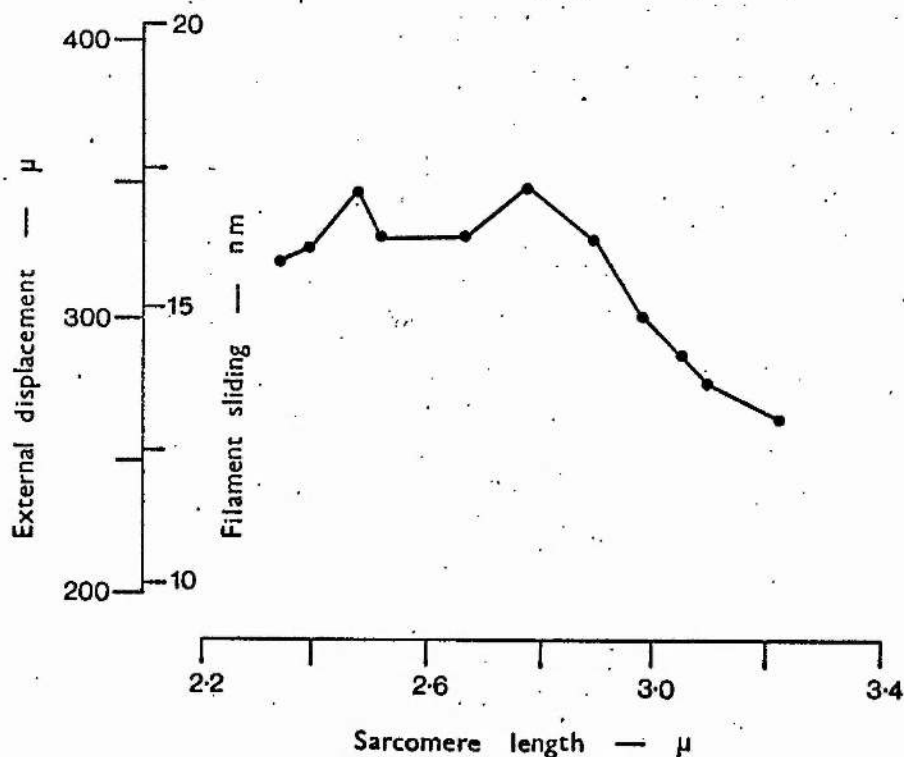


Fig. 3.14. Values for filament sliding required to reach S_2 , calculated from the external length change, plotted against sarcomere length.

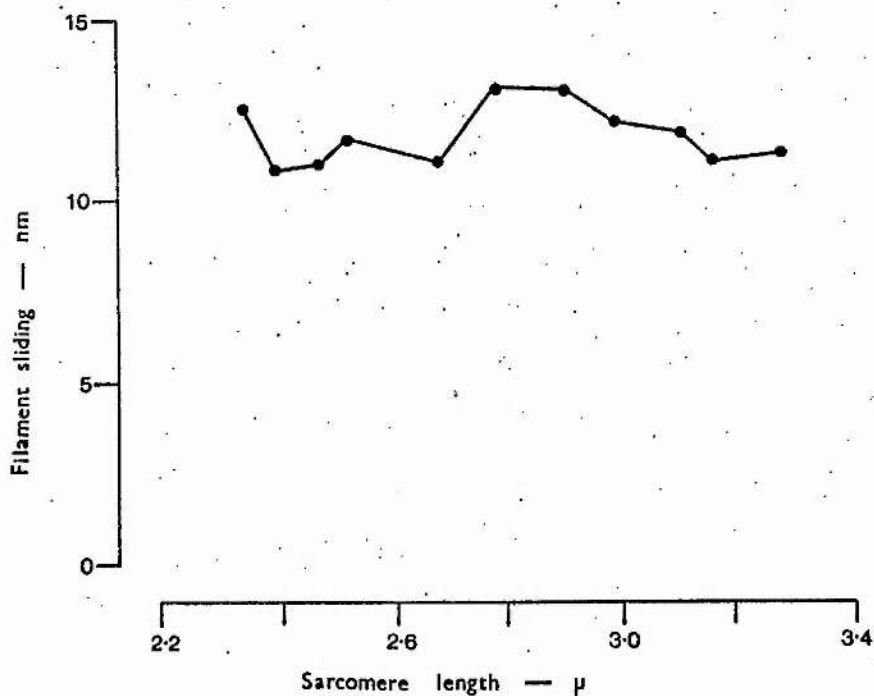


Fig. 3.15. Values for filament sliding required to reach S_2 , obtained from direct recordings of sarcomere movements; Filament sliding is relatively constant, giving a mean value of 12.3 ± 0.9 nm per half sarcomere (± 1 S.D. : $n=10$).

capable of holding immediately before rapid 'give' (total muscle tension at S_2 , P_{S_2}) ought to show a similar inverse dependence on sarcomere length. The values obtained are plotted against sarcomere spacing in Fig. 3.11. They decrease linearly with increasing sarcomere length (above $2.5 \mu\text{m}$) and the regression line intercepts the abscissa at a value of $3.66 \mu\text{m}$, which again is close to the theoretical value of $3.65 \mu\text{m}$.

Fig. 3.12 (inset) shows P_{S_2} plotted against P_0 . The linear relationship between these two dependent variables shows that the ratio P_{S_2}/P_0 is constant at all sarcomere lengths, so it can therefore be concluded that the holding force per cross-bridge is independent of sarcomere length and hence of the lateral spacing of the actin and myosin filaments.

Relative sliding movement of the filaments required to reach S_2 at different muscle lengths. The relative sliding movement of the filaments up to the point at which the sarcomeres show rapid 'give' can be calculated from the external length change in the way described earlier. Fig. 3.13, 1 - 4, show several traces made at increasing muscle lengths and from these it can be seen that less extension is needed to reach S_2 at long muscle lengths. The values are plotted against sarcomere length in Fig. 3.14. Also shown are the corresponding values for relative filament sliding, again based on the assumption that all of the length change is transmitted to the sarcomeres. Filament movements are found to be relatively constant for muscle lengths corresponding with sarcomeres less than $2.9 \mu\text{m}$ in length, but become

progressively smaller as muscle length is increased further. By contrast, the actual amount of sarcomere extension needed to reach S_2 , measured directly from the diffraction spectra, remains fairly constant (to within $\pm 8\%$) over the range of sarcomere lengths from $2.34 - 3.27 \mu\text{m}$ (Fig. 3.15). The mean value for the filament displacement was found to be $12.3 \pm 0.9 \text{ nm}$ ($\pm 1 \text{ S.D.}$; $n=10$). This is the extent of sliding of the filaments required to generate maximum tension in the contractile mechanism.

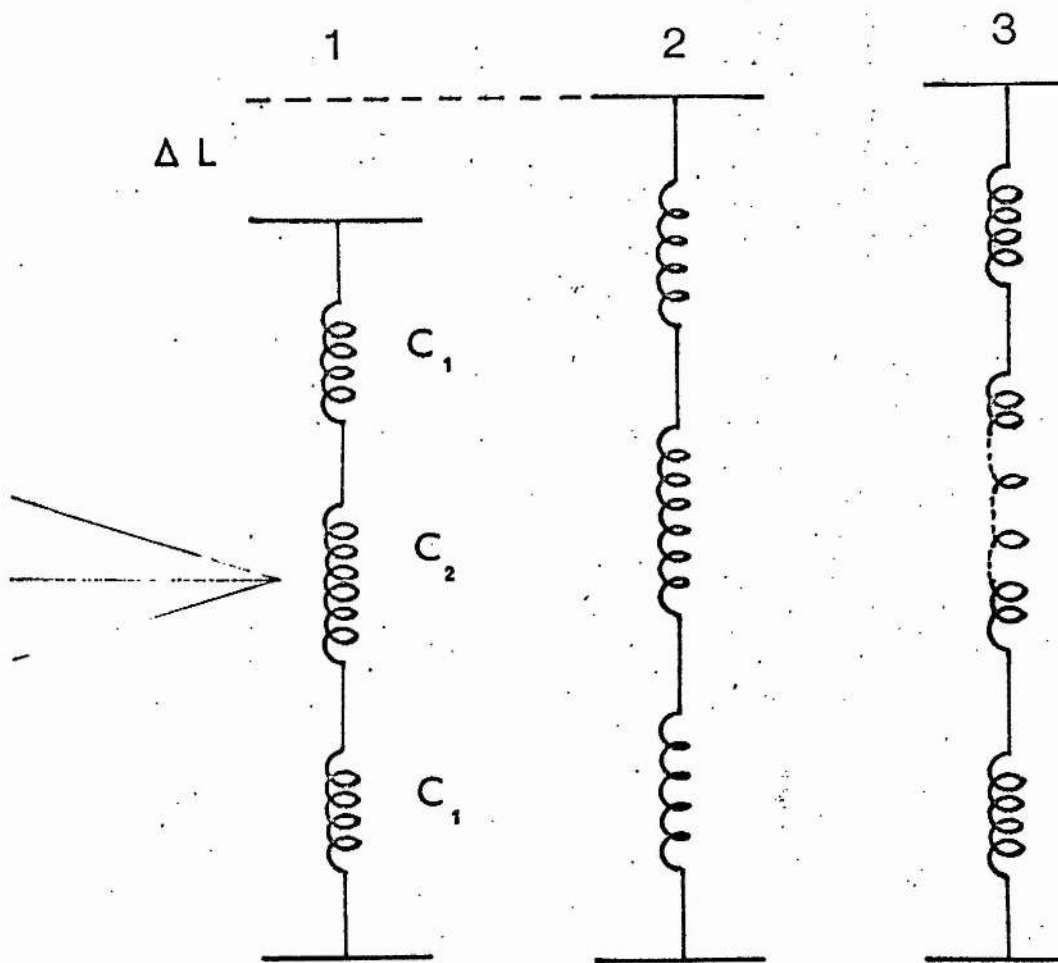


Fig. 3.16. Proposed account of the length changes occurring in the sarcomeres (C_2) and series compliances (C_1) during a stretch applied to a contracting muscle.

- 1) Before the application of the length change.
- 2) Just before rapid 'give' at S_2 .
- 3) Just after rapid 'give', showing breakage and extension of C_2 .

DISCUSSION

It has been shown that the tension response of a muscle to long stretches is highly non-linear, with two points of inflection, the second of which, S_2 , corresponds with an abrupt increase in length of the sarcomeres. The simplest interpretation of this phenomenon is that extension of an active muscle ultimately causes detachment of the cross-linkages holding the filaments together and that shortening of the extended series elastic elements (elastic recoil) brings about a rapid extension of the sarcomeres.

This can best be understood by reference to Fig. 3.16. The muscle is here represented as three compliances in series, C_2 being the contractile component (sarcomeres) and the two labelled C_1 being inert (non-contractile) elements located at each end. In a muscle at rest the stiffness of the contractile component is very small compared with that of the series elastic elements, and consequently, ramp stretches produce almost uniform extension of the sarcomeres (Fig. 3.3). However, in a fully activated muscle the stiffness of the contractile component is very much greater than at rest, and as a result, some of the length change is absorbed by extension of the series elastic elements. Clearly, this situation holds only for as long as the linkages remain patent. If displacement of the filaments exceeds a certain critical value then the cross-bridges become detached; when this happens, the elastic tension stored in the series

elements (C_1) then causes sudden extension of the sarcomeres.

The extent of the sliding movement required to bring about rapid 'give' can either be calculated from the amount of external length change applied or from direct observations of the movements of the sarcomeres. It has been seen that the former method gives confusing results which can easily be accounted for in terms of the model described above. However, when direct observations of sarcomere movements are made, several points of interest emerge. First, the amount of filament displacement required to produce rapid 'give' is relatively constant, at around 12 nm, at all muscle lengths. Secondly, the tension generated at S_2 , that is to say the maximum force that the contractile element can bear, is linearly related to filament overlap. This last point implies that the binding force between the myosin cross-bridges and the actin filament is constant and not influenced by the lateral separation of the filaments.

The argument put forward previously to account for the abrupt changes in sarcomere length at S_2 does not explain two important features of the phenomenon. First, it is clear that rapid sarcomere extension halts even though the series elastic elements are still extended beyond their rest length, and the reason why this occurs is not immediately apparent; secondly, how is the high level of tension maintained after S_2 , at a time when all the cross-bridges will have been broken? These difficulties are resolved by considering rapid 'give' as a transition between two steady states. Prior to stretch the muscle is exerting a steady

force and the filaments are relatively static. In the early stages of a stretch, up to S_2 , the filaments and the population of cross-bridges actively involved in generating force are displaced from their equilibrium position and tension in the muscle rises. At S_2 cross-bridges are forcibly detached and the series elastic elements shorten abruptly at the expense of the sarcomeres. Now, it can be shown that the change in length of the series elastic elements during rapid 'give' (about 0.4 mm) is small compared with the total amount by which they have been extended (2.4 mm, comprising some extension during stretch and some, the greater part, during the development of tetanic tension). There can be no question that rapid 'give' is terminated by cross-bridges remaining attached to the filaments; in Fig. 3.6 for example the total amount of filament displacement up to the end of rapid 'give' is 33nm, a figure which is greatly in excess of current estimates for the maximum working range of a cross-bridge. It follows, then, that the resistance to movement of the filaments must arise from the reattachment of cross-bridges previously broken, or the attachment of cross-bridges to new sites on the actin filament which become accessible as a result of movement. It is easy to envisage that initial attachment of a few cross-bridges will tend to slow down the rate of filament sliding, thereby increasing the probability for the attachment of further linkages, slowing down the filaments still further until in the limit, rapid extension is halted. During the remainder of the stretch a new steady state is established in which cross-bridges attach, as and when sites become

available, are extended until they develop maximum tension and break, and then reattach at a new position further along the actin filament. In this way, tension should remain fairly constant beyond S_2 as is often found experimentally. Moreover, if the rate constant for attachment of cross-bridges is relatively high the maintained level of tension during this phase ought to be roughly constant over a wide range of stretch velocities and this too is borne out experimentally (Chapter VI). Of course, if the velocity of stretch is greatly increased, a point will be reached where attachment is not possible, and it might then be predicted that tension would fall steeply beyond S_2 . Sugi's (1972) experiments, employing exceedingly rapid stretches ($100 \times 10^3 \text{ s}^{-1}$), do indeed show a large, abrupt fall in tension which is consistent with this.

Stiffness of cross-bridges. The stiffness of the sarcomeres up to S_2 must be a collective property of those cross-bridges involved in generating force, and an estimate of the mean stiffness of a single cross-bridge can thus be derived if the total number of linkages contributing to the effect is known. The stiffness of the sarcomeres is given by $\Delta P / \Delta S$ where S is sarcomere length and P is tension per unit area of the muscle. A sarcomere extension of 23.0 nm generates a tension of $6.85 \times 10^4 \text{ N.m}^{-2}$ at a sarcomere length ($2.39 \mu\text{m}$) where isometric force, and therefore filament overlap, is maximal; the maximum stiffness of each half sarcomere is therefore $5.95 \times 10^{12} \text{ N.m}^{-2}$ per metre extension. The number of cross projections on the thick filaments in each

half sarcomere, for a cross sectional area of 1 m^2 , is 5×10^{16} (H. E. Huxley, 1963) and assuming that all of these are actively involved in force production simultaneously, then the stiffness of a single bridge is $2.39 \times 10^{-4} \text{ N.m}^{-1}$. A small correction is necessary to allow for the extracellular space, which amounts to about 12% of the muscle volume (D.K. Hill, 1965). The value then becomes $2.68 \times 10^{-4} \text{ N.m}^{-1}$. This must of course represent the minimum stiffness since it is possible (indeed, probable) that not all of the projections on the thick filament are actively engaged in producing force at any one time. Estimates range from 20 % (Huxley & Brown, 1967) to as much as 80% (Matsubara, Yagi & Hashizume, 1975). Until more is known about the numbers involved, all that can be said is that the stiffness of a single cross-bridge lies within the range $3 - 15 \times 10^{-4} \text{ N.m}^{-1}$.

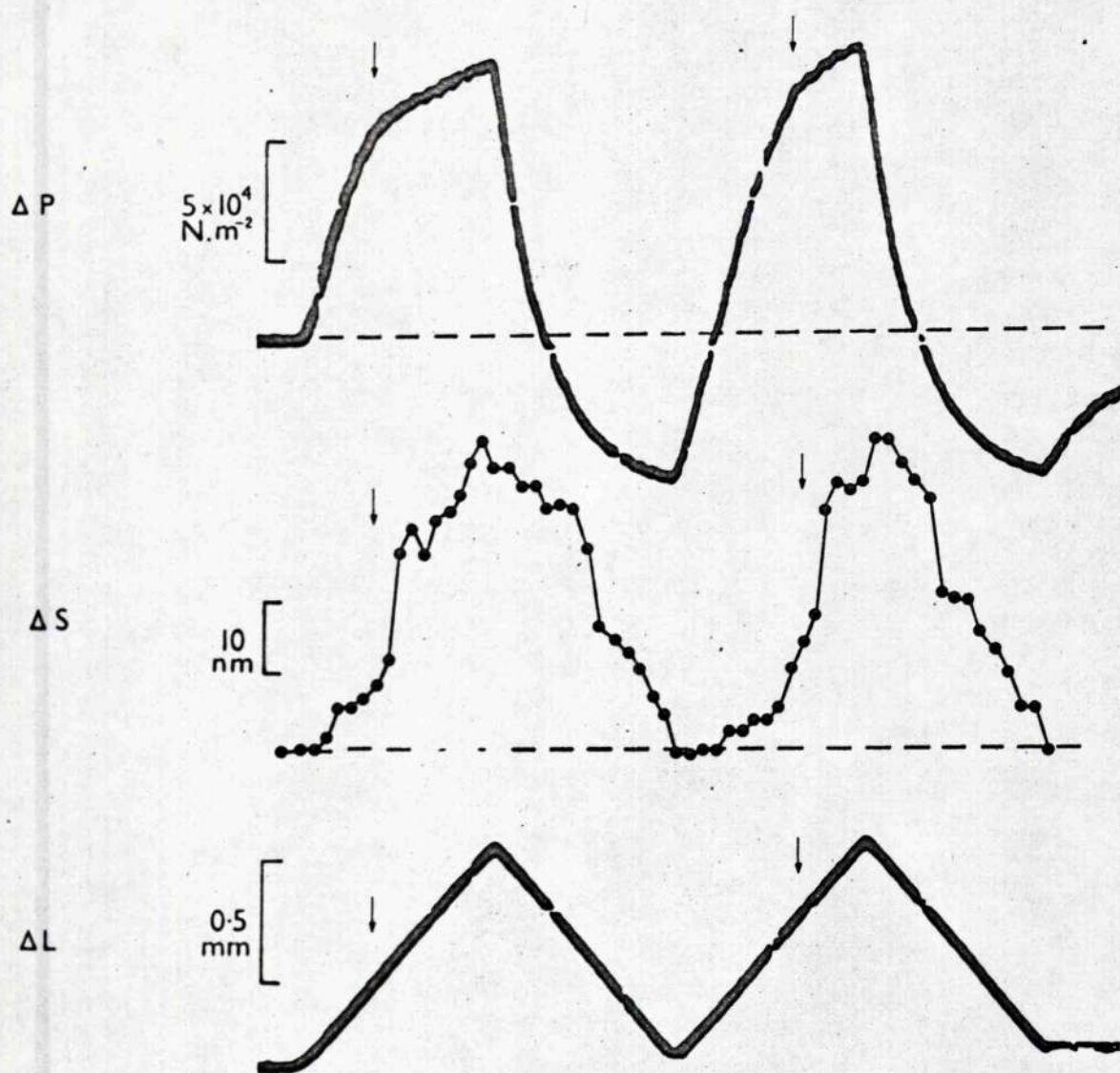


Fig. 4.1. Tension responses (ΔP) and sarcomere length changes (ΔS) during a double stretch and release cycle (ΔL) of $1020\mu\text{m}$ (at 4.08 mm.s^{-1}), applied during the plateau of an isometric tetanus. The point S_2 is arrowed for both first and second stretches.

CHAPTER IV

TENSION RESPONSES AND SARCOMERE MOVEMENTS DURING CYCLICAL LENGTH CHANGES OF LARGE AMPLITUDE.

It has been shown that the major features of the tension response to large stretches can be attributed to the behaviour of the cross-bridges that form temporary linkages between the actin and myosin filaments. The experiments to be presented here were designed to obtain further information on their mechanical properties, and to this end, muscles were subjected to cyclical length changes (stretches and releases) of large amplitude.

Tension changes and sarcomere movements during the second stretch of a double stretch and release cycle. When a stretch is followed by a release of the same amplitude and the muscle is immediately subjected to a second stretch, the form of the tension response and the movement of the sarcomeres is markedly different from that seen during the first stretch. Fig. 4.1 shows the tension response and the sarcomere movements in a muscle stretched, released and restretched by $1020\mu\text{m}$ at a velocity of 4.08 mm.s^{-1} . The temperature was 2.5°C . Only the changes during the first and second stretches will be considered at this time; reference will be made later to what happens during the releases.

The form of the tension responses during the first stretch and the

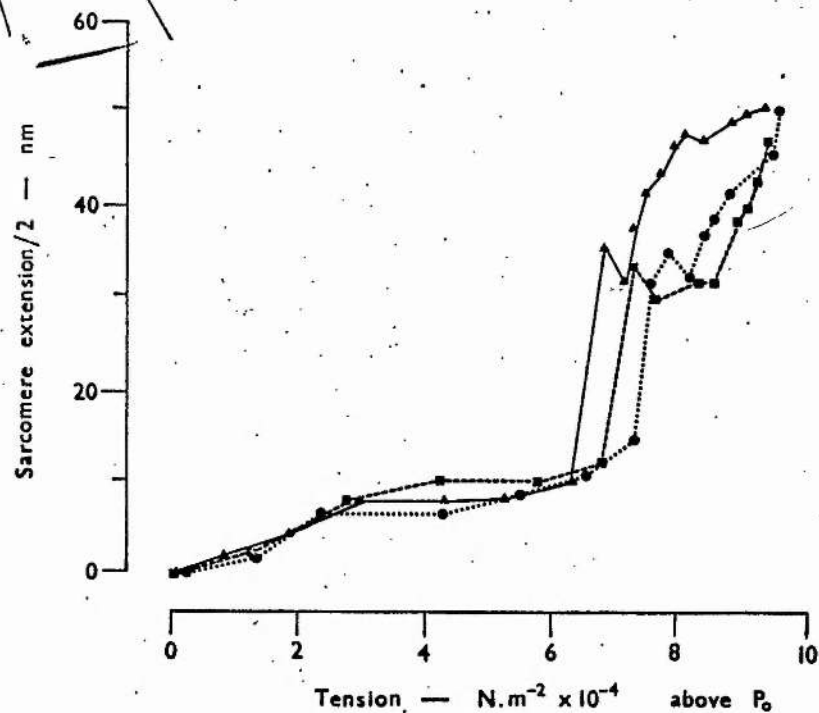


Fig. 4.2. Sarcomere length/tension diagrams, obtained during a first cycle stretch, from three different muscles.

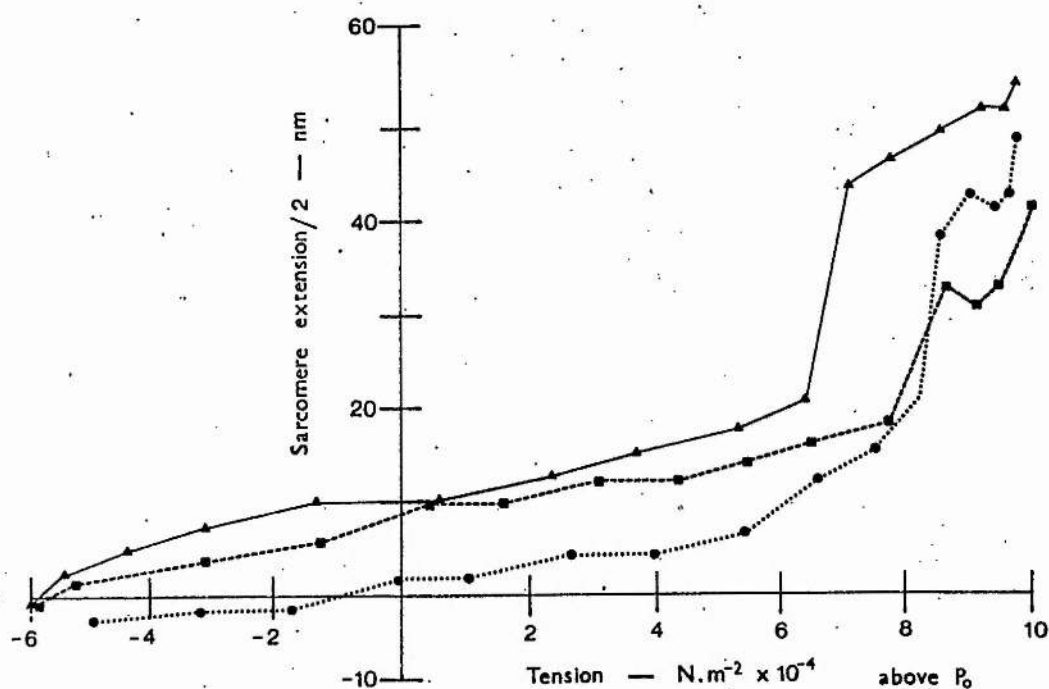


Fig. 4.3. Sarcomere length/tension diagram, obtained during a second cycle stretch, for three different muscles.

changes in sarcomere length are broadly similar to those described earlier, (Chapter III, Fig. 3.1). The results from three different muscles can be summarised as follows. First, the point S_2 and the rapid 'give' phenomenon occur for a relative sliding movement of 11.5 ± 0.9 (1 S.D.) nm per half sarcomere. Secondly, following release of the muscle, tension falls to $0.73 \times P_0$, and sarcomere length returns approximately to the value at peak isometric tension. The form of the tension increment produced by the second stretch is very different. There are several features of interest. First, the point S_2 is reached for a displacement of 18.3 ± 1.0 nm, which is approximately 1.6 x further than during a first stretch. Secondly, the tension increment up to S_2 is approximately 1.56 x greater. Third, the absolute tension held by the muscle at S_2 is about $1.38 \times P_0$ for a first stretch and $1.41 \times P_0$ for the second.

Length/tension relation of sarcomeres during first and second stretches.

The results for the three muscles referred to above are presented in the form of a sarcomere length/tension diagram in Fig. 4.2 (1st cycle) and 4.3 (2nd cycle). Filament displacement is plotted against tension above and below P_0 . The average stiffness of the sarcomeres during the period before rapid 'give' in the case of the first stretch is $5.8 \times 10^{12} \text{ N.m}^{-2}$ per metre extension of each half sarcomere, which is not greatly different from the value for sarcomere stiffness during a second stretch, $5.3 \times 10^{12} \text{ N.m}^{-2}$ per metre extension of each half sarcomere.

At S_2 sarcomere stiffness falls abruptly. An estimate of the change

in stiffness can be made by comparing the slopes of the relevant parts of the length/tension diagram. The mean value for sarcomere stiffness during rapid 'give' in the case of a first stretch is found to be approximately 30 x less than during the early part of the stretch (up to S_2) and approximately 23 x less in the case of a second stretch.

The stiffness of the sarcomeres rises again in the period following rapid 'give'. The extent to which it recovers during this phase is rather variable, but usually approximates to a value some 4.5 - 5.0 x smaller than the maximum sarcomere stiffness during a first stretch, and 5.5 - 6.0 x smaller in the case of a second stretch.

Velocity of sarcomere extension during rapid 'give' and the extent of movement of the sarcomeres. In all the experiments, the externally applied length change was made at a velocity of 4.08 mm.s^{-1} . If all the extension was taken up by the sarcomeres, the filaments in each half sarcomere would slide at a speed of $0.18 \mu\text{m.s}^{-1}$. During rapid 'give', the speed of lengthening is greatly in excess of this value. The results for three muscles gave a mean value of $1.42 \mu\text{m.s}^{-1}$, or approximately 8.0 x faster than the external length change. (This figure was estimated from the graph relating sarcomere extension to cine-frame number, and therefore represents the minimum speed of sliding during rapid 'give'.)

During the period of steady lengthening after rapid 'give' the mean value is $0.23 \mu\text{m.s}^{-1}$, which is close to the figure to be expected if filament sliding follows the external length change. The extent of

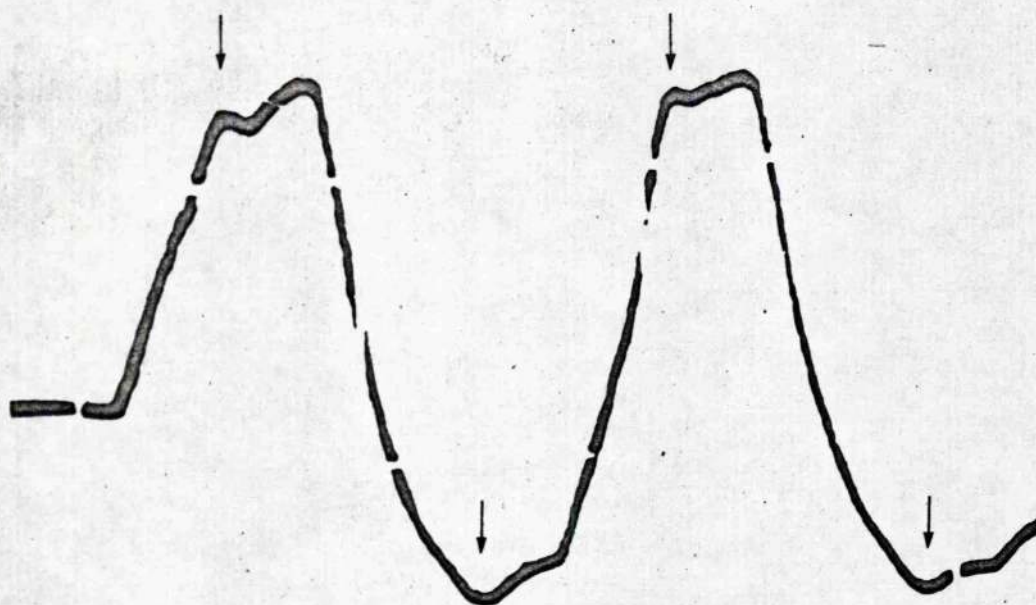


Fig. 4.4. Oscilloscope trace of the tension changes observed during cycles of stretch and release (same pattern as Fig. 4.1.), applied to a contracting muscle. When tension falls to a level, considerably below P_0 , during a release, sarcomeres are often capable of bringing about a rise in the level of tension, although the muscle is still being shortened at a velocity of about 4mm.s^{-1} .

The point of inflection during release, is referred to as $-S_2$, although all traces do not show it as clearly as that illustrated here.

The points S_2 and $-S_2$ are shown arrowed.

filament sliding during rapid 'give' is found to be 21.4 nm for a first stretch and 20.0 nm for a second. This brings the total sarcomere extension to about the value calculated on the assumption that the whole of the externally applied length change is taken up by the sarcomeres.

Changes of sarcomere length and tension during release. Fig. 4.1 shows that the changes in sarcomere length and tension during a release are not the converse of those seen during a stretch, although there are certain similarities. First, tension falls steeply during the early part of a release, at a time when sarcomere length is changing relatively slowly. Secondly, when the sarcomeres have returned to about the length corresponding with that reached at the end of rapid 'give' (during the preceeding stretch) the speed of shortening increases abruptly, and this corresponds with a reduction in the rate of tension decline; indeed, in some records tension may either level off, or even increase (eg. Fig. 4.4) during the later stages of a shortening step. The point corresponding with rapid shortening of sarcomeres and the decrease in the rate of fall of tension is designated '-S₂'. The amount of filament displacement required to reach this point is not constant, but depends upon the amount of sarcomere extension taking place during the interval following rapid 'give' and the end of the preceeding stretch. The results from the first and second cycles of Fig. 4.1 serve to clarify this point. During the first cycle, the sarcomeres are extended by 37.0 nm in this period and abrupt shortening during the release occurs when the sarcomere length has been altered by 36.0 nm in the opposite

direction. The values for the second cycle are considerably less; 24.0 and 19.0 nm respectively. The differences between first and second cycles arise because a greater amount of the external length change is required to reach S_2 in the case of a second stretch, and therefore less is available to extend the muscle in the period following rapid 'give'.

Velocity and extent of rapid sarcomere shortening during release. During the rapid phase of sarcomere shortening the filaments move at a surprisingly high velocity. If the filaments followed the external length change, then they would slide past each other at a velocity of $0.18 \mu\text{m} \cdot \text{s}^{-1}$, and in the early part of a release they move at about this speed (mean; $0.14 \mu\text{m} \cdot \text{s}^{-1}$, for the same three records of Figs. 4.2, 4.3). However, during rapid shortening, the filaments move very much faster than this, at a speed not less than $1.1 \mu\text{m} \cdot \text{s}^{-1}$. It is interesting to compare this figure with the maximum rate of sliding of the filaments in an unloaded isotonic contraction. A.V. Hill (1970) gave a mean value of $1.4 \times 10^{-3} \text{s}^{-1}$ for a whole sartorius at 0°C , which is equivalent to about $1.7 \mu\text{m} \cdot \text{s}^{-1}$ for each half sarcomere. So, in rapid shortening during release the filaments move at a rate which is comparable with that in an unloaded isotonic contraction, even though the tension borne by the muscle at this time is close to the maximum isometric tension. The extent of rapid shortening during release is found to be 12.0 nm per half sarcomere for a first cycle release and 13.0 nm per half sarcomere for a second.

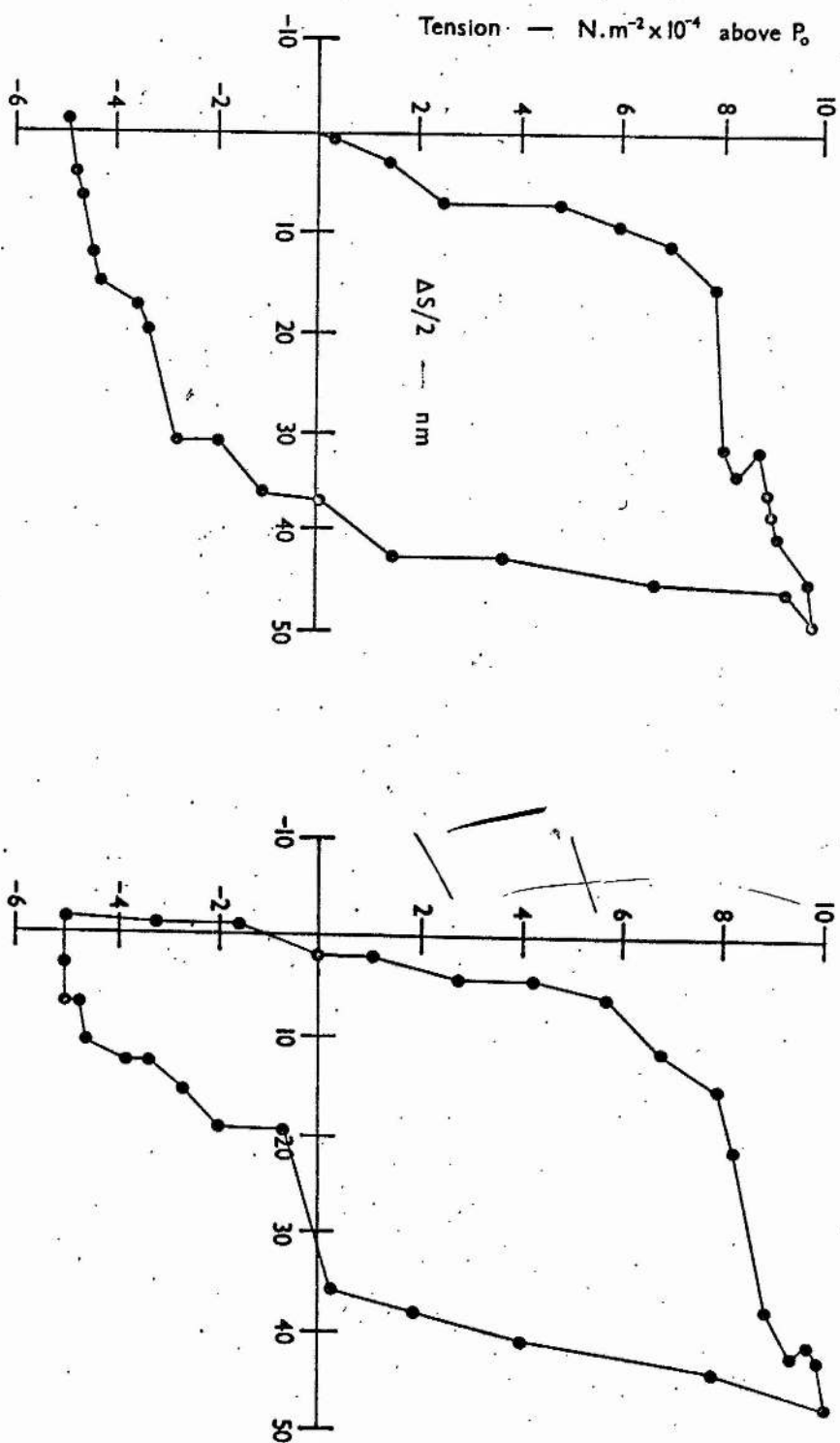


Fig. 4.5. Sarcomere length/tension diagrams for both first (1) and second (2) cycles of stretch and release. Points form 'clockwise loops'. Values for extension per half sarcomere are given in nm. Individual points are the means from the three muscles in Figs. 4.2 and 4.3, but the axes are interchanged.

Length/tension diagram for sarcomeres during release. During the early part of a release, tension falls steeply for a relatively small decrease in sarcomere length; sarcomere stiffness during this phase is comparable with that seen during the early part of a stretch (Fig. 4.5). A mean value is $6.8 \times 10^{12} \text{ N.m}^{-2}$ per metre extension of each half sarcomere for a first cycle, and $9.0 \times 10^{12} \text{ N.m}^{-2}$ per metre extension of each half sarcomere, in the case of a second cycle release.

At the point designated $-S_2$, sarcomere stiffness falls abruptly, although the transition from the relatively high level of stiffness seen at the beginning of the length change is less clearly defined than in the case of a stretch. None the less, an estimate of the change in stiffness can be made by comparing the slopes of the relevant parts of the length-tension diagram, and this reveals that mean sarcomere stiffness during rapid shortening in a first release is about 15 x less than during the early part of a release and about 18 x less for a second release.

In the period between the end of rapid shortening and the end of the length change, muscle stiffness is very variable (as it is during the corresponding phase of a stretch). This is due largely to the ability of some muscles actively to generate force at this time, producing a rise in the level of muscle tension, although the shortening step is still continuing.

Tension changes during a delayed second stretch and release cycle. It is clear from what has been said that the previous history of a muscle greatly influences the form of the tension response to stretch; the degree

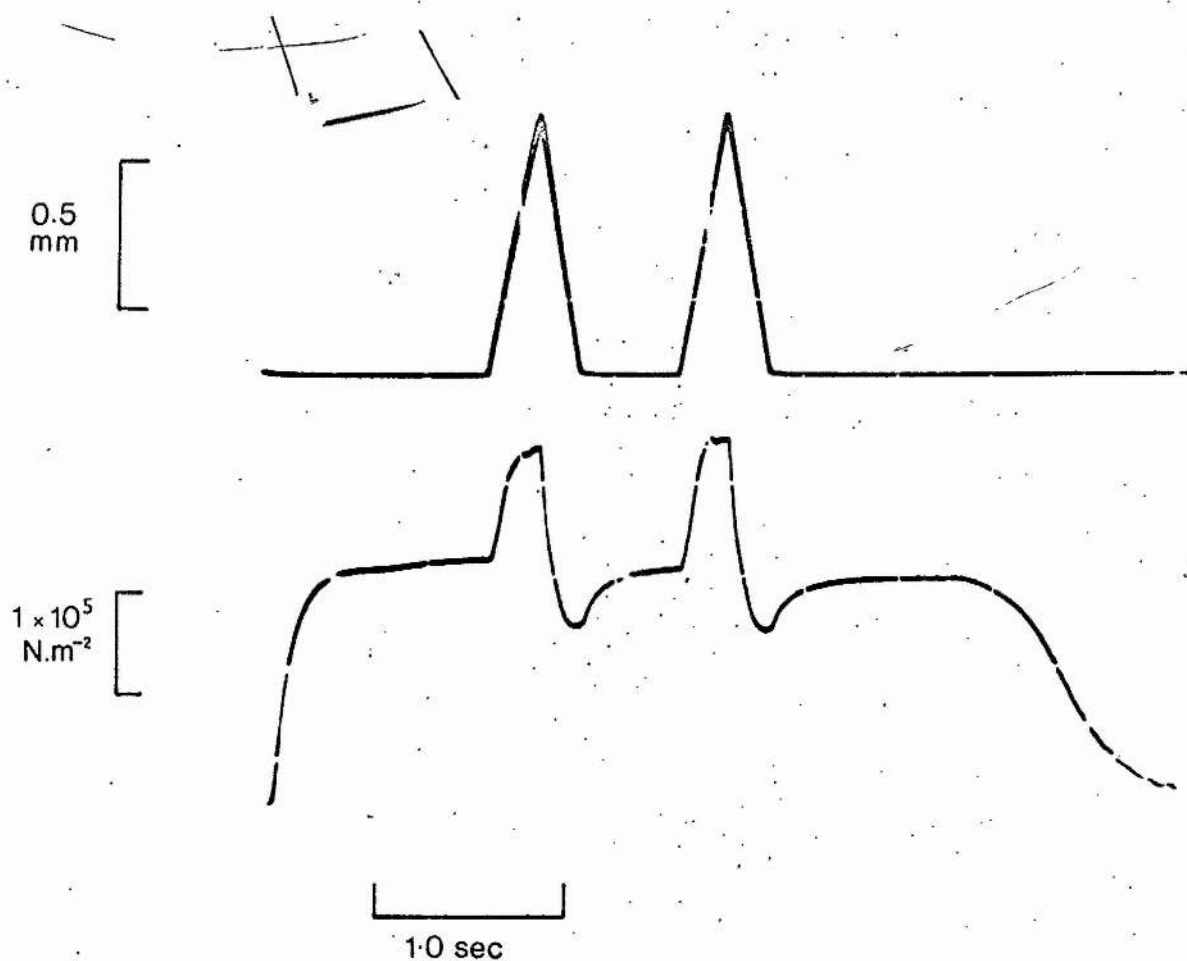


Fig. 4.6. Tension changes (lower trace) produced by a DDSR cycle (upper trace), applied during the plateau of a tetanus.

of extension required to reach the point S_2 for a second stretch is always considerably greater (about 50%) than for a first stretch. This result poses an interesting question: does the tension response of a muscle to a second cycle stretch also differ from that of a first when it is delayed by several hundred milliseconds?

Fig. 4.6 shows the effect of a double stretch and release cycle applied at the peak of a tetanus. A delay of 500 ms was allowed between the end of the first release and the beginning of the second stretch. A comparison of the tension responses to each stretch shows that this interval is sufficient to allow some recovery to take place. The amount of extension required to reach S_2 in the delayed second stretch is greater than during the first stretch ($435\mu\text{m}$, compared with $390\mu\text{m}$), although the important point to emphasize is that the difference is much less than for a second stretch applied immediately after release ($630\mu\text{m}$). Moreover, tension at S_2 rises to a higher value ($1.49 \times P_0$, compared with $1.38 \times P_0$ during the first stretch) and the transition at S_2 is more abrupt. The effects of delayed stretches have not been investigated in any detail, but it is possible that complete recovery will occur if sufficient time is allowed between successive cycles.



DISCUSSION

Working hypothesis.

It is necessary at this time to introduce a working hypothesis in order to explain the results obtained in this and the preceding chapter and to serve as a base for further experiments. It will be seen that many features of the tension records and sarcomere movements can be accommodated in the Huxley-Simmons model, which envisages the cross-bridge as being made up of an instantaneous elastic component with Hookean characteristics (their AB linkage; see Fig. 1.16), in series with a force generating element having both elastic and viscous properties. It will be recalled that the S_1 subunit of myosin, in which actin binding and ATPase activity reside, is thought to have a small number, n , of attachment sites ($M_1 M_2 \dots M_n$) through which it can bind to corresponding sites on an actin active region ($A_1 A_2 \dots A_n$). It is postulated that simultaneous attachment of the myosin head at two consecutive sites (say, $A_1 M_1$ and $A_2 M_2$) constitutes a stable linkage, and that subsequent movement of the myosin head along the actin active region proceeds in a series of discrete steps, each having a progressively lower potential energy than the preceding one.

Huxley & Simmons consider that the most likely number of attachment sites is four, with three stable positions and the full range of movement taking place in two steps. They have shown that an abrupt decrease of length (completed in less than 1 ms), equivalent to about 5.0 nm movement

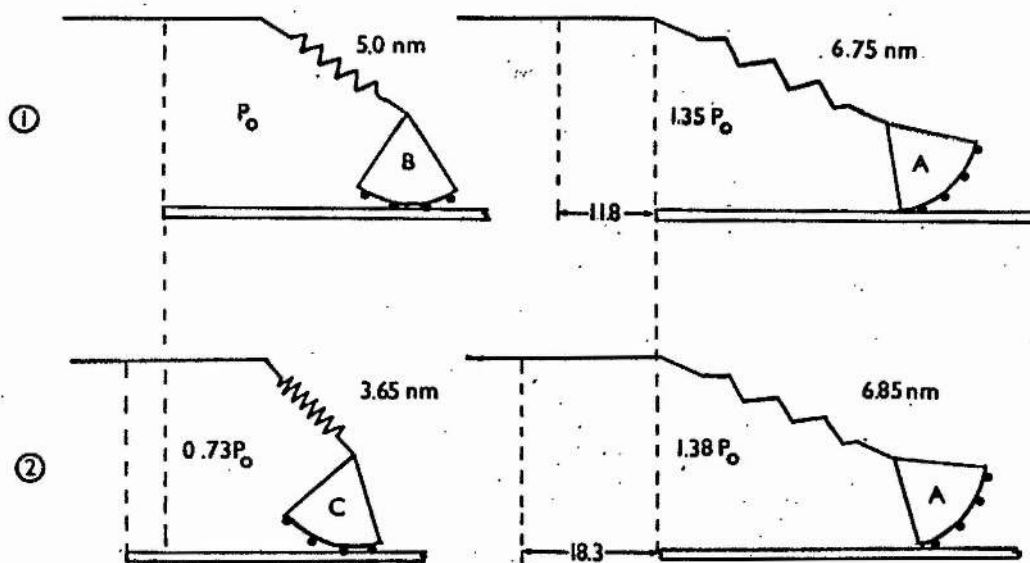


Fig. 4.7. A possible scheme for the changes of orientation of the cross-bridge, which are thought to occur during first (1) and second (2) stretches.

- A. Mean head position at S_2 for first and second stretches
- B. Mean head position at P_0 , before the application of a first stretch.
- C. Mean head position at the end of a first release, i.e., immediately before a second stretch.

per half sarcomere, is sufficient to cause isometric tension to fall to zero, and that during the few milliseconds following release, substantial tension recovery occurs. Progressively less tension is recovered when steps in excess of 5.0 nm are applied, and for displacements exceeding 13 nm, no rapid tension recovery is possible. Thus, when a muscle is maintaining peak isometric tension, the instantaneous elastic elements must, on average, be extended by about 5.0 nm beyond their unloaded (zero tension) length.

Fig. 4.7 summarises the events which it is thought might take place during stretches such as those employed in the present experiments. For simplicity, only a single head will be considered. The position the head adopts will depend upon both the potential energy gradient tending to cause it to rotate forwards, and the elastic tension generated in the AB link, which acts to oppose this movement. It is postulated that at peak tension the majority of the heads spend most of their time in position B ($A_2M_2 - A_3M_3$), and that in this position the AB linkages are, on average, extended by 5.0 nm. Thus, a rapid shortening step change of 5.0 nm (sufficiently rapid to occur before the head has had time to rotate) will abolish tension altogether. During the few milliseconds immediately after the length change the heads will move to adopt position C ($A_3M_3 - A_4M_4$) and re-extend the AB linkage, so redeveloping tension. From Huxley's recent T_1 and T_2 curves (Huxley, 1974), it appears that in rotating from B to C, the linkages are extended by less than 5.0 nm, because peak isometric tension is not fully regained; instead, tension

recovers to about $0.78 \times P_0$, suggesting that the linkages are restretched by about $0.78 \times 5.0 = 3.9 \text{ nm}$.

Consider what may happen to the system when the muscle is subjected to a ramp and hold stretch. During the early part of the stretch (up to S_1) tension is generated by extension of the AB linkage and the head maintains its position. When tension reaches $1.075 \times P_0$ (tension at S_1), the myosin head begins to rotate backwards against its natural tendency to move to the next position of lower potential energy. Tension continues to rise after S_1 , which means that the applied length change is being taken up both by rotation of the head, and by further extension of the AB linkage. Rapid sarcomere 'give' occurs at S_2 , when muscle tension has reached $1.38 \times P_0$, and for a filament displacement of 11.5 nm .

The question is, how much of this movement is translated into rotation of the head and how much is absorbed by extension of the AB link? Since the two elements are in series, the AB link is holding a tension of $1.38 \times P_0$ at S_2 , and it must therefore be extended by $1.38 \times 5.0 \text{ nm} = 6.9 \text{ nm}$. The extra extension of the AB link generated by the applied length change is thus $6.9 - 5.0 = 1.9 \text{ nm}$. Rotation of the head must then account for $11.5 - 1.9 = 9.6 \text{ nm}$ of movement.

Consider what happens during a second stretch, following a preceding release. Tension falls to $0.73 \times P_0$ at the end of the release, so at the commencement of a second stretch, the AB link is extended by $0.73 \times 5.0 \text{ nm} = 3.65 \text{ nm}$. Total filament displacement to S_2 for a second stretch is 18.30 nm and this corresponds with a tension of $1.41 \times P_0$, which

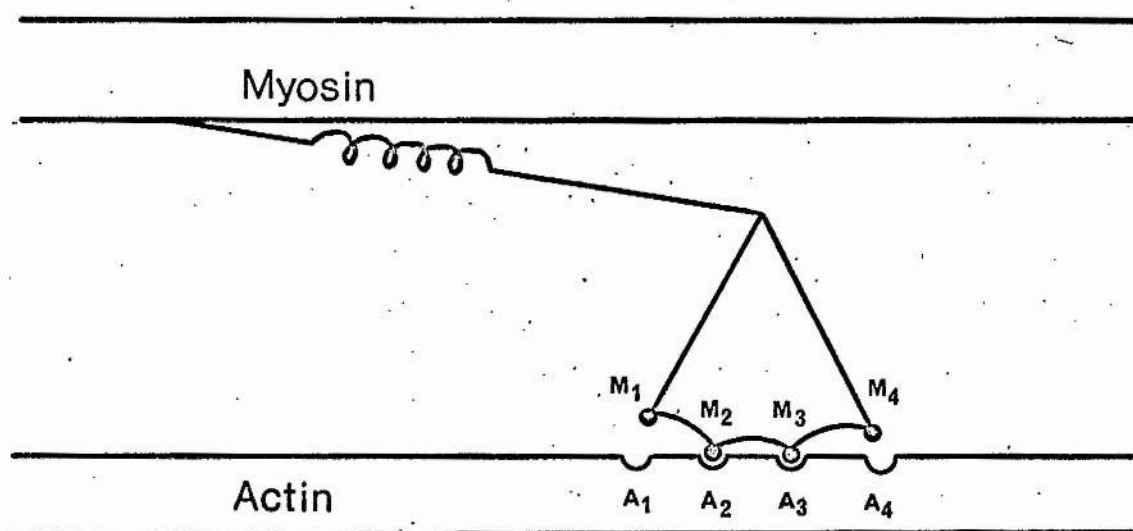


Fig. 4.8. Diagram of a myosin cross-bridge attached to the actin active region in position B ($A_2M_2 - A_3M_3$).

gives a value of 7.05 nm (1.41×5.0 nm) for extension of the AB linkage. Thus, of the 18.3 nm movement of the filaments $7.05 - 3.65 = 3.40$ nm goes into extending the AB linkage, leaving 14.9 nm to be accounted for by rotation of the head.

The important conclusion to emerge from this analysis is that the stable positions corresponding to peak isometric tension and those occupied by the heads at the end of a release are separated by a distance of $14.9 - 9.6 = 5.3$ nm.

The range of filament displacement required to reach S_2 during a first stretch has been shown to be approximately twice that required in rapid release to abolish isometric tension (9.6, compared to 5.0 nm). This may seem surprising at first, but the explanation is quite straight forward. Consider Fig. 4.8. Initially, the head attaches to the actin filament through the two sites A_1M_1 and A_2M_2 , rotates to position B ($A_2M_2 - A_3M_3$) and in so doing generates full isometric tension by extension of the AB link (5 nm). Hence, an abrupt shortening step of 5 nm abolishes tension completely. Now, during stretch, 5 nm of movement will force the head back to position $A_1M_1 - A_2M_2$ but will not be sufficient to cause forcible detachment. The figures obtained experimentally imply instead that the single site A_1M_1 can remain attached for a further 4.5 - 5.0 nm of movement before it too is forcibly broken.

The experiments described in this chapter permit one to speculate on the nature of the actin active region. The results are entirely consistent with the Huxley-Simmons model and suggest a structure approximately

15.0 nm in length, comprising 4 equally-spaced attachment sites, separated by about 5.0 nm (4.8 - 5.4 nm). This distance is comparable with the centre to centre spacing of the actin subunits that constitute the thin filament (Hanson, 1968) and it is conceivable, therefore, that each attachment site is located on a single monomer.

CHAPTER V

THE EFFECT OF TEMPERATURE AND VELOCITY OF LENGTH CHANGE ON THE FORM OF THE TENSION RESPONSE.

In the experiments referred to in the preceeding chapters, relatively slow length changes were applied to the muscle by comparison with those employed by Huxley & Simmons in their experiments. This was unavoidable because the cine camera used to record the movements of the diffraction spectra had a maximum operating speed of only 64 frames per second, which limited the sampling rate to one observation per 15 ms. The important point at issue in making the experiments to be presented in this chapter was: do such relatively slow stretches allow sufficient time for cross-bridge cycling to occur?

There are two, related ways of investigating this question; first, to study the effect of varying the velocity of stretch on the form of the tension record; and secondly, to examine the temperature dependence of the tension response. It was reasoned that if the rate of cycling of the cross-bridges has a significant effect on the response, then altering the temperature at a given velocity of stretch, or alternatively, varying the velocity of stretch at constant temperature, ought to provide some assessment of its importance.

It was decided at the outset to measure two features of the tension

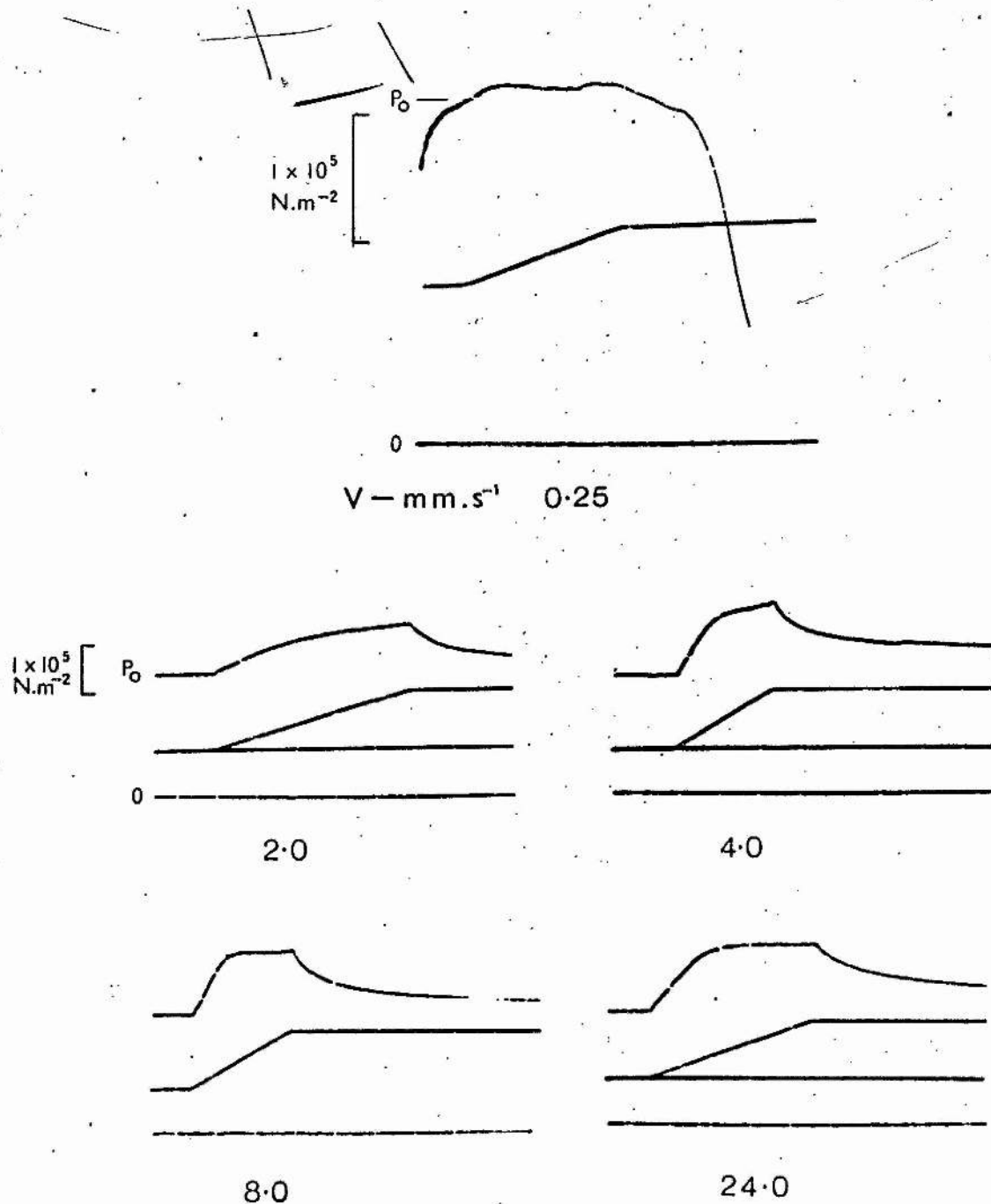


Fig. 5.1. A series of records showing the tension responses produced by subjecting a contracting muscle to ramp and hold stretches of $1060\mu\text{m}$, at velocities from $0.25 - 24\text{mm.s}^{-1}$ ($0.009 - 0.86 \times 1_0$). Stretch velocities are shown below each record, in mm.s^{-1} . The applied length changes are shown, along with the tension base line (0).

The top record was made at a higher gain, because the tension generated by a stretch at 0.25mm.s^{-1} , is small.

record:

- 1) The maximum 'holding force' supported by the sarcomeres at the point S_2 , where rapid extension occurs; this is referred to hereafter as P_{S_2} .
- 2) The mean stiffness of the muscle up to this point (E_m).

With regard to the measurement of muscle stiffness, the tension increment produced on stretching to S_2 was necessarily related to the external length change imposed on the muscle, since for the reason given above, the movement of the diffraction spectra could not be followed with sufficient time resolution to permit observations to be made over the range of velocities investigated.

It was assumed initially that both P_{S_2} and E_m would be proportional to the number of active cross-bridges holding the filament together and that this number would be inversely related to their speed of cycling. Accordingly, it was anticipated that below a certain critical speed of stretch the response ought to show a dependence on velocity, but not above it. This will be shown to be so. However, experiments in which temperature was varied over a wide range (0 - 30 °C) revealed a striking difference in the way in which the critical velocities for P_{S_2} and E_m varied and consequently, they raise some doubt about the original assumption that both parameters are related in a simple way to the speed of cross-bridge cycling. Indeed, from the evidence it appears that there may be two parallel reactions involving ATP hydrolysis, to which P_{S_2} and E_m are

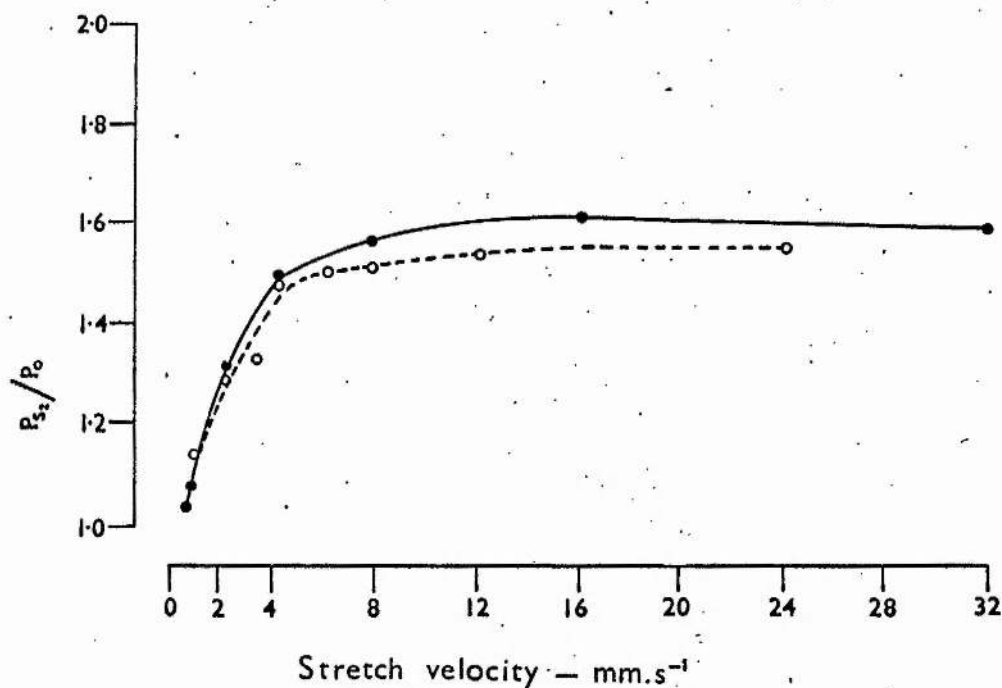


Fig. 5.2. Values for the tension generated at S_2 (P_{S_2}), expressed as a multiple of the isometric tension (P_0), plotted against the speed of stretch. Results are from two muscles.

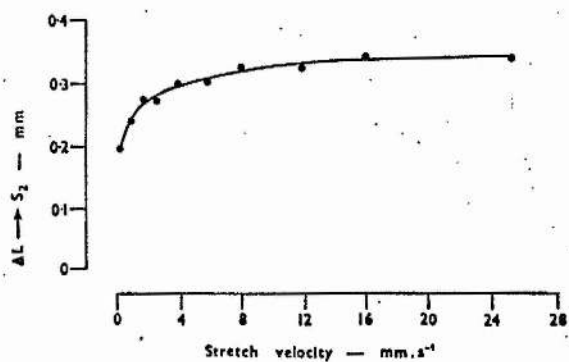


Fig. 5.3. Muscle extension required to reach S_2 , plotted against the speed of stretch.

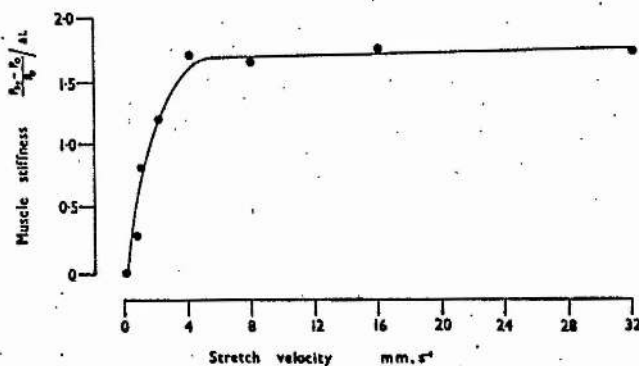


Fig. 5.4. Muscle stiffness, given by $\frac{\Delta P}{P_0} / \Delta L$, plotted against the speed of stretch.

separately related. If further experiments should prove this to be so, then a detailed study of these two muscle parameters may afford an experimental approach by means of which the two processes may be studied in the living, intact muscle.

Dependence of P_{S_2} on velocity of stretch. Several records showing the tension response produced by subjecting a contracting muscle to a ramp and hold stretch of $1060 \mu\text{m}$ at velocities ranging from $0.25 - 24 \text{ mm.s}^{-1}$ are shown in Fig. 5.1. The muscle was stimulated tetanically at a temperature of 0°C . The point S_2 at which rapid sarcomere extension occurs is visible in all records, although for slower stretch velocities the response is generally more rounded in form. The results for two experiments in which the maximum tension borne by the sarcomeres (P_{S_2}) expressed as a multiple of the isometric tension (P_0) is plotted against velocity of stretch are shown in Fig. 5.2. The value of P_{S_2}/P_0 increases in a roughly linear fashion with increasing velocity, reaching a maximum of 1.55 at about 4 mm.s^{-1} ; thereafter, it remains more or less constant. Thus, there is a range of velocities over which P_{S_2}/P_0 is highly velocity dependent and a range over which it shows little or no dependence.

The particular velocity marking the transition between these two ranges (3.8 mm.s^{-1} in this instance) is referred to as the critical velocity and is denoted by C_v . For practical purposes it can be considered to represent the minimum velocity of stretch required to give an 'undistorted' tension response, in the sense that there is insufficient time for an

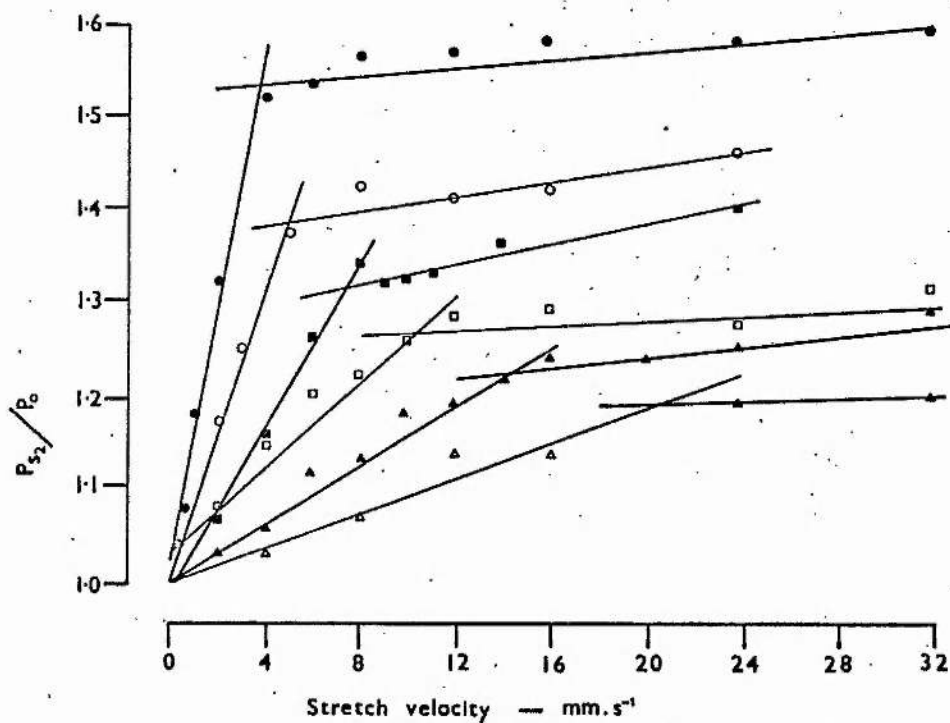


Fig. 5.5. A family of curves for P_{S_2}/P_0 plotted against speed of stretch, at the following temperatures:-

●—● 0°C; ○—○ 6°C; ■—■ 12°C; □—□ 18°C;
▲—▲ 23°C; △—△ 30°C.

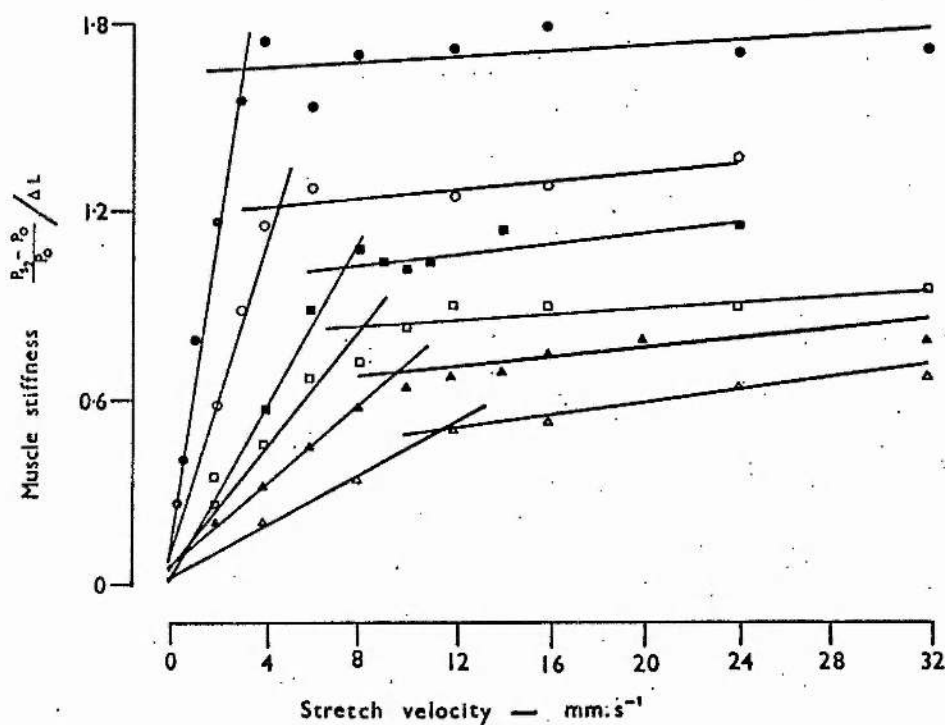


Fig. 5.6. A family of curves for muscle stiffness plotted against speed of stretch, at the same temperatures as shown in Fig. 5.5.

appreciable number of the cross-bridges to execute their 'normal' forward movement and detach. It will be recalled that the preceeding experiments involving the measurement of diffraction spectra were made at about 0°C and employed stretches at a velocity of 4mm.s^{-1} .

Dependence of muscle stiffness (E_m) on velocity of stretch. The stiffness of the muscle, E_m , is given by:

$$\frac{\Delta P/P_0}{\Delta L_m}$$

where $\Delta P = P_{S_2} - P_0$.

and ΔL_m = external length change required to reach S_2 .

Fig. 5.3 shows that ΔL_m is independent of the velocity of stretch for speeds greater than about 4mm.s^{-1} , but falls from approximately $300\mu\text{m}$ to $190\mu\text{m}$ over the range $0.25 - 4\text{mm.s}^{-1}$. The values obtained for E_m (arbitrary units) are plotted against speed of stretch in Fig. 5.4. The overall shape of the curve is similar to that obtained when P_{S_2}/P_0 is plotted against velocity. In this particular instance, for an experiment made at 0°C , C_v is found to be 3.5mm.s^{-1} .

Dependence of C_v for P_{S_2}/P_0 and E_m on temperature. If the values of C_v for both parameters are related to the rate of cycling of the cross-bridges, then they ought to be increased by raising the temperature.

Fig. 5.5 shows a family of curves for P_{S_2}/P_0 against stretch velocity

Temperature °C	CV P_{S_2}/P_0	CV E_m
0	3.8	3.5
6	5.0	4.8
12	7.5	7.4
18	10.5	9.0
23	14.5	10.1
30	21.8	13.0

Table 5. Critical velocity values for P_{S_2}/P_0 (column 2) and E_m (column 3) for each of the experimental temperatures (column 1).

at a series of temperatures ranging from 0 - 30°C. The curves have the same form as those shown in Fig. 5.2 , but the discontinuity representing C_V is displaced to the right, towards higher velocities , at the higher temperatures. Table 5 , column 2 lists the values of C_V for each of the temperatures studied. They increase approximately 6x on raising the temperature from 0°C to 30°C.

A similar family of curves relating E_m to stretch velocity at different temperatures is shown in Fig. 5.6. C_V values at each of the temperatures are listed in Table 5 , column 3 and should be compared with those obtained for PS_2 .

This comparison reveals an interesting difference in the way in which the C_V 's for PS_2/P_O and E_m vary with temperature. For temperatures up to 12°C they are not markedly different (as would be expected if the C_V for both parameters was related to cross-bridge cycling in a simple way), but beyond this temperature the C_V for E_m shows a relatively slight dependence on temperature, as compared with the corresponding values for PS_2/P_O . Thus, over the range 12 - 30°C, the critical velocity for E_m increases only 1.76 x, whereas over the same range of temperatures there is a 3-fold increase in C_V for PS_2/P_O .

The point is more strikingly demonstrated when the C_V 's are plotted against temperature. The value for PS_2/P_O increases in an exponential fashion, with a Q_{10} of 1.78 (Fig. 5.7). On the other hand, the increase in C_V for E_m is more complex, and the curve (Fig. 5.8) appears to

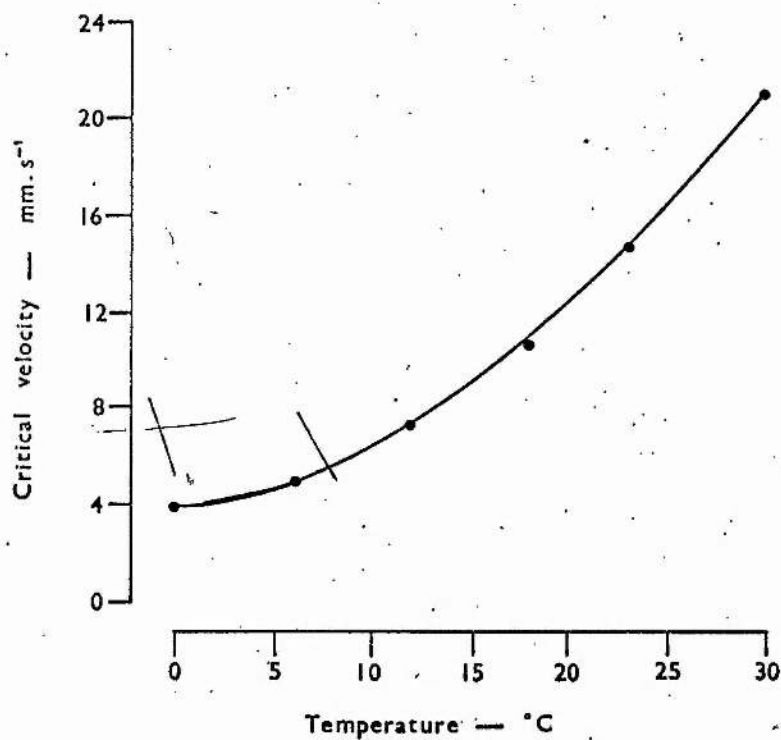


Fig. 5.7. Critical velocity (C_v) values for Ps_2/PO plotted against temperature.

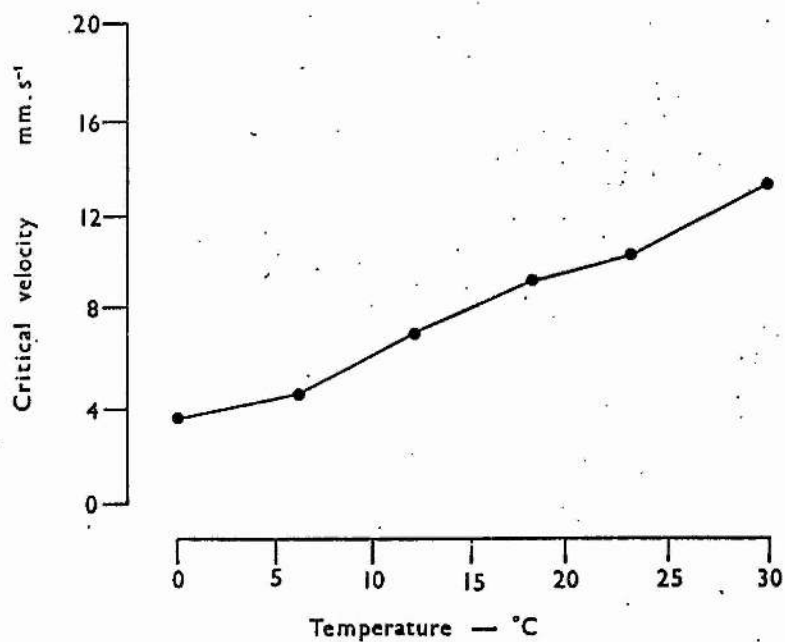


Fig. 5.8. Critical velocity (C_v) values for Em plotted against temperature.

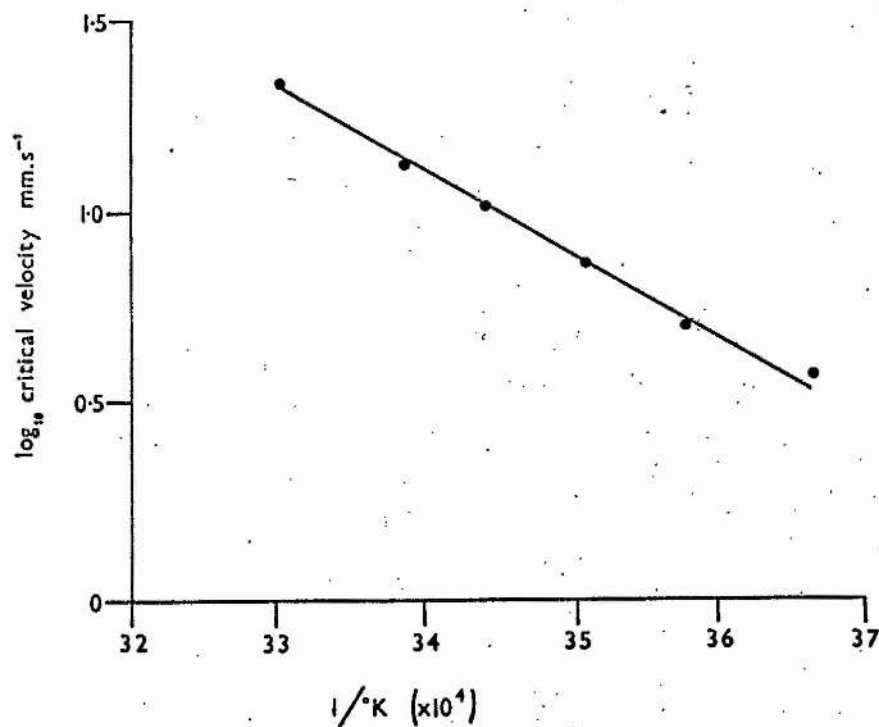


Fig. 5.9. The same data as that shown in Fig. 5.7, but displayed in the form of an Arrhenius plot: $\log_{10} C_v$ against $1/\text{absolute temperature}$.

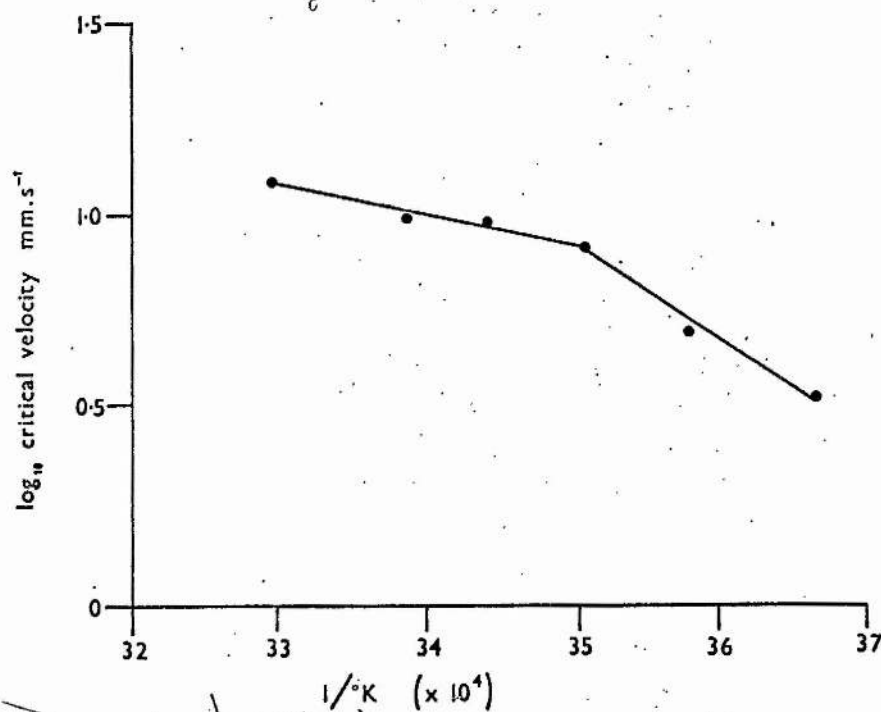


Fig. 5.10. The same data as that shown in Fig. 5.8, but displayed in the form of an Arrhenius plot.

consist of two segments; one in the range $0 - 12^{\circ}\text{C}$, with a Q_{10} of 1.78 and one in the range $12 - 30^{\circ}\text{C}$ with a Q_{10} of 1.44.

This result questions the original assumption that the critical velocities for both parameters are related directly to cross-bridge cycle time. Two obvious points are raised: first, which, if either, of the two C_v 's more accurately reflects cross-bridge cycle time and second, what is the significance of the transition temperature (12°C) separating the two halves of the curve for E_m ?

In attempting to answer these questions it is useful to present the data in the form of Arrhenius plots, in which the $\log_{10} C_v$ is plotted against the reciprocal of the absolute temperature, so that the activation energies of the (unidentified) rate-limiting steps can then be estimated. The activation energy, E , is obtained from the slope, S , of the line, and is given by:

$$E = S \cdot 2.303R$$

where R = universal gas constant.

Figs. 5.9 and 5.10 show Arrhenius plots of the C_v values for P_{S_2}/P_O and E_m . The plot for P_{S_2}/P_O gives a single straight line, with an activation energy of $9.78 \text{ kcal. mol}^{-1} \cdot ^{\circ}\text{K}^{-1}$. The corresponding plot for E_m is more complex, consisting of two straight segments, intersecting at 12°C and yielding activation energies of $12.5 \text{ kcal. mol}^{-1} \cdot ^{\circ}\text{K}^{-1}$ (below 12°C) and $4.0 \text{ kcal. mol}^{-1} \cdot ^{\circ}\text{K}^{-1}$ (above 12°C).

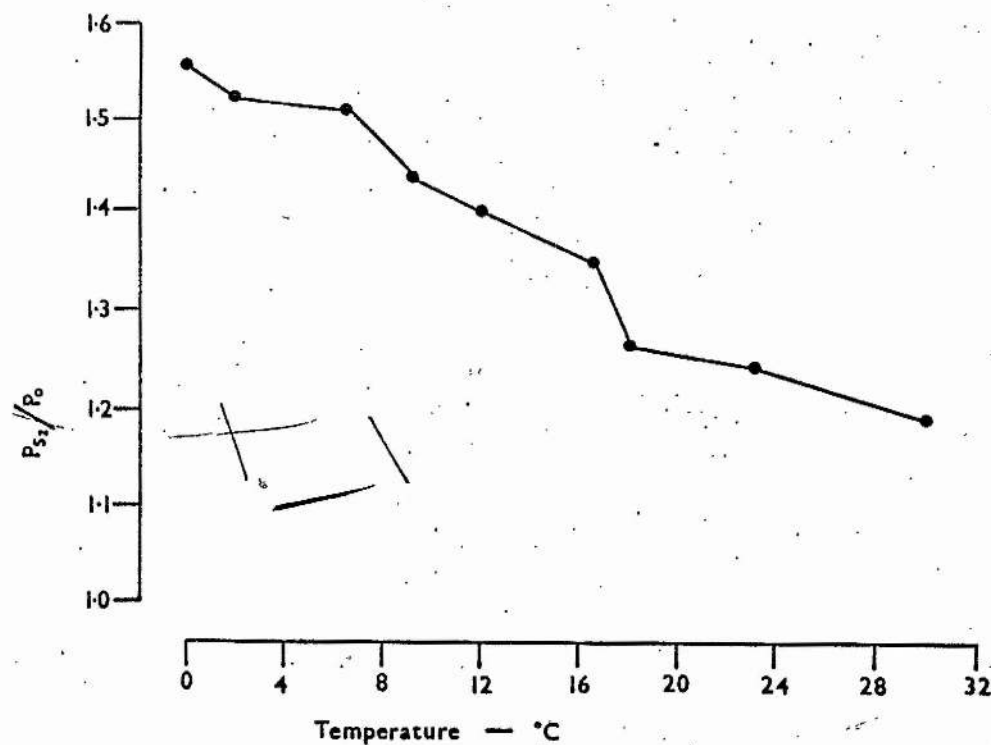


Fig. 5.11. Plateau values for P_{S_2}/P_0 plotted against temperature. Velocity of stretch: 24mm.s^{-1} .

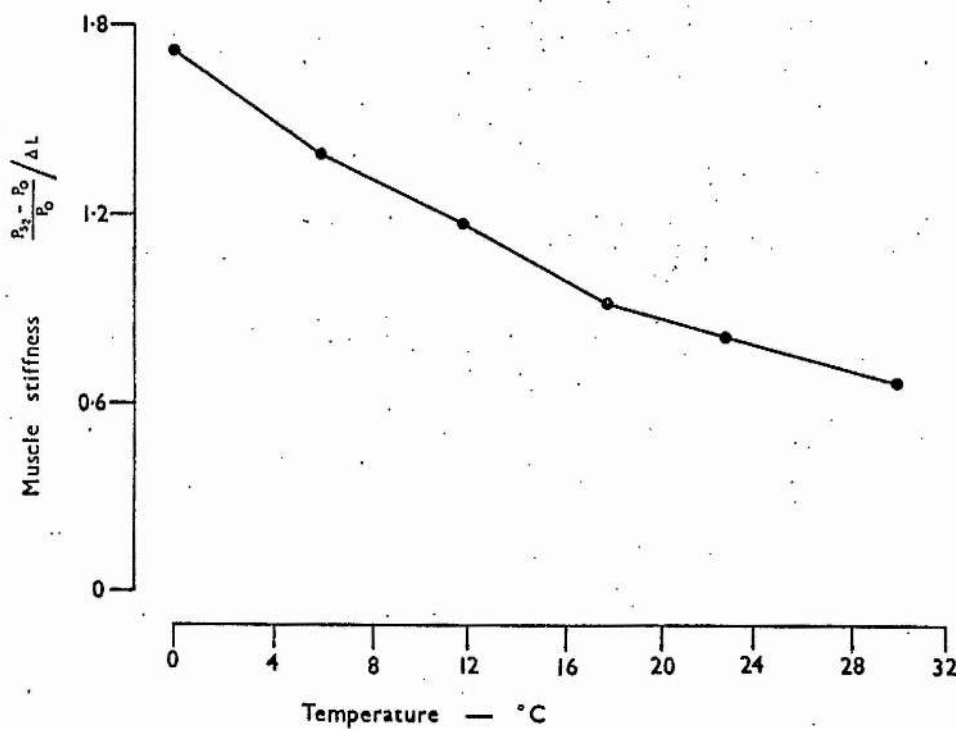


Fig. 5.12. Plateau values for E_m plotted against temperature. Velocity of stretch: 24mm.s^{-1} .

Dependence of maximum P_{S_2}/P_O and E_m values on temperature. The maximum (plateau) values for P_{S_2}/P_O and E_m show a relatively small, inverse dependence on temperature Figs. 5.11 and 5.12 show the values obtained by stretching at 24mm.s^{-1} plotted against temperature. At this speed of stretch the response is not markedly affected by cross-bridge cycling, since 24mm.s^{-1} is well above the critical velocity at all temperatures. P_{S_2}/P_O decreases in a roughly linear manner with increasing temperature, from 1.50 - 1.20 in the range $0 - 30^\circ\text{C}$, a 1.3 fold decrease. E_m shows a greater dependence on temperature, decreasing by 2.13 x over the same temperature range. It will be noted that neither P_{S_2}/P_O nor E_m show the large temperature dependence which would be expected for a chemical process.

DISCUSSION

The aim in making this series of experiments was to see if the tension responses are markedly affected by the velocity of stretching. The experiments of the preceeding chapter were conducted at $0-2.5^{\circ}\text{C}$, using comparatively slow speeds of stretching (about $4\text{ mm}\cdot\text{s}^{-1}$) for the reasons already given. It has been shown that at this temperature, the C_V is about $3.8\text{ mm}\cdot\text{s}^{-1}$, below which PS_2/P_0 and E_m show an almost linear dependence on velocity, but above which the values are relatively unaffected by any further increase in speed. It may be safely concluded, therefore, that the method of analysis used earlier to account for the tension responses and concomitant changes in sarcomere length in terms of the Huxley & Simmons model is not seriously compromised by having ignored temporarily the possibility of cycling of cross-bridges during the period of stretch.

It may seem surprising at first sight to find that such slow stretches (approximately $1/10$ th of the maximum velocity of shortening of the sarcomeres during an unloaded, isotonic contraction) are sufficient to eliminate the effects of cross-bridge cycling, but the recent work of Curtin, Gilbert, Kretzschmar & Wilkie (1974) has shown that the mean cycle time of the cross-bridges during an isometric contraction is rather long; they arrive at a figure of around 340 ms at 0°C .

In the event the experiments have provided additional information of

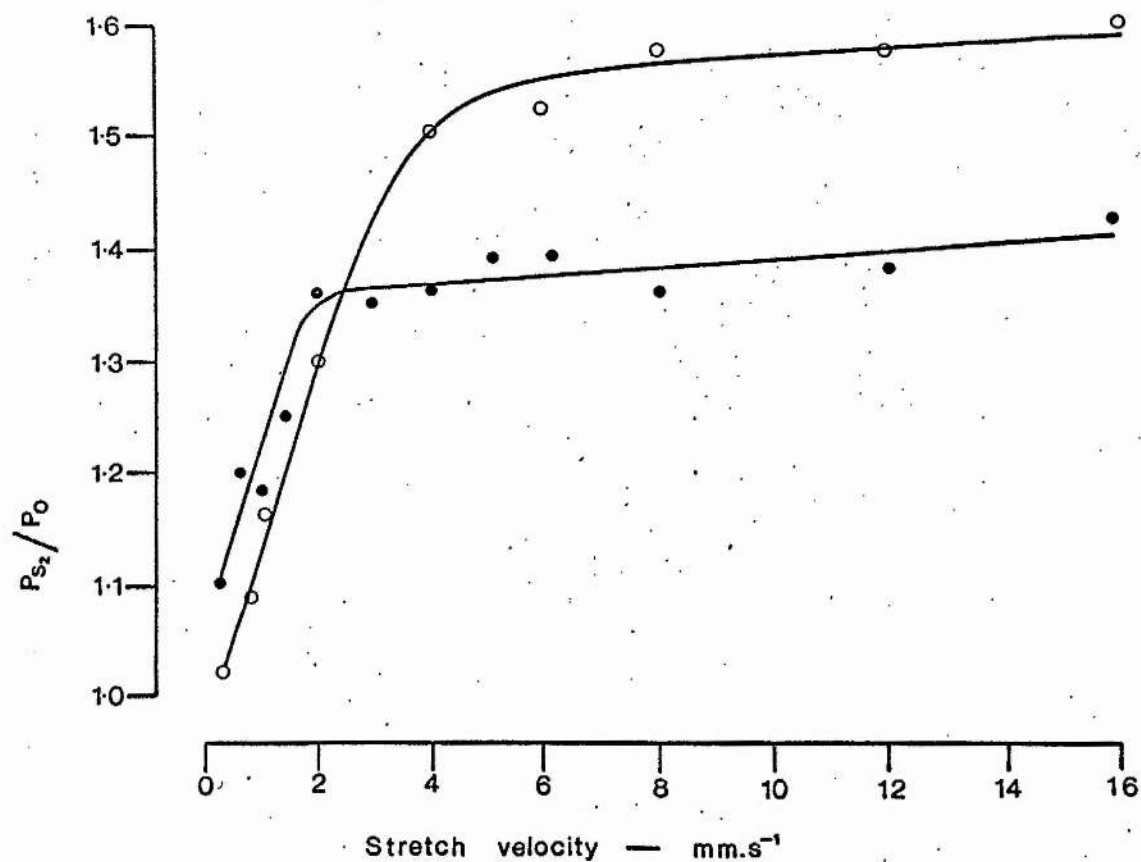


Fig. 5.13. The velocity dependence of P_{S_2}/P_O for frog sartorius (open circles) and toad sartorius (filled circles).

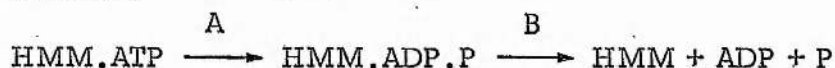
Temperature : 0°C .

considerable interest. The original assumption had been that P_{S_2}/P_0 and E_m would provide a straight forward index of the rate of cross-bridge cycling. The rationale was simply that both the maximum holding force and muscle stiffness ought to depend only on the number of cross-bridges linking the filaments together, which would in turn be inversely related to the speed of cycling. There are a number of consequences of this view. First, the C_v 's ought to increase with increasing temperature, since the rate of cycling will be greater at higher temperatures. This point is taken up again later. Secondly, C_v values ought to be proportional to the intrinsic speeds of shortening of different kinds of muscle. (A comparison of the velocity dependence of P_{S_2}/P_0 for frog and toad sartorius is shown in Fig. 5.13. It is well known that toad muscle contracts at about half the speed of frog muscle (Hill, 1970); and the two curves shown here, for an experiment made at 0°C , show that the critical velocity for toad sartorius is also about half of that for frog muscle.) Third, the maximum values for P_{S_2}/P_0 and E_m (i.e. values obtained by stretching at or above the critical velocity) ought to show a relatively small dependence upon temperature. It is important to be clear about what is being measured in each case. The maximum holding force (P_{S_2}) has been identified as the tension borne by the cross-bridges immediately prior to being forcibly detached (position C, Fig. 4.7 in the preceding chapter). The nature of the chemical bonds holding the myosin head to the actin filament is unknown, but an increase of temperature would be expected to decrease

the bond strength by virtue of an increase in thermal motion. Similarly, the stiffness of the linkage, assuming it has a 'normal' (not rubber-like) elasticity, and hence the value of E_m , would show a decrease with increasing temperature. Both predictions are born out by the experimental results, and in each case the temperature dependence is small, as would be anticipated for a purely physical process.

The observed effects of varying temperature on the C_v 's of PS_2/P_0 and E_m are more difficult to interpret. Once again, it is important to bear in mind the conformational changes contributing to PS_2/P_0 and E_m in terms of the model used earlier. First, the stiffness of any one cross-bridge is determined by (i) the inherent stiffness of the AB link and (ii) the degree to which the myosin head resists being forced backwards against its natural tendency to rotate forwards. The stiffness of the whole muscle will depend on these two factors and also upon the number of cross-bridges contributing to the effect. On the other hand, PS_2/P_0 will depend on (i) the holding force of each head at the point where it has been forced to rotate backwards and has reached position C; and (ii) the number of cross-bridges linking the filaments together. The resistance to backward movement of the head, which must contribute to the stiffness, would not be expected to influence PS_2 . It is reasonable therefore to seek to account for the observed difference in the temperature dependence of these two variables in terms of a change (occurring at about 12°C) in the tendency of the head to resist the movement imposed upon it by the length change.

Barany (1967) has shown that the ATPase activity of fresh, frog myofibrils has a similar dependence on temperature to the C_v values for E_m . Below 12°C the activation energy for rate limiting step in the splitting of ATP is found to be $22.8 \text{ kcal.mol}^{-1}.\text{°K}^{-1}$, and above this temperature, it falls to $13.7 \text{ kcal.mol}^{-1}.\text{°K}^{-1}$. The absolute magnitudes of the activation energies found by Barany and those obtained from the corresponding segments of the Arrhenius plots for the critical velocities of E_m are very different, but it is significant that the transition temperature occurs at the same point and this is of considerable interest. Lymn & Taylor (1970) identified the rate-limiting step in the hydrolysis of ATP as being the dissociation of the products of the reaction from HMM. Their scheme was as follows:



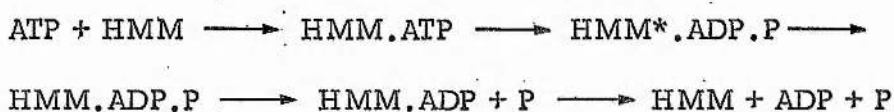
with reaction B being rate limiting rather than A.

However, according to Malik & Martonosi (1972), product dissociation is rate-limiting only at low temperatures (6°C) and not at higher temperatures (23°C). These authors found that at the higher of the two temperatures, product dissociation (step B) is greatly accelerated and the rate of hydrolysis of ATP is then governed by an unidentified intermediate step. They did not investigate the kinetics of the reaction at temperatures other than 6°C and 23°C, so it is impossible to say where the transition occurs; nevertheless it is tempting to speculate that it corresponds with the transition temperature for the critical velocity observed here, and

Temp. range	Activation Energies (k cal.mol ⁻¹ .°K)			
	PS ₂ /P _O	E _m	PS ₂ /P _O + E _m	ATP splitting
0 - 12°C	9.8	12.5	22.3	22.8
12 - 30°C	9.8	4.0	13.8	13.7

Table 6. Activation energies obtained from the C_v values for PS₂/P_O and E_m over two temperature ranges. The activation energies for ATP splitting (Barany, 1967) are shown for comparison.

for the ATPase activity found by Barany. Malik & Martonosi do not arrive at any conclusion regarding the nature of the rate-limiting step at higher temperatures, but Trentham, Bardsley, Eccleston & Weeds (1972) suggest that it may be an intermediate myosin-product complex which undergoes a conformational transition to the final myosin-product complex, the rate of this transition governing the overall rate of the reaction:



It is conceivable that this intermediate stage is the rate limiting step at higher temperatures, with the dissociation of HMM·ADP·P being rate limiting at lower temperatures.

Are there two reactions during cross-bridge cycling which consume ATP?

The interest in the present results stems from the possibility that measurements of P_{S_2}/P_O and E_m may provide information about the temperature dependence of two different reactions involving the hydrolysis of ATP. It will be recalled that the activation energy for the splitting of ATP by fresh, frog myofibrils at temperatures in the range 0–12°C is 22.8 kcal.mol⁻¹.°K⁻¹, and above 12°C the value is 13.7 kcal.mol⁻¹.°K⁻¹. If the activation energies for the C_v 's for P_{S_2}/P_O and E_m are examined over these two ranges (Table 6, facing) it transpires that their sum approximates very closely to the overall values obtained by Barany for the rate limiting step in the hydrolysis of ATP.

It is interesting to speculate, on the basis of these figures, that the overall rate of splitting of ATP by fresh myofibrils represents the sum of two different, parallel reactions, both involving the splitting of ATP, but having markedly different temperature coefficients, and that estimates of the C_v for P_{S2}/P_O and E_m under different conditions may afford a means of investigating the two reactions independently of one another, in the living muscle. Of course it has to be admitted that the close agreement between the activation energies may be purely coincidental, but this seems improbable.

Effect of regulatory proteins on the temperature dependence of actomyosin

ATPase activity. While it would be premature to push the above line of reasoning too far, there is one relevant paper which deserves special mention. Hartshorne, Barns, Parker & Fuchs (1972) studied the temperature dependence of ATP hydrolysis by natural actomyosin and desensitised actomyosin (rabbit protein), and found that in contrast to natural actomyosin, the Arrhenius plot for the ATPase activity of the desensitised preparation is linear over the range 0 - 40°C; this led them to conclude that the regulatory protein system influences the temperature dependence in some way. Thus, in the absence of either Ca^{++} or troponin A, they found the Arrhenius plot to be linear at temperatures below 40°C. The dependence of the C_v for E_m on temperature may therefore be related in an as yet unknown way to the effects of the regulatory protein system.

Economy of ATP usage during stretch. Recent experiments by Curtin & Davies (1973) have shown that the breakdown of ATP in a contracting muscle (poisoned with FDNB) is greatly reduced by stretching, and that this increased economy of ATP utilization is influenced by the velocity of stretch. It would be interesting to be able to make a careful comparison between the velocity dependence of ATP consumption and the velocity of P_{S_2}/P_O and E_m . Unfortunately, Curtin & Davies' ATP determinations were all made on muscles which had contracted at 0°C , where the velocity dependence of P_{S_2}/P_O and E_m is practically identical; no observations were made on muscles contracting at higher temperatures. Furthermore, their changes in velocity were achieved by altering both the amplitude and duration of stretch, which makes the results difficult to interpret. Nevertheless, one important feature they report is that the rate of breakdown of ATP decreases with increasing velocity of stretch, reaching a minimum value (approximately 10% of the rate of breakdown in an unstretched muscle contracting isometrically) at a velocity of $3.65 \text{ mm} \cdot \text{s}^{-1}$. This figure compares closely with the C_v values for P_{S_2}/P_O and E_m at 0°C . If the splitting of ATP during a maintained tetanus is proportional to the rate of cross-bridge cycling (after having made the appropriate correction for ATP consumed by the calcium pumping activity of the sarcoplasmic reticulum), then the reduction of ATP consumption during stretch would suggest that the rate of cycling is much reduced (to about 1/10th of the rate in an unstretched isometric contraction) or alternatively, that under such conditions ATP is not required for cross-bridge detachment.

CHAPTER VI

TENSION RESPONSES TO LENGTH CHANGES OF SMALL AND INTERMEDIATE AMPLITUDE.

The tension responses of a contracting muscle to large amplitude length changes, sufficient to displace the filaments beyond the point at which the cross-bridges become detached from the actin filament, have been fully described in Chapters III and IV. Tension recordings which best illustrate the responses of a muscle to long stretches tend to obscure the less pronounced effects which occur at S_1 . In the experiments to be described in this chapter, relatively small stretches and releases were applied to contracting and resting muscles. These were sufficiently large to exceed S_1 , but not S_2 .

Sarcomere movements were not recorded, as the resolution of the laser diffraction system is not sufficient to follow the movements produced by length changes smaller than those required to reach S_1 (1.55 nm per half sarcomere), but the movements recorded during long stretches have shown the extent to which the external length change is taken up by the contractile elements in the whole period up to S_2 , and from these it is possible to estimate the maximum amount of extension which can occur up to S_1 .

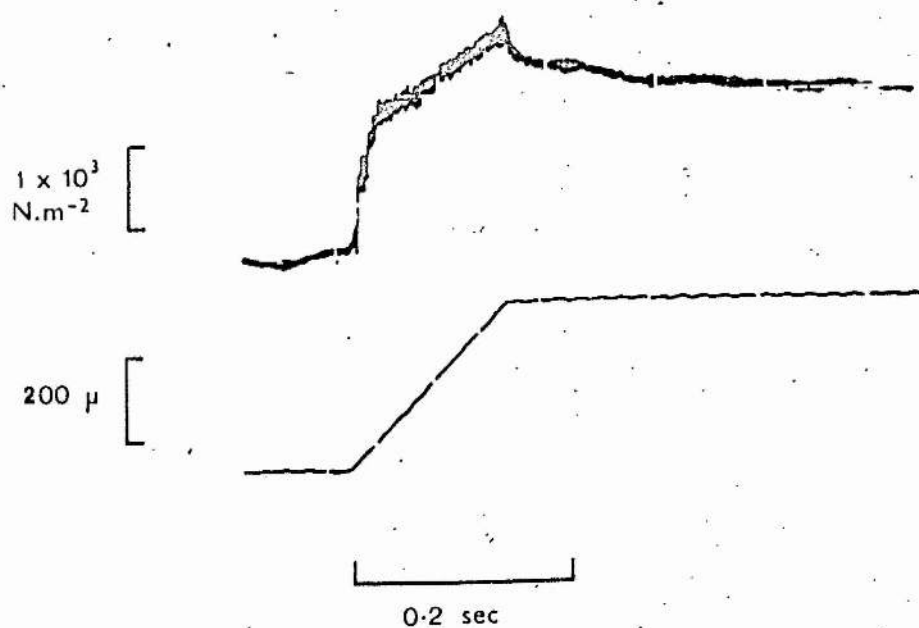


Fig. 6.1. Tension produced in a resting muscle (upper trace) by a ramp and hold stretch of $200\mu\text{m}$ (lower trace). The inflection at S_1 is clearly visible.

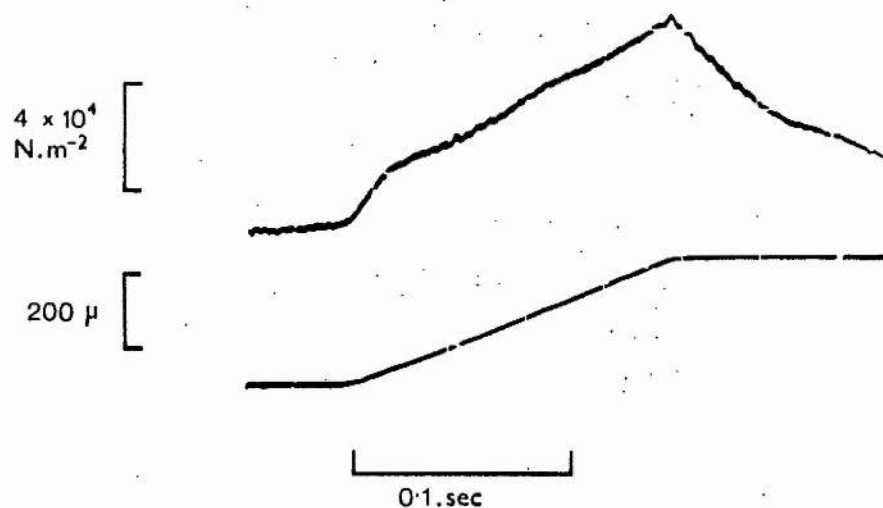


Fig. 6.2. Tension produced in a contracting muscle (upper trace) by a ramp and hold stretch of $300\mu\text{m}$ (lower trace). The inflection at S_1 is clearly visible.

Intermediate amplitudes.

Tension responses of resting and contracting muscle to single ramp and hold stretches of intermediate amplitude. It has been known for many years that a frog's sartorius at rest exerts a small force (Hill, 1949) even when it is held at a length substantially below the standard length in the body, and there is evidence that this is due to a form of interaction between the filaments (Hill, 1968, 1970 a,b). It is thought that this tension, called by Hill the filamentary resting tension, or FRT, is generated by a small number of relatively long-lived cross-connections between the filaments and that these are also responsible for the characteristic short-range elastic properties of a resting muscle.

Fig. 6.1 illustrates the form of the tension response produced in a resting muscle by a ramp and hold stretch of $200\mu\text{m}$. The stiffness of the muscle is high during the early part of the stretch (about $35\mu\text{m}$) but thereafter the resistance to stretch falls, and tension rises less steeply (in some instances, may actually fall) during the remainder of the stretch. The mean degree of extension required to produce this abrupt change in stiffness is found to be $35.8 \pm 2.4\mu\text{m}$ (± 1 S.D.; $n = 5$). This is comparable with the extension required to reach S_1 in a contracting muscle.

Fig. 6.2 shows the tension responses of a tetanised muscle to a stretch of $300\mu\text{m}$ at a velocity of $2\text{ mm}\cdot\text{s}^{-1}$. It is similar in form to that of a resting muscle. Tension rises steeply until the muscle has been extended by about $40\mu\text{m}$ (mean $42.1 \pm 1.5\mu\text{m}$; $n = 7$), at which point (S_1) muscle

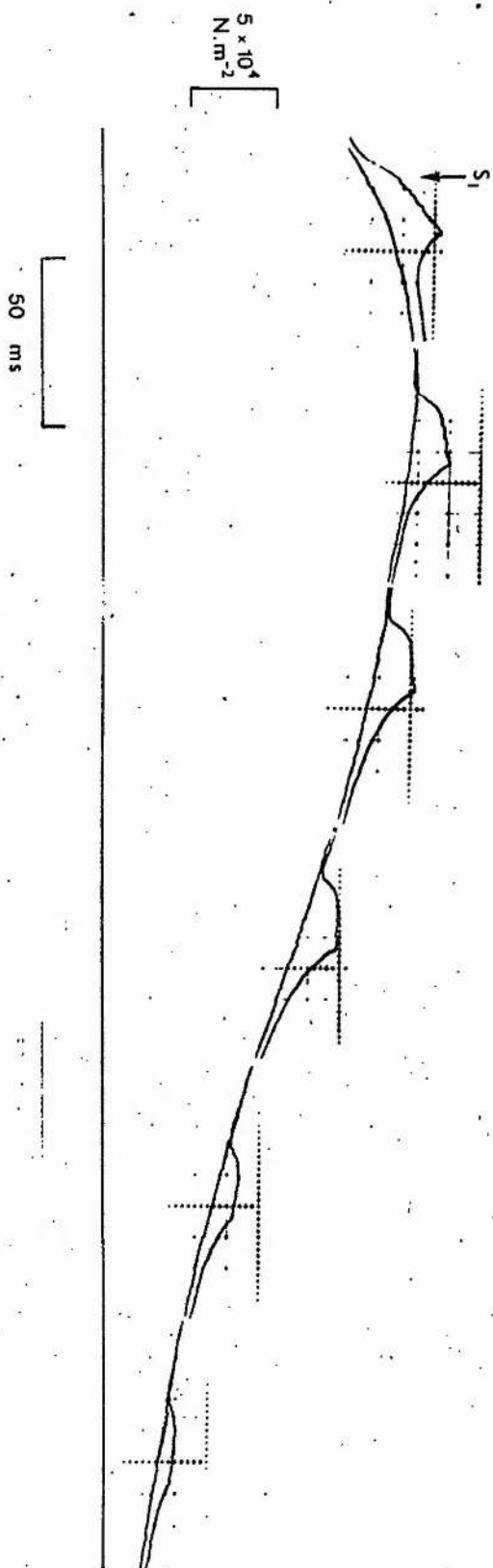


Fig. 6.3. Tension responses of a muscle, to a ramp and hold stretch of 200 μm , applied at different times after a single shock. The record was constructed from 12 consecutive twitches. A stretch was applied to every second twitch, delayed progressively longer after the stimulus.

stiffness falls and tension rises at a slower rate. Although the form of the responses is similar in both cases, the tension generated in a contracting muscle at S_1 is approximately 20 - 30 x larger, reflecting a much greater short range stiffness.

It is of interest that the amount of extension required to reach S_1 in a muscle at rest is usually slightly less than in a contracting muscle. On the basis of sarcomere measurements made during large amplitude stretches, it would be anticipated that a greater proportion of the external applied length change will be taken up by the sarcomeres in a resting muscle than in a contracting muscle, and this difference may be more apparent than real; it is probable that the actual filament displacements involved in reaching S_1 are the same in each case, although unfortunately this possibility cannot be verified experimentally at the present time.

In resting muscle, the degree of activity can be taken as being relatively constant, with little movement of the filaments taking place, apart from that imposed by the applied length change, and the same may be true of a tetanised muscle, once the plateau of isometric tension has been attained. It is therefore of interest to compare the short range elastic behaviour of a muscle under these conditions, with that seen during a single twitch, where the level of muscle activity is changing continuously and a considerable degree of filament movement must take place, even under 'isometric' conditions. Fig. 6.3 shows the tension responses of a muscle to ramp and hold stretches applied at different times during a twitch. It can be seen that the tension increment (up to

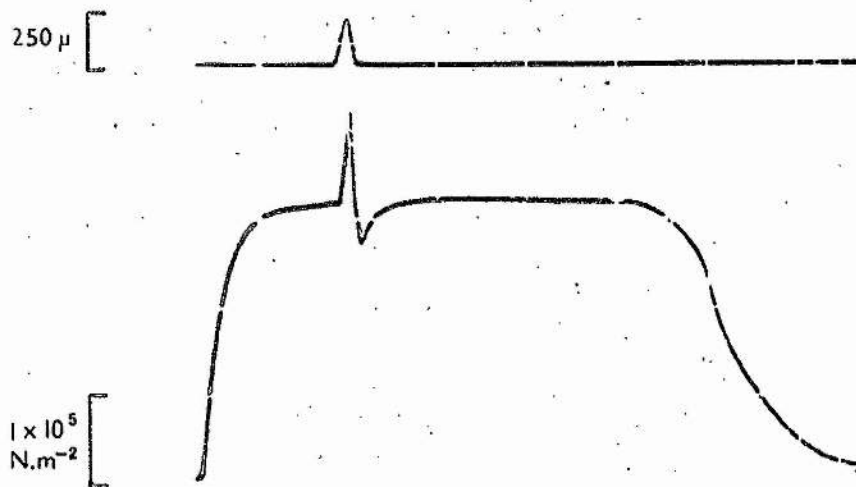


Fig. 6.4.

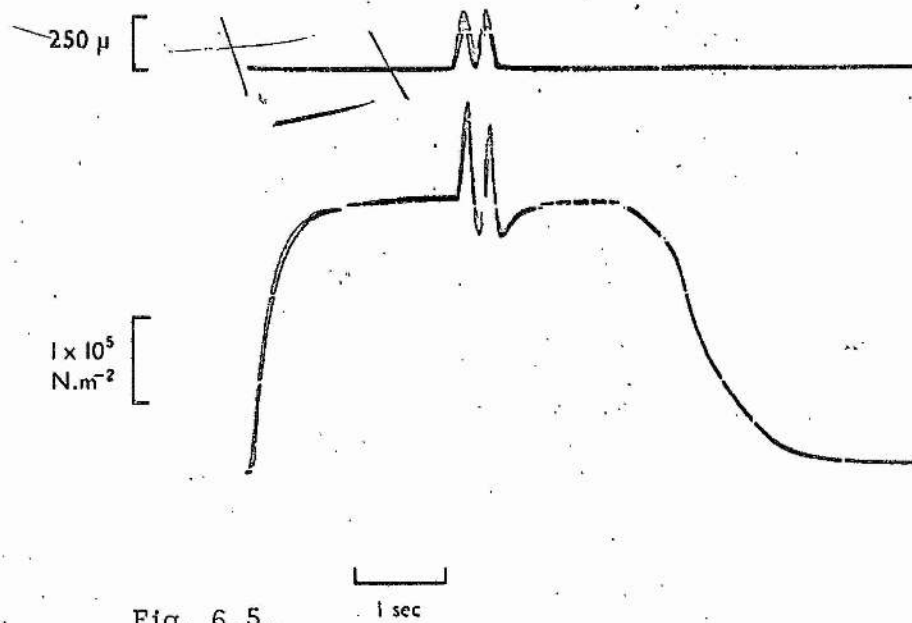


Fig. 6.5.

Figs. 6.4 and 6.5 The effect of a single (6.4) and double (6.5) stretch and release cycle of $260\mu\text{m}$ at 4mm.s^{-1} ; applied to a muscle during the plateau of a tetanus.

S_1 changes throughout the twitch. At peak tension the value is $1.6 \times 10^4 \text{ N.m}^{-2}$ falling to $0.4 \times 10^4 \text{ N.m}^{-2}$ after 350 ms. The higher value, which is equivalent $0.072 \times P_0$ (where P_0 is the peak tetanic tension) is similar to that found during a tetanus ($0.075 \times P_0$; chapter III). This is of considerable interest, since it implies that the stiffness of the muscle at the peak of a twitch is comparable with that during a tetanus, although careful measurements of the sarcomere extensions would be necessary before any further conclusions could be drawn. This is not possible with the resolution available at present.

It seems likely that the point S_1 represents the elastic limit of a component in the muscle which is involved in generating filamentary resting tension as well as the twitch and tetanus tension. The greater level of tension generated in a contracting muscle and the higher level of short range stiffness can be attributed to a larger number of these elements acting in parallel.

Tension changes during cyclical length changes of intermediate amplitude.

Fig. 6.4 shows the effect of a single stretch and release cycle of $260 \mu\text{m}$, at a velocity of 4.16 mm.s^{-1} , applied to a muscle at the peak of a tetanus. Tension rises to a maximum value of $1.30 \times P_0$, its rate of rise appearing fairly constant because the sweep speed is too slow to reveal any discontinuity at S_1 . During release, tension falls very steeply at first, then more slowly and finally reaches a level of $0.90 \times P_0$. Tension then recovers to about the peak isometric value over the next 300 ms.

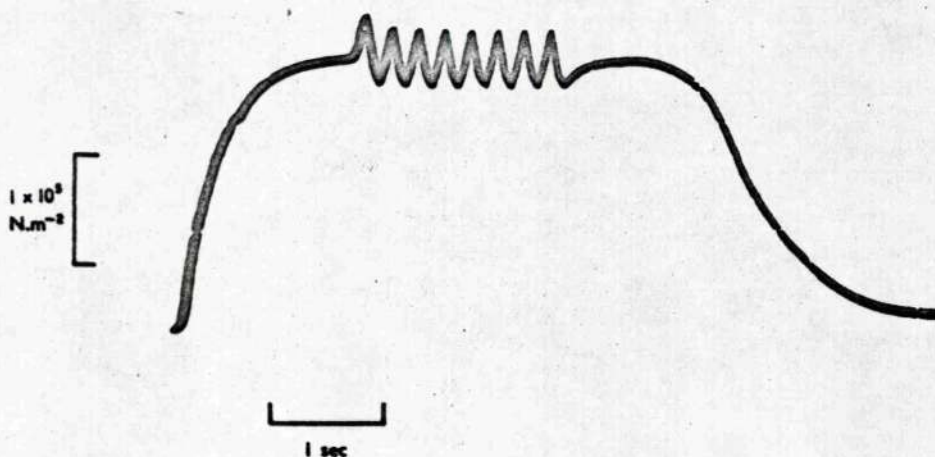


Fig. 6.6. Tension changes produced by eight consecutive cycles of $180 \mu\text{m}$, applied at the peak of a tetanus, showing the unique, asymmetrical shape of a first cycle.

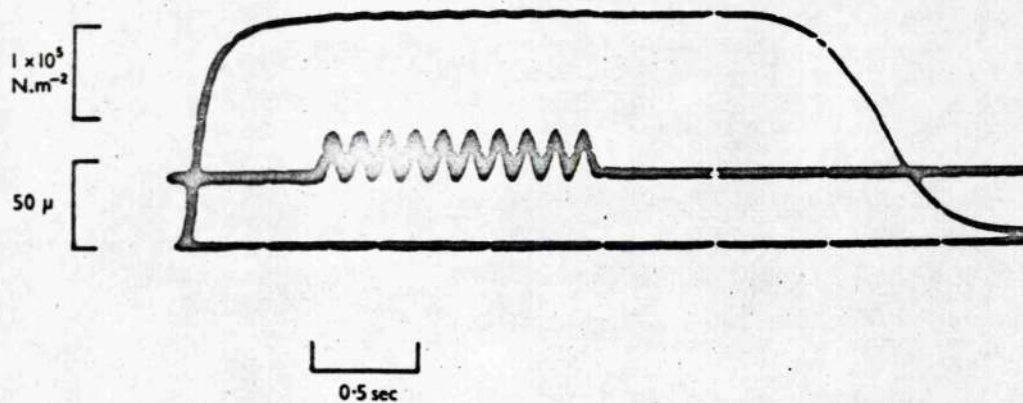


Fig. 6.7. The tension responses of a tetanised muscle to ten cycles of stretch and release of $30 \mu\text{m}$.

It is interesting to note that the tension lost during the release is considerably greater than that generated during the stretch which immediately precedes it. A similar result is seen during a single cycle of long length changes (exceeding S_2) when about 1.8 x more tension is lost in release than is generated by the preceding stretch. Fig. 6.5 shows the tension record produced by a double stretch and release cycle of intermediate amplitude applied during a tetanus. The rate of rise of tension (stiffness) during the second stretch is almost identical to that seen during the first; consequently, the same tension increment is generated by both stretches, although the maximum tension reached is lower at the end of the second stretch, because the stretch commences at a lower tension level.

During a second release tension falls to $0.87 \times P_0$, marginally lower than that reached after a first release ($0.90 \times P_0$), but the tension change during a second release is smaller. Finally, the muscle redevelops tension over the next few hundred milliseconds, until the peak isometric level is regained.

Small amplitudes.

Tension responses to cycles of small amplitude. A consistent feature of the response to cycles of large and intermediate amplitude is the fact that the tension lost during a first cycle release is always greater than that generated by the stretch which precedes it; about 80% more in the

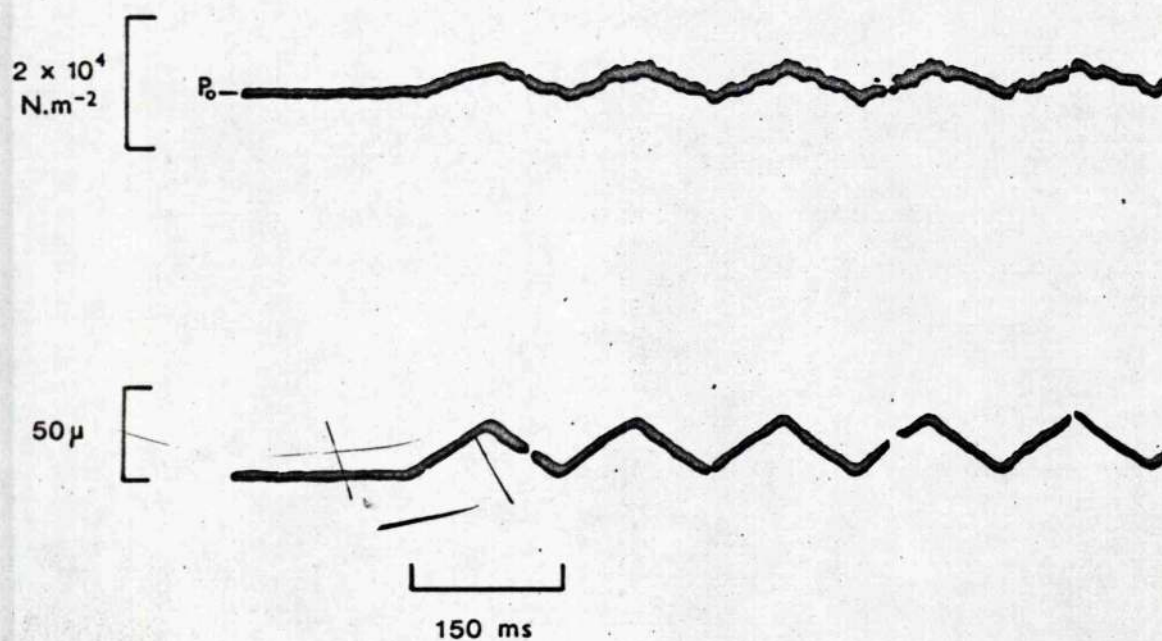


Fig. 6.8. The same conditions as Fig. 6.7 but at higher gain and sweep speed. The tension record closely follows the changes in muscle length.

case of cycles of $\sim 1\text{mm}$ and about 40% more in the case of cycles of $\sim 250\mu\text{m}$. By contrast, the tension lost in a second (or subsequent) cycle is approximately equal to that generated by the preceding stretch. This is clearly shown in Fig. 6.6. The tension response to small amplitude stretch and release cycles ($\pm 30\mu\text{m}$) does not show this striking asymmetry.

Fig. 6.7 shows a typical recording of the tension changes produced by a number of consecutive cycles of stretch and release, of $30\mu\text{m}$. The small 'saw-tooth' oscillations correspond to the changes in length. The overall shape of the tetanus is unaffected by the length changes. Similar recordings are depicted in Fig. 6.8. At the higher gain, the tension changes are seen more clearly; tension rises and falls in an almost linear manner, following closely the fluctuations in length. Thus, it appears that over the range $0 - 30\mu\text{m}$ the muscle behaves as a normal elastic body, the tension generated by stretch being equal to that lost during release.

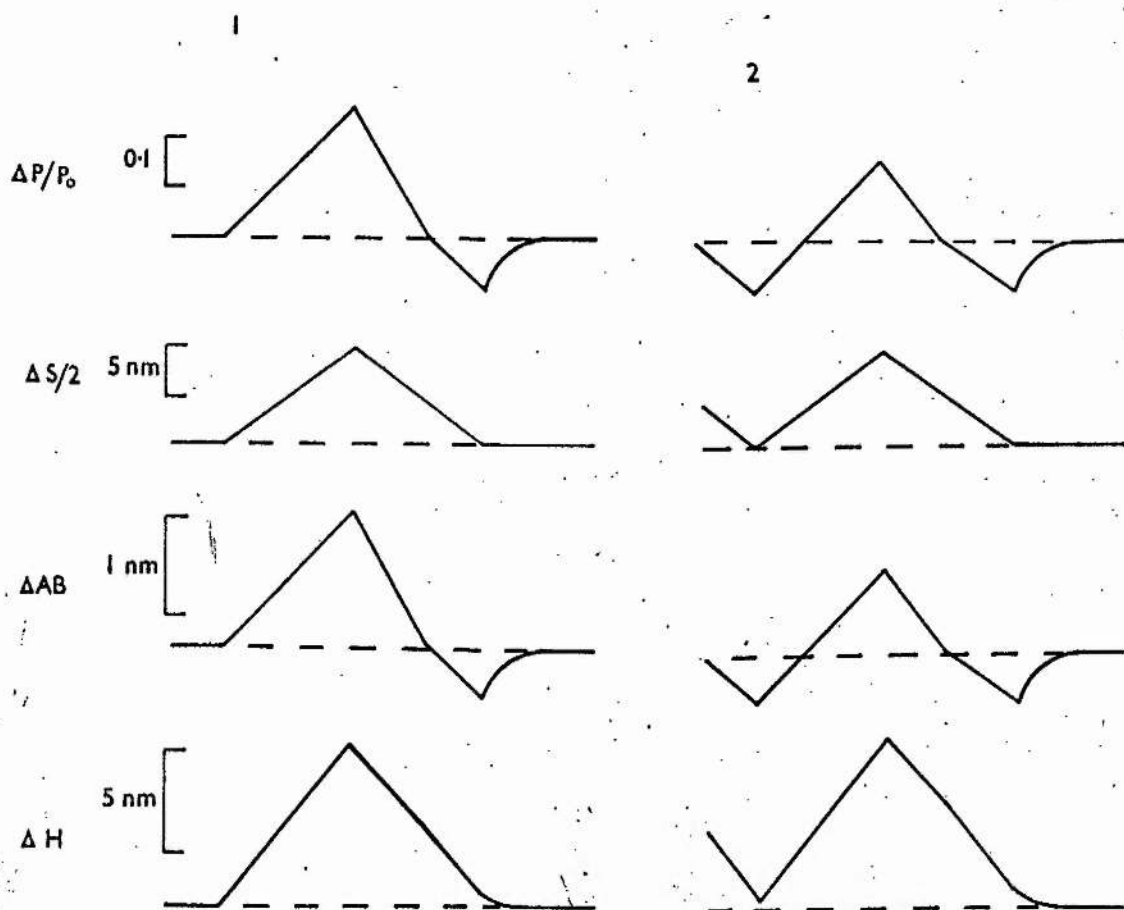


Fig. 6.9. Suggested changes in the length of two cross-bridge elements, the AB link (ΔAB) and the myosin head (ΔH), during first (1) and second (2) cycles of stretch and release. Tension changes, related to P_0 ($\Delta P/P_0$) and concomitant sarcomere movements ($\Delta S/2$), are also shown.

DISCUSSION

A model which accounts satisfactorily for the behaviour of a muscle subjected to large amplitude length changes (exceeding S_2) was presented in the previous chapter, and it is of interest now to consider how well it can account for the tension responses seen in muscle subjected to stretch and release cycles of intermediate amplitude. Large and intermediate amplitude cycles produce responses which differ in two important respects. First, the tension level reached at the end of first and second stretches is approximately equal for large amplitudes, but not for intermediate ones. Secondly, the loss of tension during both first and second releases is always approximately the same for large amplitudes, but the second is always less for intermediate amplitudes.

An attempt will be made to evaluate the changes occurring in the length of two identifiable elements of the cross-bridge, the force generating head and the elastic link through which force is transmitted to the filaments, during first and second cycles of $260\ \mu\text{m}$ (Huxley & Simmons, 1971 a; Fig. 1.17).

Fig. 6.9 illustrates:

- 1) Changes in muscle tension ($\Delta P/P_0$).
- 2) Changes in the length of each half sarcomere ($\Delta S/2$) and thus the extent of relative filament sliding. (Sarcomere length was not monitored, but results obtained for cycles of large amplitude give an indication of the degree of filament movement expected for cycles of $260\ \mu\text{m}$).

- 3) Calculated changes in the length of the elastic AB link (ΔAB).
- 4) Calculated changes in the length of the contractile component, accounted for by rotation of the myosin head (ΔH).

Consider the events during a single cycle. The tension generated by the stretch reaches a value of $1.30 \times P_0$ and from the findings of Huxley & Simmons this represents a mean extension of the AB link of $1.30 \times 5.0 \text{ nm} = 6.5 \text{ nm}$, or an increase of 1.5 nm above its length at peak isometric tension. On the assumption that approximately $\frac{2}{3}$ of the external length change is taken up by the sarcomeres, the relative sliding movement of the filaments would be 9.2 nm , and rotation of the head must then account for $9.2 - 1.5 = 7.7 \text{ nm}$, which is significantly less than that required to cause cross-bridge detachment ($9 - 10 \text{ nm}$; see chapter III). During release, tension falls abruptly at first, reaching the P_0 value at a time when the filaments have moved back by 5.16 nm . Clearly, as tension equals P_0 the length of the AB link must now be 5.0 nm , and so the myosin head can only have rotated by 3.66 nm ($5.16 - 1.50 \text{ nm}$), implying that forward rotation has lagged behind the movement of the filaments.

In the period remaining, until the end of the release, tension falls to a level of $0.9 \times P_0$, although its decay is less rapid than during the early part of the release. Consequently, the length of the AB link must decrease to $0.9 \times 5.0 \text{ nm} = 4.5 \text{ nm}$, 0.5 nm below its length at peak isometric tension, and so the head must still be further backwards than in its equilibrium position before the preceding stretch. Following the end of the release, tension rises towards the P_0 level with a half time of

approximately 70 ms, and so the AB link is being extended back to its P_0 length of 5.0 nm by forward rotation of the head to its mean equilibrium position.

A similar sequence of events is proposed for a second cycle. At the beginning of a second stretch, tension is at $0.9 \times P_0$, filament extension is zero and the AB link is 0.5 nm from its equilibrium position. The stretch then produces a rise in tension to $1.21 \times P_0$ which is approximately the same increment as that produced by a first stretch. This is reasonable, as cross-bridge detachment is minimal and hence muscle stiffness should be the same as in a first stretch. At $1.21 \times P_0$ the AB link has a length of $1.21 \times 5.0 \text{ nm} = 6.05 \text{ nm}$ which is 1.55 nm above its length at the end of release ($6.05 - 4.50 \text{ nm}$), filament sliding is the same as in a first stretch (9.2 nm) and so head rotation must account for $9.2 - 1.55 = 7.65 \text{ nm}$. Tension falls rapidly during the early part of the release, until P_0 is reached (for a smaller length change than during a first release) at a time when the filaments will have moved by only 4.2 nm, the AB link is at its P_0 extension of 5.0 nm and the head has rotated to 5.0 nm from its equilibrium position. As the release proceeds, tension falls below P_0 to a level of $0.9 \times P_0$, the same as at the end of a first release, the AB link shortens to 0.5 nm below its P_0 length and the head rotates to within 0.5 nm of its mean equilibrium position. Finally, after the release, tension rises to P_0 with a half time of approximately 70 ms (the same as after a single cycle and so the AB link must return to its P_0 extension of 5.0 nm, accompanied by rotation of the head to its mean equilibrium position.

If this interpretation of the results is correct, it leads to a number of interesting conclusions. Firstly, the rate at which the head is capable of rotating is relatively slow, because even at release velocities as low as 4.16 mm.s^{-1} it is unable to prevent the AB link from shortening more than it was extended during the preceding stretch. Huxley & Simmons (1971a) have shown that the speed with which tension can be regained in rapid recovery, by rotation of the head, becomes less as the tension level increases, so it is not unreasonable to suppose, for a release from a tension above P_0 , the speed with which the head is capable of reextending the link may be very low. Secondly, once tension has declined to a level close to P_0 it falls less rapidly although, presumably, the filaments continue to move at the same rate. This can be attributed to the ability of the head to rotate forwards more rapidly at tensions less than peak isometric, and so reduce the rate of shortening of the AB link. This explanation also helps to account for the fact that the tension level at the end of a second or subsequent cycle is the same as at the end of a first cycle. Although tension is lower at the beginning of a second release than a first, the P_0 level is reached for a smaller length change and so the head is able to begin more rapid forward rotation earlier, thereby preventing tension from falling as far during a second release.

The argument presented is involved and relies heavily on an important assumption: that sarcomere movements during intermediate cycles of stretch and release are symmetrical. There is no direct evidence that this is so. Nevertheless, the important features of the responses, in

particular the difference between first and second cycles, can be reproduced by the model proposed earlier to account for tension changes during longer stretches and releases.

Finally, the symmetrical nature of the tension responses to very short length changes shows that the muscle behaves like a Hookean elastic body and lends support to the idea that tension generated up to S_1 is due solely to extension of the AB link without rotation of the attached myosin heads.



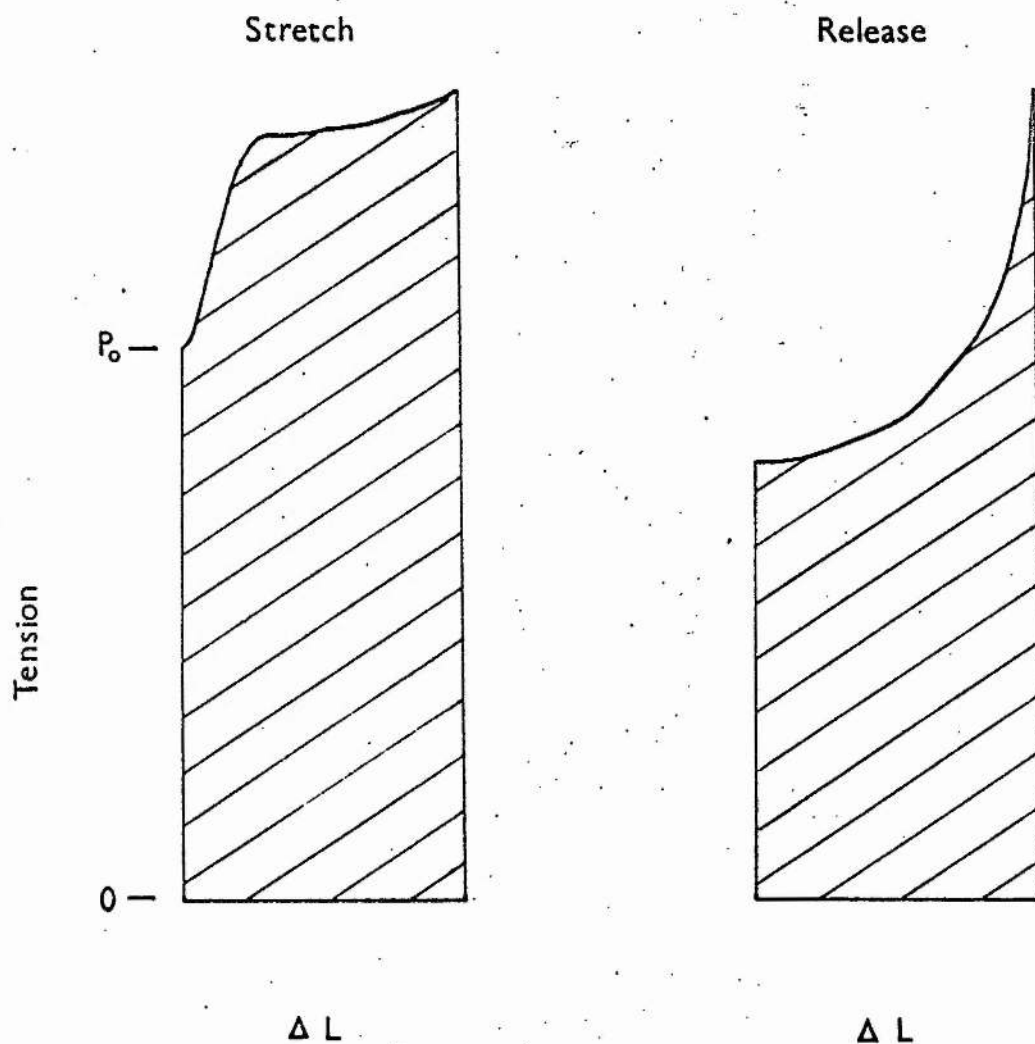


Fig. 7.1. The work done on a muscle during stretch is given by the area under the length/tension curve (left). Most of the work is recovered during release (right). The difference in area represents the work absorbed by a muscle during a cycle of stretch and release.

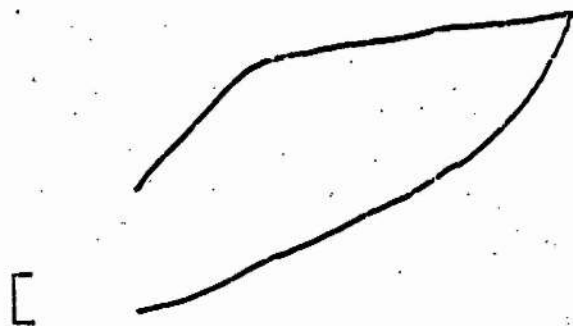
CHAPTER VII

WORK ABSORBED BY CONTRACTING MUSCLE DURING CYCLES OF STRETCH AND RELEASE.

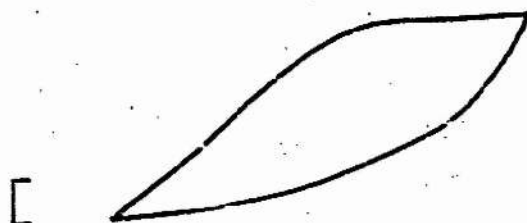
The structure responsible for the early increase of tension during stretch has been referred to as the short range elastic component, but so far no evidence has been presented to justify the assumption that it is truly an elastic element. The experiments described in this chapter were undertaken to investigate this point.

Tetanic contractions were again employed and the muscle was subjected to stretch followed immediately by a release of the same amplitude and velocity. The displacement signal from the servo system which controlled the stretcher was fed to the X-plates of the oscilloscope, and the output from the tension recorder, to the Y-plates. A Devices 'Digitimer' was used to modulate the beam intensity, via the Z-input, so that only the events occurring during stretch and release were recorded. Length/tension 'loops' were thus obtained for cyclical length changes of different amplitude and constant velocity. All the experiments in this section were made at a temperature of 0°C and at a velocity of 4 mm.s^{-1} , which is just above the critical velocity (see Chapter V).

The work done on the muscle during stretch is given by the area under



1025 μm



872 μm

Fig. 7.2. Length/tension loops recorded during first (upper trace) and second (lower trace) cycles of stretch and release.

The amplitude of the length change is shown below each trace. The scale bars represent $5 \times 10^4 \text{ N.m}^{-2}$.

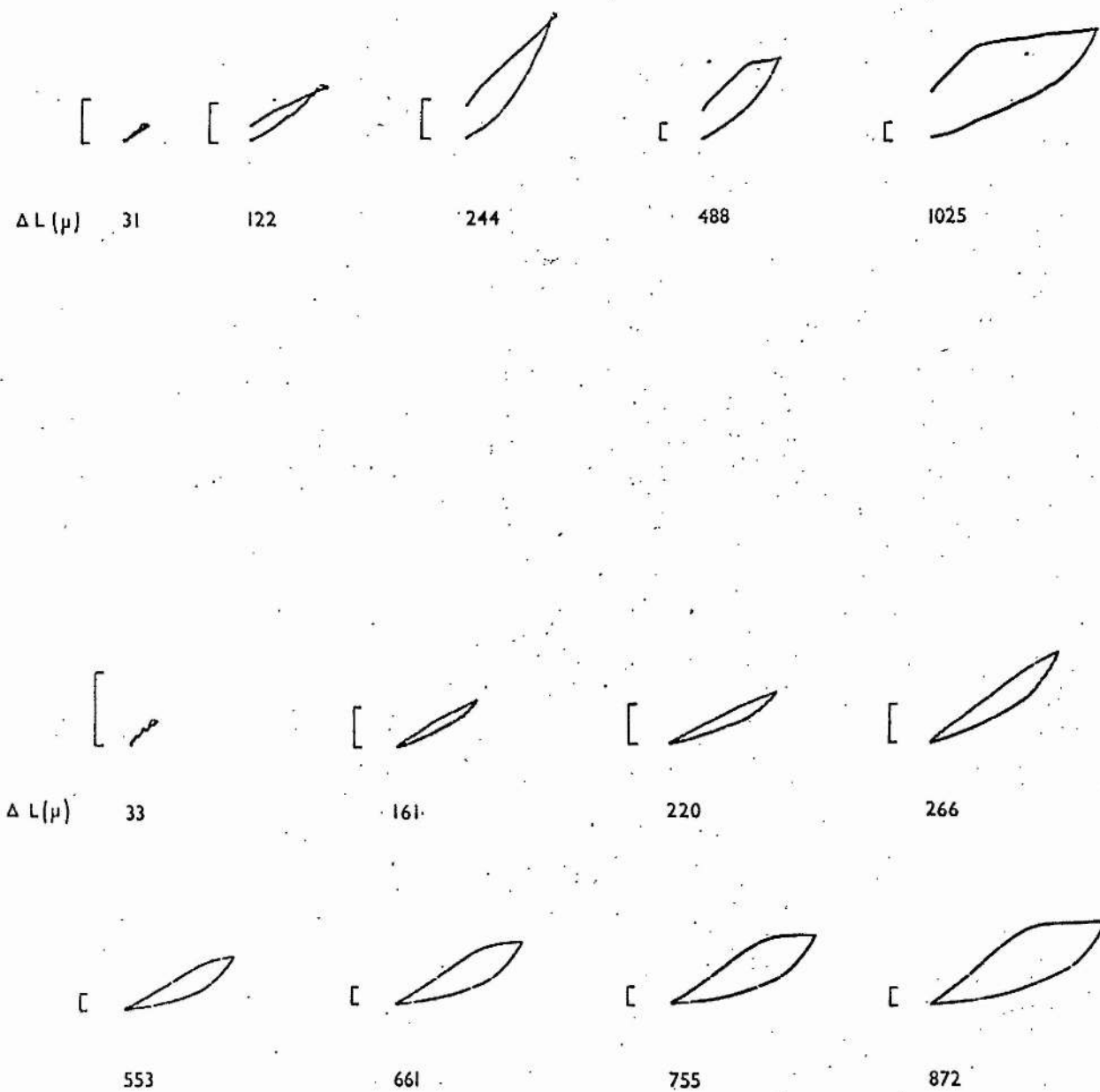


Fig. 7.3. Two series of length/tension loops, produced by cycles of amplitude. First cycles (upper series) and second cycles (lower series).

Cycle amplitude is shown below each trace. Scale bars represent $5 \times 10^4 \text{ N.m}^{-2}$.

the length/tension curve, depicted diagrammatically in Fig. 7.1.A. The major part of this is returned during a subsequent release (7.1.B). However, the tension change during release is not simply the reverse of that produced by stretching, and with the exception of cycles involving very short length changes, the amount of work returned is invariably less; the oscilloscope trace describes a clockwise loop, the area of which represents the amount of non-returnable work done by the mechanical system on the muscle.

Work absorbed in stretch and release cycles of different amplitudes. The tension response of a contracting muscle to length changes of different amplitudes has already been described in detail. It has been shown that the level of tension existing immediately before and immediately after a single stretch and release cycle of large amplitude is not the same; typically, tension at the end of a release from a previous stretch falls to about $0.7 \times P_0$. However, tension before and after the second cycle of a double stretch and release combination is the same. Fig. 7.2 shows length/tension loops of a) a single cycle of stretch and release and b) the second cycle of a double combination. It can be seen that the loop of a second cycle is closed whereas that of a single is not. In both cases part of the work done in stretching the muscle is not recovered in releasing.

A series of loops produced by cycles of different amplitudes is shown in Fig. 7.3; traces from both first and second cycles are included and the differences in shape between the two are apparent. (In similar

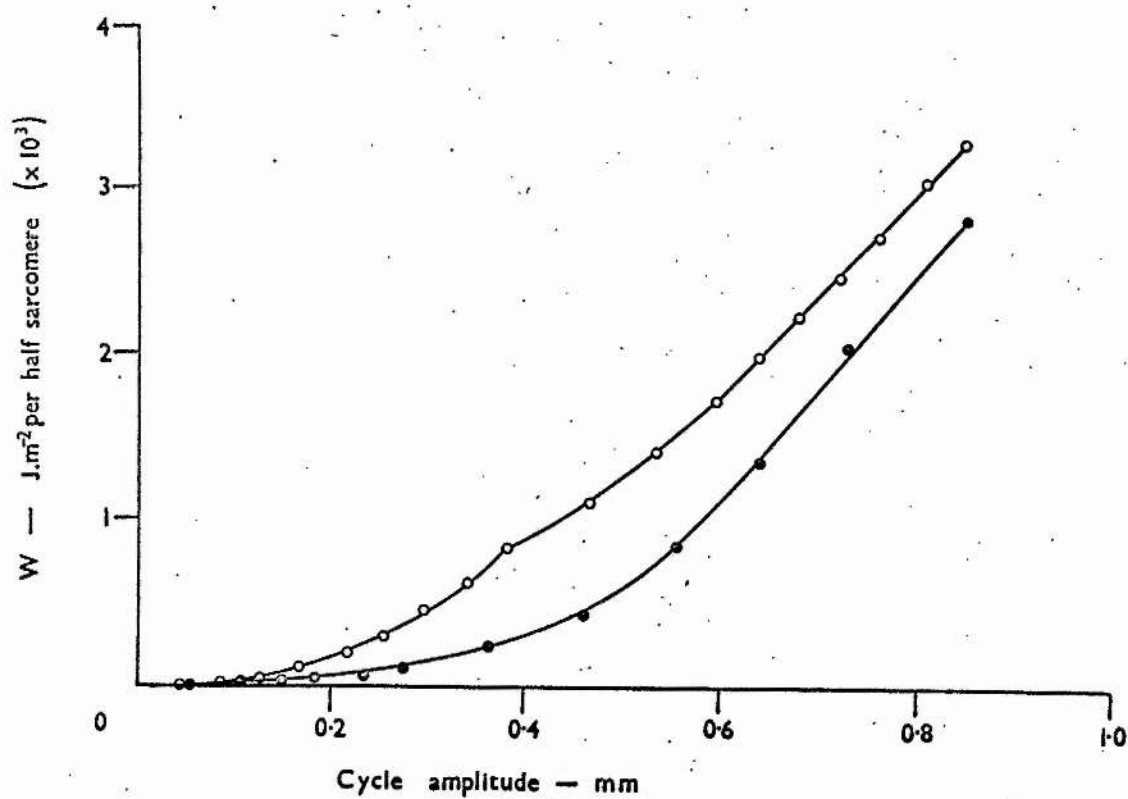


Fig. 7.4. The areas of first cycle loops (open circles) and second cycle loops (filled circles), expressed as the work (W) absorbed per half sarcomere, plotted against the amplitude of the applied length change.

experiments with cat soleus muscle Rack & Westbury (1974) studied only cycles in which the level of tension was the same before and after the application of a stretch and release, and so their records depict only closed loops).

The areas of first and second cycle loops are plotted against the amplitude of the length changes imposed on the muscle in Fig 7.4. The work absorbed by the muscle (W) increases with increasing amplitude but not in a simple fashion. The two curves show several features of particular interest. Consider the curve for the open loops, generated by a single stretch and release cycle. First, during cycles of small amplitude (less than $40\text{ }\mu\text{m}$) no measurable work is absorbed by the muscle; indeed, it appeared from some records that the muscle actually does a small amount of work on the system (oscilloscope trace described an anti-clockwise loop), although it is difficult to be sure that this type of response is a genuine property of the muscle. Secondly, over the range of cycle amplitudes from 40 to $380\text{ }\mu\text{m}$, the non-returnable work becomes progressively larger, although the increase is not linear; and thirdly, between $380\text{ }\mu\text{m}$ (the amount of extension required to reach S_2) and $840\text{ }\mu\text{m}$ (end of stretch) it continues to rise in a linear fashion, to reach a final value of $2.74 \times 10^{-3} \text{ J.m}^{-2}$ per half sarcomere.

The curve of W against cycle amplitude for closed loops (second or subsequent cycle) is similar in form, but differs in one important respect; following the extension where no non-returnable work

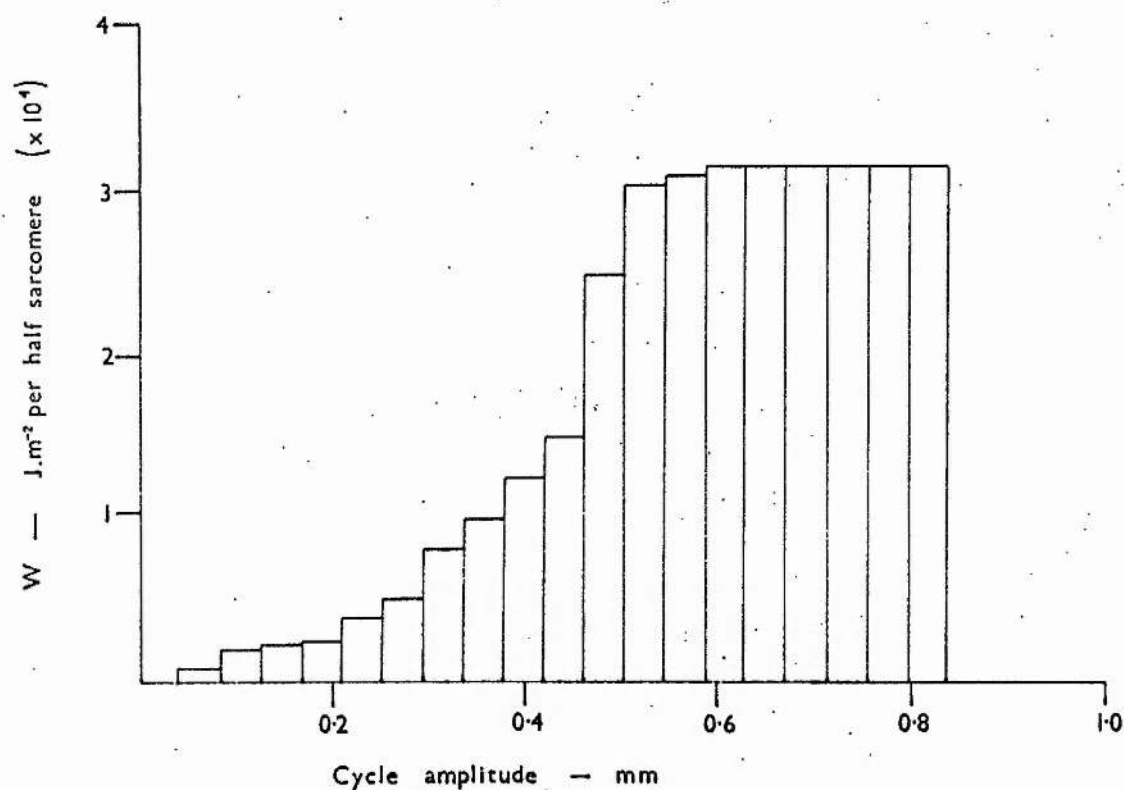
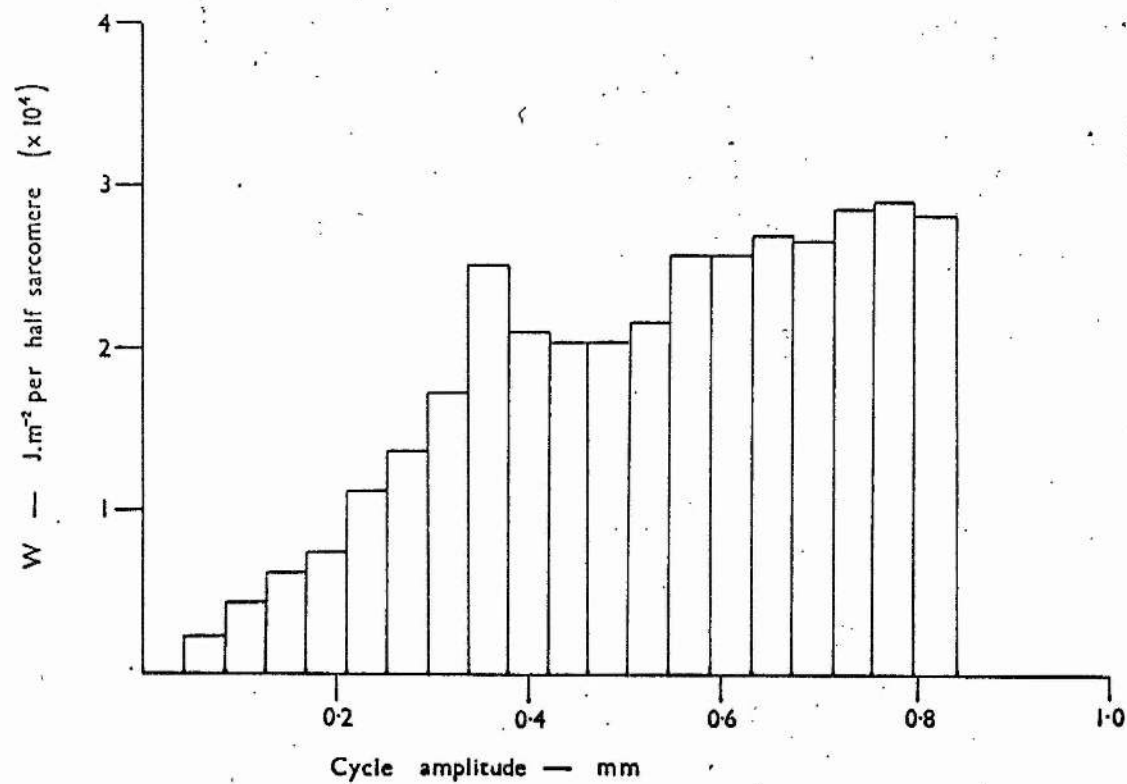


Fig. 7.5. (a and b). The non-returnable work (W) for amplitude increments of $42\text{ }\mu\text{m}$, obtained by subtracting the areas of two successive loops, where the amplitude of stretch differs by $42\text{ }\mu\text{m}$.

can be recorded, the values increase more gradually with increasing amplitude than in the case of the curve for open loops, and it is not until about $540\mu\text{m}$ (close to S_2 for a second stretch) that any discontinuity in the curve is apparent. Beyond this amplitude the curve is almost exactly linear, up to $870\mu\text{m}$, where a value of $2.30 \times 10^{-3} \text{ J.m}^{-2}$ per half sarcomere is reached.

The effect of cycle amplitude on W is more clearly depicted in Fig. 7.5, where the non-returnable work for length increments of $42\mu\text{m}$ is given in the form of a histogram. The abscissa is the range of extension over which the work is estimated; i.e. the areas of two loops of amplitudes differing by $42\mu\text{m}$ (say $84\mu\text{m}$ and $126\mu\text{m}$) are compared and the difference is taken to represent the extra work absorbed in stretching and releasing the muscle over the range ($84 - 126\mu\text{m}$) concerned.

Predictably, the increment from $0 - 42\mu\text{m}$ has a negligible value. However, from $42 - 336\mu\text{m}$ the work increments become progressively larger, until a maximum is reached at $336 - 378\mu\text{m}$, after which they show a transient decrease, finally increasing again to the maximum value. In the case of Fig. 7.5.b, the initial increase in size is more gradual and continues until 546 to $588\mu\text{m}$, thereafter remaining constant up to $840\mu\text{m}$.

Work absorbed by the sarcomeres. It is important to know where the absorption of work occurs in the muscle, so an experiment was made

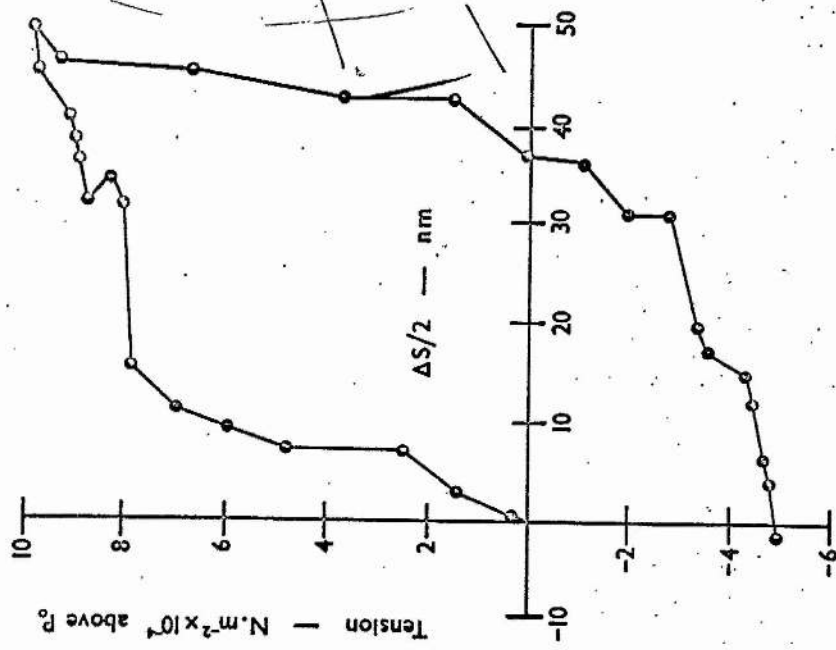


Fig. 7.6.

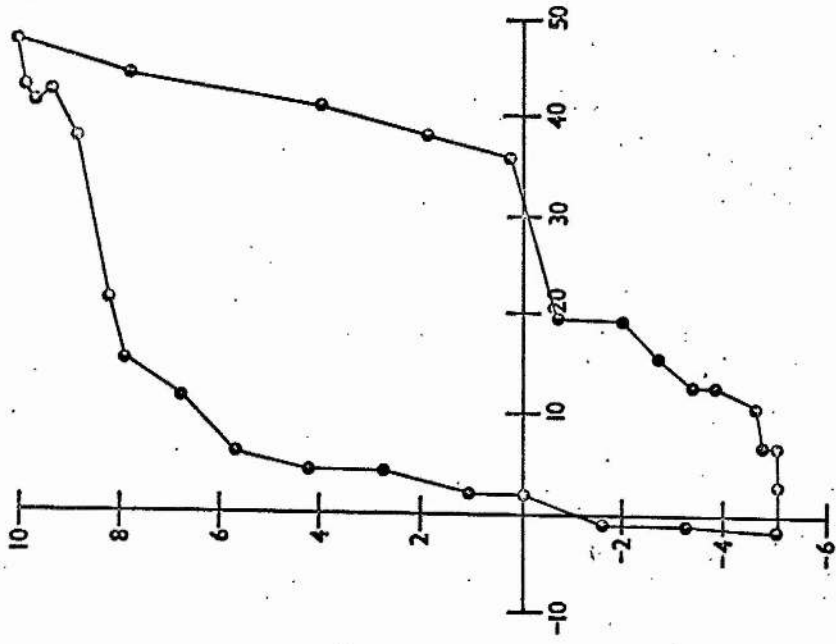


Fig. 7.7.

Figs. 7.6., 7.7. Sarcomere length / tension diagrams for both first (7.6) and second (7.7) cycles of stretch and release. Individual points are the means from three muscles.

in which sarcomere movements were monitored during first and second cycles of stretch and release (as in Chapter 4) and the results are expressed as a length/tension 'loop' for the sarcomeres, rather than for the whole muscle. It is assumed that tension recorded at the muscle extremities is equal to that borne by each half-sarcomere, which is reasonable for short muscle lengths where resting tension is negligible.

Fig. 7.6 shows a length/tension diagram for the sarcomeres, for a muscle subjected to a first stretch and release cycle of $1020\text{ }\mu\text{m}$. Again, the work done in stretching the sarcomeres, which is not recovered during release, is represented by the area enclosed by the loop and yields a value of $4.04 \times 10^{-3} \text{ J.m}^{-2}$ per half sarcomere. Work absorbed by the whole muscle, as estimated from the applied external length change/tension plot, gave a value of $4.60 \times 10^{-3} \text{ J.m}^{-2}$ per half sarcomere.

The sarcomere length/tension diagram for a second cycle of the same amplitude is given in Fig. 7.7 and W in this case is $3.15 \times 10^{-3} \text{ J.m}^{-2}$ per half sarcomere, compared with the value for the whole muscle of $3.75 \times 10^{-3} \text{ J.m}^{-2}$ per half sarcomere.

These results show that the major part (80 - 85%) of the work absorption occurs within the sarcomeres themselves. Furthermore, they reaffirm the observation that the work absorption during a first cycle is significantly greater than that absorbed during a second cycle. This latter point poses an interesting question; is the absorption of work uniformly greater for a first cycle, or is it consumed preferentially during

a particular phase of the cycle? The answer is readily obtained by integrating the part of the histogram showing work absorbed per $\sim 40\mu\text{m}$ increment, up to S_2 in each case. For a first cycle this amounts to $0.70 \times 10^{-3} \text{ J.m}^{-2}$ per half sarcomere, and for a second cycle $0.75 \times 10^{-3} \text{ J.m}^{-2}$ per half sarcomere. Thus, the greater amount of work absorbed during a first cycle of large amplitude (substantially in excess of S_2) must be associated with the greater amount of filament sliding which takes place after S_2 is exceeded.

The following figures for the experiment of Fig. 7.4 serve to illustrate the point. The external length change was $840\mu\text{m}$. S_2 for the first cycle stretch occurred at $380\mu\text{m}$ and for the second cycle stretch, at $540\mu\text{m}$. Thus the amount of the applied length change associated with extension of the filaments beyond S_2 is therefore $840 - 380 = 460\mu\text{m}$ (1st cycle) and $840 - 540 = 300\mu\text{m}$ (2nd cycle). The ratio of the second to first cycle is then $300 / 460 = 0.65$. The total work absorbed in each case amounted to $4.7 \times 10^{-3} \text{ J.m}^{-2}$ per half sarcomere (1st cycle) and $3.75 \times 10^{-3} \text{ J.m}^{-2}$ per half sarcomere (2nd cycle). The amount absorbed for cycles of amplitude just sufficient to reach S_2 was $0.70 \times 10^{-3} \text{ J.m}^{-2}$ per half sarcomere (1st cycle) and $0.75 \times 10^{-3} \text{ J.m}^{-2}$ per half sarcomere (2nd cycle), so that the extra work associated with filament sliding beyond S_2 is $(4.7 \times 10^{-3}) - (0.70 \times 10^{-3}) = 4.0 \times 10^{-3} \text{ J.m}^{-2}$ per half sarcomere (1st cycle) and $(3.75 \times 10^{-3}) - (0.75 \times 10^{-3}) = 3.0 \times 10^{-3} \text{ J.m}^{-2}$ per half sarcomere (2nd cycle). The ratio of this extra work (second: first)

is thus $3.0 \times 10^{-3} / 4.0 \times 10^{-3} = 0.75$. This is similar to the value of 0.65 obtained for the ratio of the extra length change associated with sliding beyond S_2 .

Unfortunately, this analysis relies on a comparison of external length changes and not internal filament movements; the degree of agreement might reasonably be expected to have been closer if the sarcomere movements had been monitored in this experiment.

Work absorbed by the sarcomeres in stretching a muscle to S_2 . It is of interest to measure the work done on the sarcomeres when the muscle is extended to the point where the cross-bridges detach and rapid 'give' occurs. This is done by relating total force on the muscle to filament displacement over this range. During a first cycle stretch, the amount of filament sliding associated with backward rotation of the myosin head is estimated to be 10 nm. (see Chapter 4), and during a second cycle stretch, 15 nm. The product of muscle force and displacement gives the required figure for the work done, and the values so obtained are $3.18 \times 10^{-3} \text{ J.m}^{-2}$ per half sarcomere (1st cycle) and $4.29 \times 10^{-3} \text{ J.m}^{-2}$ per half sarcomere (2nd cycle).

DISCUSSION

It is pertinent to consider whether the way in which a muscle absorbs work during cycles of stretch and release is compatible with Huxley & Simmons' model and if the results reveal any additional information about the properties of the cross-bridge.

It was found that there is no detectable work done on a muscle when it is subjected to cyclical length changes of amplitude less than about $40\mu\text{m}$, corresponding with the elastic limit S_1 , and this result is consistent with the suggestion that the early, steep increase of tension up to S_1 is developed in the elastic AB linkage, without rotation of the attached head; the work done on extending the linkage is wholly returned during a subsequent release. This result justifies the use of the term short range elastic component to describe the structure responsible for the tension responses to short stretches.

Beyond S_1 the work absorbed per unit increment of length (Fig. 7.5) increases progressively up to S_2 , the point at which rapid sarcomere extension occurs. For example, the extra work done in performing a cycle of $168\mu\text{m}$ as compared with one of only $126\mu\text{m}$ (a $42\mu\text{m}$ increment) amounts to $0.6 \times 10^{-3} \text{ J.m}^{-2}$ per half sarcomere (1st cycle), whereas a similar length interval, this time between $210\mu\text{m}$ and $252\mu\text{m}$ consumes $1.1 \times 10^{-3} \text{ J.m}^{-2}$ per half sarcomere. It is clear that the net absorption of work

increases the further cross-bridges are deformed from their mean starting position. In contrast, for cycles of amplitude sufficient to exceed S_2 , the work absorbed per unit length increment remains roughly constant as the filaments are made to slide further beyond the point of rapid 'give'. This behaviour is to be anticipated, if the major part of the tension supported by the muscle beyond S_2 is borne by frictional (or other dissipative) forces, with the work done being degraded into heat. It is clearly very different from what happens during cycles of amplitude such that cross-bridges are deformed but not broken. This reinforces the argument that rapid 'give' of sarcomeres results from a fundamental change in the state of a muscle.

The difference in the work done on stretching to S_2 during first and second cycles and its ATP equivalent. It was shown earlier (Chapter IV) that the amount of extension required to reach S_2 during a second cycle stretch, that is, one starting from a tension level below P_0 , is substantially greater than that required to produce rapid 'give' of sarcomeres during a stretch applied at the peak of a tetanus, and it was suggested that this difference arose because the mean position of the attached myosin heads was different at the commencement of each stretch (see Fig. 4.8). If this is correct, then the difference in the work done in extending the filaments up to S_2 in each case represents the work required to force the head to switch from one preferred position (C) to the other (B).

It is of interest to calculate the ATP equivalent of this extra work, for the following reason; if detachment of the head during extension from the two attachment sites of position C in Fig. 4.8 consumes most work found to accompany switching of the head from C \rightarrow B, and if the same bonds must first be broken in a normal (unstretched) contraction, then it is legitimate to equate the ATP equivalent of this work with the energy cost for cross-bridge detachment. Now, in the case of a second cycle stretch, the work done (W_2) in extending a muscle up to S_2 is $4.27 \times 10^{-3} \text{ J.m}^{-2}$ per half sarcomere, and in the first stretch (W_1), $3.18 \times 10^{-3} \text{ J.m}^{-2}$ per half sarcomere, so the difference ($W_2 - W_1$) = $1.09 \times 10^{-3} \text{ J.m}^{-2}$ per half sarcomere. The number of cross projections on the myosin filament is estimated to be $5 \times 10^{16} \text{ m}^{-2}$ per half sarcomere (Huxley, 1963), which gives a figure $1.09 \times 10^{-3} / 5 \times 10^{16} = 0.2 \times 10^{-19} \text{ J}$ for the extra work associated with each one. The enthalpy change resulting from the conversion of ATP \rightarrow ADP in the muscle is $5 \times 10^4 \text{ J.mole}^{-1}$ (Offer, 1974), equivalent to $5 \times 10^4 / 6 \times 10^{23} = 0.8 \times 10^{-19} \text{ J}$ per molecule, or 4x greater than the work done in the switching of one cross-bridge from position C \rightarrow B. Thus, the hydrolysis of one molecule of ATP would provide ample energy to cause detachment of a single head, although the efficiency of the process would be rather low (about 25 %, with the remainder of the enthalpy change appearing as heat). However, it is well known from X-ray diffraction studies of contracting muscle that not all of the cross-projections form connections (cross-bridges) with the actin filament at any one time. Huxley & Brown (1967) estimate

that only 20 % are so attached during an isometric tetanus. The work required to cause switching from position $C \rightarrow B$ would then amount to 1×10^{-19} J; a single molecule of ATP might then only just be adequate for detachment and, moreover the efficiency of the process would have to be very high. A more recent study by Matsubara, Yagi & Hashizume (1975) suggests that the fraction of attached cross-bridges may be as high as 80 %, which would mean that switching of one cross-bridge from $C \rightarrow B$ would require only 0.25×10^{-19} J, and one molecule of ATP would be sufficient. The efficiency of the process would then be rather low (31 %).

It would be unwise to place too much reliance on a calculation of this kind. The uncertainties arise chiefly in the widely differing estimates for the fraction of the total population of cross-projections actively involved in an isometric tetanus (20 - 80%). All that can be said is that the process of detachment may require only one molecule of ATP, in which case the energetic efficiency would lie somewhere between 30 and 100%. Unfortunately, it is impossible to be more precise at the present time.

Nature of the myosin-actin bonds. The energy required to forcibly break a cross-bridge has been estimated to be within the range $0.25 - 1.0 \times 10^{-19}$ J. This figure imposes certain limits on the kind of bonds involved in holding the myosin head to the actin active site. Consider, for example, the energetic requirements for breaking a single hydrogen

bond. The bond energy is approximately 21 kJ.mole^{-1} ; or $2.1 \times 10^4 / 6 \times 10^{23} = 0.35 \times 10^{-19} \text{ J. per bond}$, which is close to the figure given above for the energy needed to detach forcibly a single cross-bridge. Thus, it is conceivable that each point on the myosin head is linked to an actin subunit (eg. M_1A_1) through a single hydrogen bond. This is consistent with Offer's (1974) conclusions. Of course, the possibility of more numerous, weaker 'bonds' (eg. electrostatic interactions between charged sites) is not excluded. Certainly, stronger bonding would appear to be ruled out by considerations of this kind. The bond energy for the next strongest bond is around 80 kJ.mole^{-1} (for N - N) bonding, or 4x greater than for hydrogen bonding.

CHAPTER VIII

CONCLUSIONS.

The sliding filament theory (A.F. Huxley & Neidergerke, 1954 ; H.E. Huxley & Hanson, 1954) is now widely accepted as the explanation for the way in which a muscle alters its length, although much controversy still remains regarding the mechanism by which the relative force between the actin and myosin filaments is generated during contraction. The well-documented constant volume behaviour of the filament lattice (H.E. Huxley, 1953 a,b; April, 1975) imposes certain specific constraints on the kind of model that can be invoked to account for force production. This property means that the surface to surface distance of the filaments in the region where they overlap can vary from 4 - 11 nm (frog muscle ; Elliot, Lowy & Worthington, 1963 ; Elliot, 1964), yet surprisingly, the characteristic length/tension relation for frog muscle (Gordon, Huxley & Julian, 1966 b) shows that the capacity of each cross-bridge to generate tension is not affected by variations in the separation of the filaments within this range. This important consequence of the constant volume behaviour has led to a number of models being proposed which are able to account for the features of the contractile properties of muscle, to a greater or lesser degree. In some instances, the cross-projections on the thick filaments are considered to play a key role in both generating and transmitting force (H.E. Huxley, 1969 ; A.F. Huxley & Simmons,

1971b ; Podolsky & Nolan, 1971; Julian, Sollins & Sollins, 1973), but in others their status is either relegated to a passive role, with lateral expansion of the Z disk (Ullrick, 1967) or electrostatic repulsion between the filaments (Shear, 1970; Elliot, Rome & Spencer, 1970) generating the motive force; or, alternatively, are considered to be 'active' only in so far as they influence the distribution of electrostatic charges on the filaments (Ashley, 1972) and do not function as tension bearing elements. The results obtained in the present investigation can best be interpreted in terms of a model in which interaction between the myosin cross-projections and the actin filaments generates force and in which the projections themselves act as temporary mechanical linkages between the filaments. It will be seen that the findings are entirely consistent with the recent model put forward by Huxley & Simmons, (1971b), although it would be unwise to conclude from this that they are incompatible with one or more of the alternative models; these alternatives are exceedingly complex and it is not always easy to see how they can be tested experimentally.

The concept of rapid 'give' as a transition between two steady states.

The results can best be interpreted if rapid 'give' is considered as a transition between two steady states; the position at peak isometric tension, where the filaments are static (relatively so) and where the muscle is exerting a constant force, and the condition after rapid 'give' where the sarcomeres are being extended at a uniform speed and the muscle maintains a new (higher) constant force. This notion has two important

consequences :

A. For speeds of stretch in excess of the critical velocity, the changes that occur up to S_2 (tension responses and filament movements) give information about the mechanical properties (eg. stiffness) of those cross-bridges actively involved in generating force, at the time of stretch, and these transient events have provided information on the dimensions and structure of the sites of interaction between actin and myosin.

B. Changes occurring beyond S_2 give information about the force / velocity relation of muscle when it is being forcibly stretched (as opposed to shortening). Unfortunately, little can be said about the force / velocity relation during extension, because, for the reasons given earlier (Chapter VI), it was impossible to record sarcomere movements over the required range of velocities. The remainder of this discussion is therefore concerned with the information that can be obtained in the early part of a stretch, up to and including rapid 'give'.

Structure of the actin active region and the possible nature of bonding to the myosin head.

The suggestion that the myosin heads adopt 'preferred' positions is helpful in explaining one interesting and consistent feature of the responses; namely, the abrupt onset of rapid 'give' and the almost angular form of the tension response which results. It was assumed earlier (Discussion to Chapter IV) that at peak isometric tension the majority

of the myosin heads spend most of their time in an intermediate position (B, of Fig. 4.7) and relatively little time in either of the other positions. It is easy to see from Huxley & Simmons' model why this should be so. When the head attaches initially, it does so with little or no tension in the elastic linkage, consequently, it is able to rotate into the next position and in so doing, develops peak isometric tension in its link. As a result of this high tension, the activation energy for the next step is high and the probability of the head making it is therefore small. If it should chance to do so, then the likelihood of detachment (by ATP hydrolysis) is great. This means that the heads are energetically constrained to occupy an intermediate position. By similar reasoning, it can be seen that a previous release will favour movement of the head from this intermediate position to one of lower potential energy; thus, shortening during release will unload the elastic link and lower the activation energy for this step.

This concept of 'preferred' orientation of the heads leads to some interesting conclusions concerning the structure of the actin active region. By comparing the amounts of filament movement that occur on reaching S_2 for first and second cycle stretches it was possible to conclude that the sites occupied by the head at peak isometric tension and at the end of release are separated by about 5.5 nm. The overall length of the actin active region, deduced from the total distance the filaments move to reach S_2 in a second stretch, is around 15.0 nm. It is clear from Huxley & Simmons' later work (A.F. Huxley, 1974) that the amount

of filament sliding required to abolish tension is around 5.5 nm, or put another way, this is the extent of movement required to generate full isometric tension. These figures suggest a structure for the actin active region comprising 4 attachment sites (A_1, A_2, A_3 and A_4) separated by 5.0 - 5.5 nm, which interact with 4 corresponding sites (M_1, M_2, M_3 and M_4) on the myosin head. It is unlikely that this separation happens by chance to coincide with the centre to centre spacing of the actin monomers in the F-actin strands that make up the thin filament, and it is postulated that each of the attachment sites is located on successive actin monomers.

In this connection it is interesting that recent estimates of the dimensions of the S1 subunit of HMM (the component which has the ability to combine with actin and to split ATP) show it to be an elongate molecule approximately 15 nm in length and 4 nm in diameter (Moore, Huxley & DeRosier, 1970). Again, it is unlikely that this correspondence is purely fortuitous.

These considerations suggest that while the myosin head is attached to the thin filament it interacts sequentially with a region of the actin filament approximately 4 monomers in length. It is well known (Rizzino, Barouch, Eisenberg & Moos, 1970) that under appropriate conditions every actin monomer can interact with a single molecule of HMM, and as a result, local structural differences (eg. distribution of charged groups) that could give rise to variations in the affinity of the head for the actin, establishing the kind of potential gradient envisaged by Huxley & Simmons, must reside in the head itself. A comparison of the work

done in stretching model up to S_2 in first and second cycles led to the conclusion that the attachment site A_4M_4 , which together with A_3M_3 defines position C, could be a single hydrogen bond. Moreover, it emerged that the enthalpy change associated with the hydrolysis of a single molecule of ATP would supply enough energy to break this bond during a normal contraction. However, it is clear that the maximum force sustained by each cross-bridge at S_2 (assuming that all of the cross-projections on the thick filament are attached simultaneously) is 30x smaller than the force which a single hydrogen bond could bear.

The most likely explanation for this is that the head attaches to the actin filament by means of Van der Waals or electrostatic attractive forces. This idea has some merit in that it is quite easy to envisage the myosin heads having an uneven distribution of ionised groups (electronic charges) located at the points $M_1 - M_4$.

The undamped elastic component of the cross-bridge.

The idea of an undamped (instantaneous) elastic component arranged in series with the element which generates force is an important feature of Huxley & Simmons' model. Unfortunately, there are serious drawbacks associated with any quantitative discussion of the physical properties of this part of the cross-bridge. The difficulty stems from conflicting reports in the literature concerning the proportion of myosin cross-projections that are actively engaged in generating force. Huxley & Brown (1967) estimate that the number so involved may be as little

as 20% of the total, whereas a more recent X-ray diffraction study by Matsubara, Yagi & Hashizume (1975) puts the figure at 80%.

Let us assume for the moment that all of the cross-projections are actively engaged in generating force. It can then be calculated (page 57) that the stiffness of each cross-bridge is around $2.7 \times 10^{-4} \text{ N.m}^{-1}$. It was earlier postulated (working hypothesis; Chapter IV) that most of the filament sliding is associated with backward rotation of the attached myosin head, so the stiffness of the undamped, elastic component must be considerably greater than this. It has been tacitly assumed throughout that a 5 nm extension of this component generates the full isometric tension; thus the combined stiffness of all the cross-bridges is $3 \times 10^5 \text{ N.m}^{-2}$ (maximum isometric force) $/ 5 \times 10^{-9} \text{ m} = 6 \times 10^{13} \text{ N.m}^{-1}$, or $1.2 \times 10^{-3} \text{ N.m}^{-1}$ for a single cross-bridge. The 'best' estimate that can be obtained from the present results is calculated by measuring the tension increment up to S_1 (the point at which the head begins to rotate), divided by the amount of filament sliding which has occurred. Unfortunately, it is impossible to give an accurate figure for the amount of filament movement up to this point. It is, however, possible to give an upper estimate, assuming that sarcomere extension is uniform in the whole period up to S_2 . It then transpires that the stiffness of each elastic link is in the region of $3.8 \times 10^{-4} \text{ N.m}^{-1}$, or approximately $3.2 \times$ less than the figure derived from Huxley & Simmons' work. In view of the uncertainty that exists concerning the degree of sarcomere extension in the period up to S_1 , this discrepancy is not too great.

Huxley & Simmons suggest tentatively that the instantaneous elasticity in their model resides in the S2 subunit of HMM. The structure of this component of the myosin molecule is very well known. It consists of two α helical polypeptide chains (Lowey & Cohen, 1962; Weeds & Hartley, 1967, 1968) arranged in parallel, each of which has a molecular weight of about 40,000. It is therefore possible to make a reasonable estimate of its stiffness. When this is done, yielding a value of $18.5 \times 10^{-2} \text{ N.m}^{-1}$ (see below), a large discrepancy arises; the stiffness observed experimentally by Huxley & Simmons ($1.2 \times 10^{-3} \text{ N.m}^{-1}$) differs by a factor of 150, and that estimated here, by an even larger factor of 490.

Calculated stiffness of the S2 subunit of HMM. Consider each chain independently; the molecular weight of each is about 40,000 and the mean molecular weight of its constituent amino acids is 110. Each chain must then contain close to 360 amino acids. It has been shown (Pauling & Corey, 1953) that α helical polypeptide chains contain about 3.6 residues per turn of the helix, the helical structure being maintained by hydrogen bonds linking residues on successive turns. The elasticity of the whole chain is therefore governed by this bonding and so if the strength of each bond and the number of bonds is known, the stiffness of the whole chain may be estimated. If it is assumed that each amino acid forms one hydrogen bond (Pauling & Corey, 1950) then there will be 3.6 bonds per turn and 100 turns in each chain. From a mechanical point of view this arrangement would have length tension characteristics equivalent to $100/3.6 = 28$ hydrogen bonds lying in series. Given that the maximum bond strength of one hydrogen bond is $3 \times 10^{-10} \text{ N}$

(Offer, 1974) and its bond energy is $21 \times 10^3 \text{ J.mole}^{-1}$ (Fieser & Fieser, 1957) then the extension required to break it is 1.16 \AA and its mean stiffness is 2.59 N.m^{-1} . The stiffness of each chain is therefore $2.59/28 = 9.25 \times 10^{-2} \text{ N.m}^{-1}$ and for the two chains in parallel $18.5 \times 10^{-2} \text{ N.m}^{-1}$.

There are two possible reasons for this large discrepancy; either the estimate for the stiffness of the S2 subunit is wrong, based on inadequate knowledge of its tertiary molecular structure; or, as seems more likely, the major source of compliance resides in part of the linkage which does not have an α helical structure. The flexible region of the molecule which is postulated to permit outward movement of the cross-bridge (H.E. Huxley, 1969) is the most likely candidate.

Relation of the present results to other models in which the myosin cross-projections function as mechanical linkages.

There are two important models which deserve some comment; the one described by Podolsky & Nolan (1971) and that of Julian, Sollins & Sollins (1973). Ford, Huxley & Simmons (1974) have provided good evidence that early rapid tension recovery following abrupt shortening of the muscle is not due to recruitment of previously unattached cross-bridges, as postulated by Podolsky & Nolan. An important feature of their model is that cross-bridge cycling occurs on an extremely short time scale, of the order of a few milliseconds. It is difficult to reconcile this view with the data obtained from experiments on the velocity dependence of P_{S_2} . This showed that at 0°C the rate of cycling of the

cross-bridges ceases to affect P_{S_2} at velocities in excess of about 4 mm.s^{-1} . This corresponds with a speed of filament sliding of about $0.16 \mu\text{m.s}^{-1}$. The spacing of the cross-projections orientated in the direction of any given actin filament is approximately 43 nm, which means that a specific point on the actin filament will encounter, on average, 3.8 cross-bridges per second so that an interaction can occur only once every 260 ms. If Podolsky & Nolans' theory were correct, the critical velocity ought to be at least 10 x greater than is found experimentally.

The model put forward by Huxley & Simmons has certain energetic advantages. They postulate that the head can remain attached to the actin filament at a number of positions, but that detachment, accompanied by hydrolysis of ATP can only occur when the head has reached the final position. We have already seen that the head is constrained to adopt an intermediate position, from which it cannot be detached by ATP, during the maintenance of isometric tension. This means that relatively little ATP will be consumed at high loads compared with small loads where shortening is possible.

Now, the model of Julian et al, which is superficially like that of Huxley & Simmons, does not permit cross-bridges to exist in intermediate positions; they can either exist in an attached state, where they exert no tension (α), or one in which they exert maximum force (β) and from which the probability of detachment, and therefore ATP hydrolysis, is high. It would therefore seem that this must be energetically more

expensive than the Huxley & Simmons model.

Scope for further study.

The importance of looking at sarcomere movements in mechanical experiments of the kind described here cannot be over-emphasised. The present experiments were hampered because the camera used to record the movement of the diffraction spectra was able to operate at a maximum speed of only 64 frames per second, restricting the sampling rate to one observation every 15 ms. This meant that the speed of stretching had to be comparatively slow and no detailed study of the effects of varying velocity of stretch on the movements of the sarcomeres could be made. Moreover, even with this relatively poor time resolution, analysis of the results was extremely time consuming. Clearly, better resolution could be obtained with a high speed camera (up to 1000 frames per sec.), but this would not get round the problem of making measurements on each frame. A better approach would be to obtain a continuous record of sarcomere movements, as would be obtained with the kind of system mentioned earlier (Scope of the present study), employing a photoelectric cell to detect changes in the spacing of the first order spectra.

Several interesting experiments could be undertaken with a system of this kind. In particular, the relation between force and the speed of filament movement during the period after rapid 'give' could be studied by varying the speed at which the muscle is stretched. In addition, the extent of rapid 'give' at different sarcomere lengths could be measured.

The temperature dependence of sarcomere stiffness and of P_{S_2} referred to in Chapter V, is another area which deserves further study. Again, it would be necessary to monitor filament sliding in order to determine the stiffness of the sarcomeres over a wide range of temperature and velocity.

The patterns of stretch and release used in this study were limited in that it was impossible to investigate the effects of multiple stretches; each stretch, other than the first, necessarily followed a previous release, as the wave-form generator used could not be programmed to provide one stretch, followed immediately or after a delay by another one. A device has now been constructed which is able to do this. An experiment which should be made is to stretch a muscle, at a relatively slow speed (say $4 \text{ mm} \cdot \text{s}^{-1}$), to a point beyond rapid 'give' where the tension levels off and then either halt the stretch for a period of time and then subject the muscle to a second stretch; or, alternatively, increase the velocity of stretch immediately. In the former case, tension will start to fall in the period between first and second stretches, and if sufficient time is allowed (say 500 ms) for attachment and reattachment of cross-bridges to occur, then a subsequent stretch ought to produce a response essentially similar to the first, accompanied by rapid 'give' of sarcomeres. A different result is predicted for the second of these alternatives, when velocity of stretch is increased abruptly; the muscle should change quickly (perhaps, instantaneously) from one point on the force / velocity curve to another. If the second of these stretches is sufficiently rapid

it ought to effect a drop in the level of maintained force.

Finally, the variations in the discharge frequency of a muscle spindle subjected to stretch bears a striking resemblance to the form of the tension response to large amplitude stretches described in this report (Brown, 1971); so much so, that it raises the possibility that the afferent response may be determined largely by the mechanical properties of the intrafusal fibres themselves. The instantaneous impulse frequency increases rapidly during the early part of a stretch, then levels off more or less abruptly while the stretch continues. At the end of the stretch, it decays in a characteristic fashion. Primary and secondary nerve endings differ in their responses (Boyd & Ward, 1975); primary endings show a marked velocity dependence, with rapid accommodation after the length change is completed (large dynamic index) whereas secondary endings respond to the instantaneous length of the spindle and show little accommodation (small dynamic index). It would be of considerable interest to record the instantaneous rate of firing of an isolated spindle and observe sarcomere movements using the laser diffraction system, simultaneously. This would be technically difficult with mammalian spindles, but it could be attempted with the simpler frog muscle spindle, employing the 'critical curarisation' procedure to eliminate the effects of ventral root stimulation on the extrafusal fibres while recording the response of the intrafusal fibres.

REFERENCES.

- APRIL, E.W. (1975). Liquid crystalline characteristics of the thick filament lattice of striated muscle. *Nature, Lond.* 257, 139 - 141.
- ARMSTRONG, C.M., HUXLEY, A.F. & JULIAN, F.J. (1966). Oscillatory responses in frog skeletal muscle fibres. *J. Physiol.* 186, 26 - 27 P.
- ASHLEY, R. (1972). A hybrid theory of muscle contraction. *J. theor. Biol.* 36, 339 - 354.
- BARANY, M. (1967). ATPase activity of myosin correlated with speed of muscle shortening. *J. gen. Physiol.* 50, suppl. 197 - 216.
- BARRY, W.H. & CARNAY, L.D. (1969). Changes in light scattered by striated muscle during excitation-contraction coupling. *Am. J. Physiol.* 217, 1425 - 1430.
- BOYD, I.A. & WARD, J. (1975). Motor control of nuclear bag and nuclear chain intrafusal fibres from isolated living muscle spindles from the cat. *J. Physiol.* 244, 83 - 112.
- BRESSLER, B.H. & CLINCH, N.F. (1974). The compliance of contracting skeletal muscle. *J. Physiol.* 237, 477 - 493.
- BROWN, M.C. (1971). The responses of frog muscle spindles from fast and slow muscle fibres to a variety of mechanical inputs. *J. Physiol.* 218, 1 - 17.
- CARLSON, F.D. & WILKIE, D.R. (1974). *Muscle physiology*. Prentice-Hall, Inc., N.J.

- CIVAN, M.M. & PODOLSKY, R.J. (1966). Contraction kinetics of striated muscle fibres following quick changes in load. *J. Physiol.* 184, 511 - 534.
- CLEWORTH, D.R. & EDMAN, K.A.P. (1972). Changes in sarcomere length during isometric tension development in frog skeletal muscle. *J. Physiol.* 227, 1 - 17.
- CURTIN, N.A. & DAVIES, R.E. (1973). Chemical and mechanical changes during stretching of activated frog skeletal muscle. *Cold Spring Harb. Symp. quant. Biol.* 37, 619 - 626.
- CURTIN, N.A., GILBERT, C., KRETZSCHMAR, K.M. & WILKIE, D.R. (1974). The effect of the performance of work on the total energy output and metabolism during muscular contraction. *J. Physiol.* 238, 455 - 472.
- EBASHI, S. (1963). Third component participating in the superprecipitation of 'natural actomyosin'. *Nature, Lond.* 200, 1010.
- EBASHI, S. & EBASHI, F. (1964). A new protein component participating in the superprecipitation of myosin B. *J. Biochem., Tokyo.* 53, 604 - 613.
- EBASHI, S., ENDO, M., NONOMURA, Y., MASAKI, T. & OHTSUKI, I. (1966). Localization of native tropomyosin in relation to striation patterns. *J. Biochem.* 60, 607 - 608.
- ELLIOT, G.F. (1964). X-ray diffraction studies on striated and smooth muscles. *Proc. Roy. Soc. B.* 160, 467 - 472.
- ELLIOT, G.F., LOWY, J. & WORTHINGTON, C.R. (1963). An X-ray and light diffraction study of the filament lattice of striated muscle

in the living state and in rigor. *J. molec. Biol.* 6, 295 - 305.

ELLIOT, G.F., ROME, E.M. & SPENCER, M. (1970). A type of contraction hypothesis applicable to all muscles. *Nature, Lond.* 226, 417 - 420.

FIESER, L.F. & FIESER, M. (1957). *Introduction to organic chemistry.* D.C. Heath, Boston.

FLITNEY, F.W. & HIRST, D.G. (1974). Short range elastic properties of contracting frog's muscle. *J. Physiol.* 239, 119 P.

FLITNEY, F.W. & HIRST, D.G. (1975a). Rapid 'give' of sarcomeres and tension changes during servo-controlled stretches applied to contracting frog's muscle. *J. Physiol.* 246, 68 - 69 P.

FLITNEY, F.W. & HIRST, D.G. (1975b). Tension responses and sarcomere movements during length changes applied to contracting frog's muscle. *In Press.*

FLITNEY, F.W., HIRST, D.G. & STEPHENS, W.G.S. (1975). Apparatus for investigating sarcomere movements in contracting frog's muscle during servo-controlled length changes. *In Press.*

FUCHS, F. (1974). Striated muscle. *A. Rev. Physiol.* 36, 461 - 502.

GOLDSPINK, G., LARSON, R.E. & DAVIES, R.E. (1970). Fluctuations in sarcomere length in the chick anterior and posterior latissimus dorsi muscles during isometric contraction. *Experientia.* 26, 16 - 18.

GORDON, A.M., HUXLEY, A.F. & JULIAN, F.J. (1966b). The variation in isometric tension with sarcomere length in vertebrate muscle fibres. *J. Physiol.* 184, 170 - 192.

HALL, C.E., JAKUS, M.A. & SCHMITT, F.D. (1946). An investigation of cross-striations and myosin filaments in muscle. Biol. Bull. Woods Hole, 90, 32 - 49.

HANSON, J. (1968). Recent X-ray diffraction studies of muscle. Q. Rev. Biophys. 1, 177 - 216.

HARTSHORNE, D.J., BARNES, E.M., PARKER, L. & FUCHS, F. (1972). The effect of temperature on actomyosin. Biochim. biophys. Acta. 267, 190 - 202.

HASSELBACH, W. (1952). Die Umwandlung von Aktomyosin-ATPase in L- Myosin ATPase durch Aktivatoren und die resultierenden Aktivierungseffekte. Z. Naturf. 7b, 163.

HILL, A.V. (1938). The heat of shortening and the dynamic constants of muscle. Proc. R. Soc. B. 136, 195 - 211.

HILL, A.V. (1949). Is relaxation an active process ? Proc. R. Soc. B. 136, 420 - 435.

HILL, A.V. (1970). First and last experiments in muscle mechanics. Cambridge : University Press.

HILL, D.K. (1949). Changes in transparency of muscle during a twitch. J. Physiol. 108, 292 - 302.

HILL, D.K. (1953a). The optical properties of resting striated muscle. The effect of rapid stretch on the scattering and diffraction of light. J. Physiol. 119,

HILL, D.K. (1953b). The effect of stimulation on the diffraction of light by striated muscle. J. Physiol. 119, 501 - 512.

- HILL, D.K. (1965). The organization of the interfibre space in the striated muscle of the toad, and the alignment of striations of neighbouring fibres. *J. Physiol.* 179, 368 - 384.
- HILL, D.K. (1968). Tension due to interaction between the sliding filaments in resting striated muscle. The effect of stimulation. *J. Physiol.* 199, 637 - 684.
- HILL, D.K. (1970a). The effect of temperature in the range 0 - 35°C on the resting tension of frog's muscle. *J. Physiol.* 208, 725 - 739.
- HILL, D.K. (1970b). The effect of temperature on the resting tension of frog's muscle in hypertonic solutions. *J. Physiol.* 208, 741 - 756.
- HUXLEY, A.F. (1957). Muscle structure and theories of contraction. *Prog. Biophys. biophys. Chem.* 7, 255 - 318.
- HUXLEY, A.F. (1971). The activation of striated muscle and its mechanical response. *Proc. R. Soc. B.* 178, 1 - 27.
- HUXLEY, A.F. (1974). Muscular contraction. *J. Physiol.* 243, 1 - 43.
- HUXLEY, A.F. & NEIDERGERKE, R. (1954). Interference microscopy of living muscle fibres. *Nature, Lond.* 173, 971 - 973.
- HUXLEY, A.F. & PEACHEY, L.D. (1959). The maximum length for contraction in striated muscle. *J. Physiol.* 146, 55 - 56 P.
- HUXLEY, A.F. & SIMMONS, R.M. (1968). A capacitance gauge tension transducer. *J. Physiol.* 197, 12 P.

HUXLEY, A.F. & SIMMONS, R.M. (1970a). A quick phase in the series elastic component of striated muscle, demonstrated in isolated fibres from the frog. *J. Physiol.* 208, 52 - 53 P.

HUXLEY, A.F. & SIMMONS, R.M. (1971a). Mechanical properties of the cross-bridges of frog striated muscle. *J. Physiol.* 218, 59 - 60 P.

HUXLEY, A.F. & SIMMONS, R.M. (1971b). Proposed mechanism of force generation in striated muscle. *Nature, Lond.* 233, 533 - 538.

HUXLEY, A.F. & SIMMONS, R.M. (1973). Mechanical transients and origin of muscular force. *Cold Spring Harb. Symp. quant. Biol.* 37, 669 - 680.

HUXLEY, H.E. (1953a). X-ray analysis and the problem of muscle. *Proc. R. Soc. B.* 141, 59 - 62.

HUXLEY, H.E. (1953b). Electron microscope studies of the organization of the filaments in striated muscle. *Biochim. Biophys. Acta.* 12, 387 - 394.

HUXLEY, H.E. (1961). The contractile structure of cardiac and skeletal muscle. *Circulation.* 24, 328 - 335.

HUXLEY, H.E. (1963). Electron microscope studies of natural and synthetic protein filaments from striated muscle. *J. molec. Biol.* 7, 281 - 308.

HUXLEY, H.E. (1969). The mechanism of muscular contraction. *Science, N.Y.* 164, 1356 - 1366.

- HUXLEY, H.E. & BROWN, W. (1967). Low angle X-ray diagram of vertebrate striated muscle and its behaviour during contraction and rigor. *J. molec. Biol.* 30, 383 - 434.
- HUXLEY, H.E., BROWN, W. & HOLMES, K.C. (1965). Constancy of the axial spacings in frog sartorius muscle during contraction. *Nature, Lond.* 206, 1358.
- HUXLEY, H.E. & HANSON, J. (1954). Changes in the cross-striations of muscle during contraction and stretch and their structural interpretation. *Nature, Lond.* 173, 973 - 976.
- JULIAN, F.J., SOLLINS, K.R. & SOLLINS, M.R. (1973). A model for muscle contraction in which cross-bridge attachment and force generation are distinct. *Cold Spring Harb. Symp. quant. Biol.* 37, 685 - 688.
- KATZ, B. (1939). The relation between force and speed in muscular contraction. *J. Physiol.* 96, 45 - 64.
- KAWAI, A. & KUNTZ, D. (1973). Optical diffraction studies of muscle fibres. *Biophys. J.* 13, 857 - 876.
- LOWEY, S. & COHEN, C. (1962). Studies on the structure of myosin. *J. molec. Biol.* 4, 293 - 308.
- LOWEY, S., GOLDSTEIN, L., COHEN, C. & LUCK, S. (1967). Proteolytic degradation of myosin and meromyosins by a water soluble polyanionic derivative of trypsin. Properties of helical subunits isolated from heavy meromyosin. *J. molec. Biol.* 23, 287 - 304.

- LOWEY, S., SLAYTER, H.S., WEEDS, A.G. & BAKER, H. (1969).
Substructure of the myosin molecule. *J. molec. Biol.* 42, 1 - 29.
- LYMN, R.W. & TAYLOR, E.W. (1970). Transient state phosphate production in the hydrolysis of nucleoside triphosphates by myosin. *Biochemistry*, N.Y. 9, 2975 - 2983.
- MALIK, M.N. & MARTONOSI, A. (1972). The regulation of the rate of ATP hydrolysis by H-meromyosin. *Archs. Biochem. Biophys.* 152, 243 - 257.
- MATSUBARA, I., YAGI, N. & HASHIZUME, H. (1975). Use of an X-ray television for diffraction of the frog striated muscle. *Nature, Lond.* 255, 728 - 729.
- MOORE, P.B., HUXLEY, H.E. & DEROSIER, D.J. (1970). The three dimensional reconstruction of F-actin, thin filaments and decorated thin filaments. *J. molec. Biol.* 50, 279 - 295.
- NASSAR, R., MANRING, A. & JOHNSON, E.A. (1974). Light diffraction of cardiac muscle: sarcomere motion during contraction. *Ciba Foundation Symposium* 24. The physiological basis of Starling's law of the heart. Associated Scientific Publishers, Amsterdam.
- NEEDHAM, D.M. (1971). *Machina Carnis*. The biochemistry of muscular contraction in its historical development. Cambridge: University Press.
- OFFER, G. (1974). The molecular basis of muscle contraction. In 'Companion to biochemistry'. Ed. by Bull, A.T., Lagnado, J.R., Thomas, J.O. & Tipton, K.F. Longman Ltd., London.
- PAGE, S.G. (1964a). Filament lengths in resting and excited muscle. *Proc. R. Soc. B.* 160, 460 - 466.

PAGE, S.G. (1968). Fine structure of tortoise skeletal muscle.

J. Physiol. 197, 709 - 715.

PAULING, L. & COREY, R.B. (1950). Two hydrogen-bonded spiral configurations of the polypeptide chain. J. Am. chem. Soc. 72, 5349.

PAULING, L. & COREY, R.B. (1953). Compound helical configurations of polypeptide chains. Structure of proteins of the α -keratin type. Nature, Lond. 171, 59 - 61.

PEPE, E.A. (1966). Some aspects of the structural organization of the myofibril as revealed by antibody-staining methods. J. cell. Biol. 28, 505 - 525.

PODOLSKY, R.J. (1960). Kinetics of muscular contraction; the approach to the steady state. Nature, Lond. 188, 666 - 668.

PODOLSKY, R.J. & NOLAN, A.C. (1971). Cross-bridge properties derived from physiological studies of frog muscle fibres. Contractility of muscle cells. Prentice Hall, N.J.

PODOLSKY, R.J. & NOLAN, A.C. (1973). Muscle contraction transients, cross-bridge kinetics and the Fenn effect. Cold Spring Harb. Symp. quant. Biol. 37, 661 - 688.

RACK, P.M.H. & WESTBURY, D.R. (1974). The short range stiffness of active mammalian muscle and its effect on mechanical properties. J. Physiol. 240, 331 - 350.

RAMSEY, R.W. & STREET, S.F. (1940). The isometric length/tension diagram of isolated skeletal muscle fibres of the frog. J. cell. comp. Physiol. 15, 11-34.

RIZZINO, A.A., BAROUCH, W.W., EISENBERG, E. & MOOS, C.

Actin-heavy meromyosin binding. Determination of binding stoichiometry from ATP kinetic measurements. *Biochemistry*, N.Y. 9, 2402 - 2408.

RUDEL, R. & TAYLOR, S.R. (1969). The influence of stimulus parameters on contractions of frog muscle fibres. *J. Physiol.* 205, 499 - 513.

SHEAR, D.B. (1970). Electrostatic forces in muscle contraction. *J. theor. Biol.* 28, 531 - 546.

SUGI, H. (1972). Tension changes during and after stretch in frog muscle fibres. *J. Physiol.* 225, 237 - 253.

TRENTAM, D.R., BARDSLEY, R.G., ECCLESTON, J.F. & WEEDS, A.G. (1972). Elementary processes of the magnesium ion dependent adenosine triphosphate activity of heavy meromyosin. *Biochem. J.* 126, 635 - 644.

ULLRICK, W.C. (1967). A theory of contraction for striated muscle. *J. theor. Biol.* 15, 53 - 69.

WEEDS, A.G. & HARTLEY, B.S. (1967). A chemical approach to the substructure of myosin. *J. molec. Biol.* 24, 307 - 311.

WEEDS, A.G. & HARTLEY, B.S. (1968). Selective purification of the thiol peptides of myosin. *Biochem. J.* 107, 531 - 548.